

DIPLOMARBEIT

Constructing FRET biosensors for intracellular metabolite detection via fluorescence microscopy

Ausgeführt am Institut für
Systems and Synthetic Biology
Wageningen University

unter der Anleitung von dr.ir. Leo de Graaff, Laura van der Straat MSc,
Dorett Odoni MSc und ing. Tom Schonewille

sowie am Institut für
Verfahrenstechnik, Umwelttechnik und Technische Biowissenschaften
der Technischen Universität Wien

unter der Anleitung von Ao.Univ.Prof. Mag. Dr.rer.nat. Robert Mach

durch
Gwendolin Korinek
Kantweg 10
2201 Gerasdorf Oberlisse

16. Mai 2014

Abstract

In the present thesis, a FRET biosensor for quantification of C4-dicarboxylates (as previously published [1]) should be constructed. The aim was to make the sensor useable in *Aspergillus niger*. For this reason, the linkers of the biosensor were adapted to be compatible with the Funbrick system (Laura van der Straat). Two different versions of the sensor using the same core binding domain but different FRET pairs should be built in order to monitor C4-dicarboxylates such as malate, fumarate, succinate and oxaloacetate in two different cellular compartments: the cytosol and the mitochondria. After testing and characterisation of the sensor, *A. niger* should be transformed with the construct.

A FRET biosensor with the FRET pair GFP-mCherry was reconstructed in *E. coli*, purified and analysed with fluorescence microscopy. Analysis of the sensor in the cell-free extract by fluorescence microscopy showed a change of GFP emission intensity (and therefore a change of FRET ratio) upon substrate addition, which signifies that the sensor is functional. A C4 core-YFP fragment and a CFP-backbone fragment for construction of the second biosensor were built. A GFP variant with a new combination of mutations (F64L, S65T, Y66W and T203Y) ("Frog") was created. Furthermore, a new, fast optical method to screen for transformants with GFP and CFP was developed and a cloning tool to circumvent Colony-PCR is proposed.

If *A. niger* is transformed with the present FRET biosensor, it could be the first FRET biosensor for use in this fungus and lead to a much better understanding of its metabolic pathways. Further characterisation of the biosensor is recommended.

Abstract

In der vorliegenden Arbeit sollte ein FRET Biosensor zur Quantifizierung von C4-Dicarboxylaten (wie bereits publiziert [1]) konstruiert werden. Ziel war es, den Sensor für *Aspergillus niger* verwendbar zu machen. Die Linker des Biosensors wurden daher adaptiert, um mit dem Funbrick-System (Laura van der Straat) kompatibel zu sein. Zwei verschiedene Versionen des Sensors mit derselben Bindungsdomäne und unterschiedlichen FRET-Paaren sollten konstruiert werden, um C4-Dicarboxylate wie Malat, Fumarat, Succinat und Oxalacetat in zwei verschiedenen Zellkompartimenten, dem Cytosol und den Mitochondrien, zu beobachten. Nach Prüfung und Charakterisierung des Sensors sollte *A. niger* mit dem Konstrukt transformiert werden.

Ein FRET Biosensor mit dem FRET-Paar GFP-mCherry wurde in *E. coli* rekonstruiert, aufgereinigt und mit Fluoreszenzmikroskopie analysiert. Die Analyse des Sensors im zellfreien Extrakt mittels Fluoreszenzmikroskopie zeigte eine Änderung der Intensität der Emission von GFP (und damit eine Änderung des FRET-Verhältnisses) bei Substratzugabe, was zeigt, dass der Sensor funktioniert. Ein C4 Bindungsdomäne-YFP Fragment und ein CFP-Rückgrat Fragment für die Konstruktion des zweiten Biosensors wurden gebaut. Eine GFP-Variante mit einer neuen Kombination an Mutationen (F64L, S65T, Y66W and T203Y) ("Frog") wurde hergestellt. Weiters wurde eine neue, schnelle optische Screeningmethode für Transformanten mit GFP und CFP entwickelt, und ein Klonierungstool, um Kolonie-PCR zu umgehen, wird vorgestellt.

Wird *A. niger* mit dem vorliegenden FRET Biosensor transformiert, so könnte dies der erste FRET Biosensor für die Anwendung in diesem Pilz sein und wichtige neue Erkenntnisse über dessen Stoffwechselwege erschließen. Eine weiterführende Charakterisierung des Biosensors wird empfohlen.

Acknowledgements

This master thesis would not have been feasible without the help of many people.

First, I would like to emphasize the importance of the Erasmus programme. Living and working abroad is a life-changing experience, and I hope that many more students will have and seize the opportunity to go on Erasmus in the years to come. I would like to thank my Erasmus coordinator at TU Vienna, Wolfgang Linert, for making me aware of free Erasmus positions, Traude Krausler and Ellen de Jong (Wageningen UR) for their administrative efforts, as well as Irina Druzhinina, the Dean Peter Gärtner and Vice-Dean Hermann Hofbauer for their administrative help.

Second, I am deeply grateful for the help of my supervisors at Wageningen University and TU Vienna. I would like to thank Christian Kubicek who first introduced me to the workgroup of Leo de Graaff and express my gratitude to Leo de Graaff, Laura van der Straat, Dorett Odoni and Tom Schonewille for their warm welcome, encouragement and support. Last but not least, I would like to thank Robert Mach for supervising my master thesis at TU Vienna.

Third, I greatly appreciate all the help from everyone at Systems and Synthetic Biology and Microbiology, including (but not limited to) Juanan, Ruud H, Jan-Willem, Jasper, Alicia, Floor, Mike, Daan, Zyfra, Marnix, Mark, Milad, Shreyans, Kal, Philippe, Marit, Ruben, Wim and Bastian. A special Thank you goes to Jan-Willem Borst for his introduction to FRET theory and help with fluorescence spectroscopy measurements.

Fourth, I would like to thank my parents Gertrude and Fritz, my sister Tatjana, my niece Anaïs as well as my friends Birgit, Berni, Sajen, Alex, Julia, Eline, Wen, Thomas, Jake, Yu-Chu, Kerstin, David, Jingjing, Danny, Corinna, Melanie and Lennart for their feedback and moral support.

Contents

Abstract	2
Abstract	3
Acknowledgements	4
1 Introduction	8
1.1 Metabolic engineering in <i>Aspergillus niger</i> : an overview	8
1.2 Organic acids: important metabolites	9
1.2.1 Citrate	9
1.2.2 Oxaloacetate	10
1.2.3 L-Malate	11
1.2.4 Fumarate	11
1.2.5 Succinate	11
1.3 Methods of quantification of intracellular metabolites	11
1.4 Genetically encoded fluorescent/bioluminescent sensors	12
1.5 FRET sensors	13
1.5.1 General principle	13
1.5.2 Fluorophores	14
1.5.3 GFP - an important FRET fluorophore	16
1.5.4 mCherry - an important FRET fluorophore	18
1.5.5 Binding domain	19
1.5.6 Linkers	20
1.6 The Funbrick system	21
2 Aim and Approach	23
3 Materials and Methods	24
3.1 Preparative work	24
3.1.1 Media preparation	24
3.1.2 Preparation of electrocompetent cells	24
3.1.3 Preparation of protoplasts	24
3.1.4 Cultures	24
3.1.5 DNA mini- and midiprep	25
3.1.6 Concentration measurements	25
3.1.7 Restriction digests	26
3.1.8 Agarose gels	26
3.1.9 Gel extraction	26

3.2	Mutagenesis	26
3.3	In silico tasks	27
3.3.1	Sequence verification	27
3.3.2	Primer design	27
3.3.3	Molecular weight prediction	27
3.4	PCR	27
3.4.1	PCR to add restriction sites to YFP	27
3.4.2	ColonyPCR	28
3.4.3	Approaches to avoid ColonyPCR	28
3.5	Molecular cloning techniques	30
3.5.1	Overview	30
3.5.2	Mutations to obtain desired fragments	32
3.5.3	Fragments and constructs	33
3.5.4	Ligation	36
3.5.5	Transformation	37
3.6	Preparation and quantification of sensor	38
3.6.1	Cell lysis	38
3.6.2	pH measurements	38
3.6.3	Strep-tag protein purification	39
3.6.4	SDS-PAGE	39
3.6.5	BCA Assay	39
3.7	Testing of sensor	40
3.7.1	96 well-plate reader	40
3.7.2	Varian Cary Eclipse Fluorescence Spectrophotometer	42
4	Results and Discussion	43
4.1	Mutations	43
4.1.1	Analysis of GFP insert	43
4.1.2	Improved folding of GFP	43
4.2	Insertion of pyrA and YFP	45
4.2.1	Transformation of DH5 – α with Rcap C4 binding domain and mitochondrial signal	45
4.2.2	Restriction site check of YFP and Rcap C4 binding domain	45
4.2.3	Extraction of mitochondrial signal and pyrA from gel	46
4.2.4	Addition of restriction sites to YFP by PCR	46
4.2.5	Cloning of YFP into pJET	46
4.2.6	Insertion of pyrA in Funbrick	46
4.3	Insertion of first fluorophore	47
4.3.1	Insertion of CFP and GFP in pET52	47
4.4	Construction of the first FRET biosensor	49
4.4.1	Insertion of Rcap C4 in GFP-pET52 and CFP-pET52	49
4.4.2	Insertion of Rcap C4 in GFP-citA-mCherry	50
4.5	Construction of the second FRET biosensor	50
4.5.1	Insertion of YFP in GFP-Rcap C4-mCherry	50

4.5.2	Insertion of C4-YFP in CFP-Lox	51
4.5.3	Mutation of GFP-C4-YFP to CFP-C4-YFP	51
4.6	Characterisation of the FRET biosensor	52
4.6.1	Sensor measurement in the cell-free extract	52
4.6.2	Sensor purification and analysis	54
5	Conclusions	59
6	Recommendations	60
7	Abbreviations	62
	References	62
8	Appendix	67
8.1	In silico data	67
8.1.1	Primers	67
8.1.2	Sequences	68
8.2	Constructs	71
8.3	Agarose gels	72
8.4	Protocols	75
8.4.1	Project outline to build the Khanbrick	75

1 Introduction

1.1 Metabolic engineering in *Aspergillus niger*: an overview

Aspergillus niger is a well-established, generally regarded as safe "workhorse" of biotechnology. This fungus is used for industrial production of many different substances such as citrate [2] [3], xylanases [4] [5] and cellulases [6] [5]. In order to optimise production of various organic compounds, it is essential to understand the underlying biochemical processes on a morphological and metabolic level.

The morphology of filamentous fungi such as *A. niger* plays an important role for transport phenomena and productivity. Cultures may grow as freely dispersed mycelia or pellets of aggregated biomass depending on growth conditions which have to be optimised separately for every biotechnological process. While cultivation broths with pellets are less viscous than dispersed mycelia, nutrition limitations in the inner part of the biopellets can be disadvantageous [7]. Protein formation in fungal aggregates of different morphologies has been investigated with the help of a GFP-producing *A. niger* strain [7]. Fluorescence-based biosensors to localise metabolites of interest aid in studying the spatial distribution of gene expression patterns and metabolic pathway fluxes [7].

When looking at the metabolism of *A. niger*, it is important to think about compartmentalisation. Many biological processes occur within specific cell compartments. Fig. 1.1 gives a schematic overview of the most important metabolic processes in *A. niger* (Laura van der Straat) (see section 1.2).

The central element of metabolism, the TCA cycle in the mitochondria, is industrially especially relevant in *A. niger* due to the high citric acid production. Metabolites are imported from or excreted into the cytosol. In the cytosol, substrates like glucose are taken up and metabolites such as itaconate, citrate or oxalate are secreted into extracellular space.

The high industrial relevance of this pathway underlines that quantification of intracellular metabolites is crucial to understand metabolic pathways and gain valuable insights for metabolic engineering. For example, if a strain should be engineered for maximum citric acid production, a classical approach is to amplify or delete promising target genes. If a hypothetical measurement indicates that the amount of citrate in the fermentation broth is rather low, this could be attributed to a wide variety of reasons. For example, the genetic modification might not be effective. However, it is also possible that there is an increase in citrate production, but the capacity of the mitochondrial or cytosolic transporter is too low so that the majority of the metabolite is contained within the cell. Therefore, intracellular metabolite detection plays an important role as a means of feedback for metabolic engineering.

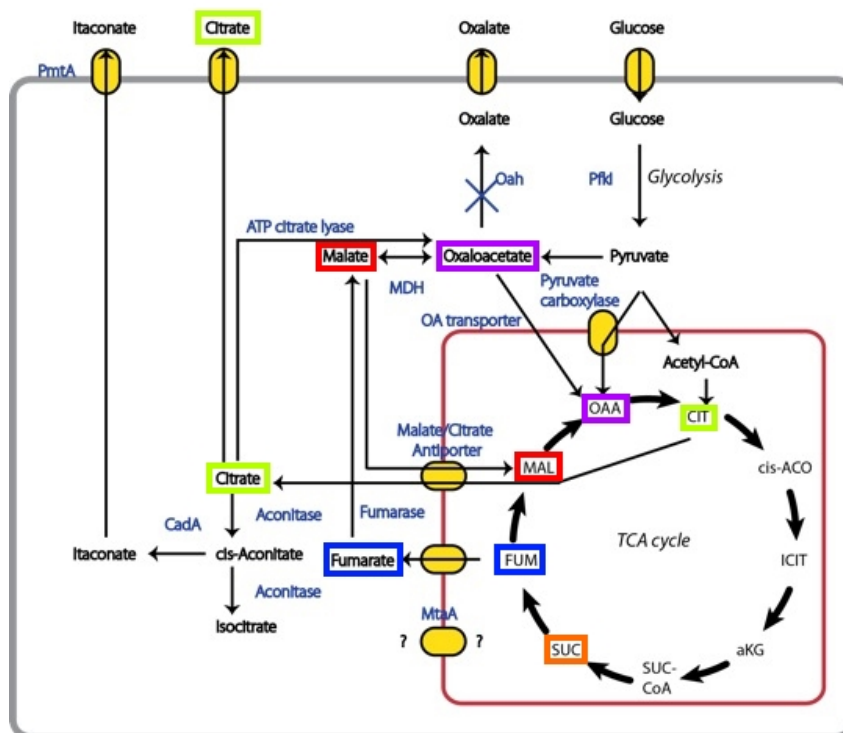


Figure 1.1: Schematic overview of important metabolic pathways in *A. niger*. Metabolites of particular interest for the present thesis were marked with frames: citrate (lemon green), malate (red), fumarate (blue), succinate (orange) and oxaloacetate (purple).

1.2 Organic acids: important metabolites

There are many substrates which play a vital role in the metabolism of *A. niger*. The present thesis focuses on citric acid, malate, fumarate, succinate and oxaloacetate due to their importance in the metabolic pathways of *A. niger*. These organic acids can be measured with the biosensors that should be built.

1.2.1 Citrate

Citric acid is accumulated if there is a metabolic dysfunction in the TCA cycle [8]. Intracellular concentrations of citrate can reach up to 4 mM [9], which is well within the limit of detection of FRET biosensors [10]. In order to reach these high concentrations and ensure continuous citric acid production, the TCA cycle has to be completed. To this end, the lack of cycle intermediates caused by the metabolic dysfunction needs to be compensated with the help of anaplerotic reactions [8].

Citric acid is mainly formed via the reactions of the glycolytic pathway [11], so a high rate of carbohydrate catabolism via the hexosebiphosphate pathway contributes to citric acid accumulation [12]. Not every carbon source is equally well suited for citric acid accumulation - while sucrose or glucose are optimal, there is little acidogenesis on galactose or lactose. A key factor in regulating citric acid production is the affinity of phosphofructokinase (PFK), the regulator

enzyme of the hexosebiphosphate pathway, to its substrate fructose-6-phosphate. Citrate is a strong inhibitor of PFK1, but this effect is antagonised by NH_4^+ ions [9]. However, recent studies by Papagianni et al. suggest that NH_4^+ ions combine with glucose to form glucosamine which is excreted into the medium. Therefore, it can be stated that PFK and α -ketoglutarate dehydrogenase are not repressed by NH_4^+ ions [11].

Citrate is produced by citrate synthase which catalyses the condensation of acetyl-CoA with oxaloacetate to form citrate and CoA. In each turn of the TCA cycle, two molecules of ATP and CO_2 are formed and oxaloacetic acid is regenerated. Citrate synthase is present in the mitochondria. Overexpression of citrate synthase does not increase citric acid production [13]. In the presence of high sugar concentrations, glycolytic flux can be controlled by trehalose-6-phosphate (T6P). The lower the concentration of T6P, the sooner citric acid accumulation is initiated [14]. Another important factor in citric acid production is the influence of manganese ions. Mn^{2+} deficiency leads to a suppression of anabolic and TCA-cycle-enzymes except for citrate synthase and thus to an overflow of citric acid as an end product of glycolysis [15]. A decrease in α -ketoglutarate dehydrogenase activity in the TCA cycle increases citric acid accumulation as well [12].

The mitochondrial tricarboxylic acid carrier competes with aconitase for citrate. If its affinity for citrate is higher, it catalyses the transport of citrate from the mitochondria to the cytoplasm [11]. This is thought to be a rate-limiting step [16]. An increased cytosolic malate concentration may stimulate export of citrate from the mitochondria by antiport of cytosolic malate [17]. The metabolite is exported from the cell. This step seems rather important for citric acid production since cell export is believed to shift the reaction balance to the production side [17].

1.2.2 Oxaloacetate

Oxaloacetate is an important element in the TCA cycle. Its concentration affects the K_m value of citrate synthase for acetyl-CoA [11]. *A. niger* is able to synthesise oxaloacetate independently from the TCA cycle [18]. This is an important anaplerotic reaction. A constitutive pyruvate carboxylase of *A. niger* is located in the cytosol. It can convert glycolytic pyruvate with CO_2 to oxaloacetate. The quantity of CO_2 used in this step equals the quantity of CO_2 released during acetyl-CoA formation. This use of CO_2 increases citric acid yields [11]. A high rate of oxaloacetate formation by pyruvate carboxylase may increase citric acid accumulation [12]. Oxaloacetate hydrolase may split oxaloacetate to form oxalate which is an unwanted toxic byproduct of citric acid fermentation. The substrate may also be converted to malate by malate dehydrogenase. Increased cytosolic malate dehydrogenase activity leads to an increase in initial citrate production rate, but is of minor importance at later stages of the fermentation [16]. The affinity of oxaloacetate to malate dehydrogenase is higher than that of oxaloacetate hydrolase. It is hypothesized that a rise in pH ($\text{pH} > 3$ [16]) favours oxaloacetate hydrolase activity [18]. The constitutively formed ATP:citrate lyase, located in the cytosol, cleaves citrate to form acetyl-CoA and oxaloacetate [12].

1.2.3 L-Malate

Intracellular malate accumulation directly precedes citric acid accumulation [16]. L-malic acid can be synthesised via the glyoxylic acid cycle from isocitric acid and acetyl-CoA [8]. The first step in this pathway is the breakdown of isocitrate by isocitrate lyase to glyoxylate and succinate. Next, malate synthase may catalyse the formation of malate from glyoxylate and acetyl-CoA. However, isocitrate lyase is absent during citrate production. Therefore, all malate and oxaloacetate is formed by carboxylation of pyruvate under these conditions [11]. It is conceivable that L-malate will be produced on an industrial scale in the near future (see section 1.2.5).

1.2.4 Fumarate

Overexpression of cytosolic fumarases (fum1, fumR from *S. cerevisiae* and *R. oryzae*, respectively), which catalyse addition of water to fumarate to form cytosolic L-malate, leads to increased citric acid production. The produced malate serves as substrate for the mitochondrial malate-citrate antiporter. The fumarate for this reaction is present in the cytosol and believed to come from the mitochondria, as no pathways in the cytosol are known [16]. Recent research showed important findings for producing fumarate in *A. niger* industrially in the near future (see section 1.2.5).

1.2.5 Succinate

Succinate can be synthesised by conversion of isocitrate by isocitrate lyase to glyoxylate and succinate. Interestingly, overexpression of the isocitrate lyase gene does not lead to an increased flux toward the glyoxylate pathway and increased succinate and malate levels, but to increased fumarate production instead. Addition of malonate, which is a competitive inhibitor of succinate dehydrogenase, does not lead to succinate production, but to an increase in citrate and oxalate production in a wildtype strain and to increased malate production in a strain with overexpression of the isocitrate lyase gene [19].

Insertion of a fumarate reductase (Frds1 from *S. cerevisiae*) which converts fumarate to succinate leads to increased citric acid production. Fumarate is exported from the mitochondria and converted to succinate by the cytosolic fumarate reductase. Although malate is preferred, succinate may serve as a substrate for the mitochondrial malate-citrate antiporter as well [16]. It is believed that succinate production can be increased by improving fumarate reductase activity, which should lead to a higher flux through the reductive branch of the TCA cycle [19].

1.3 Methods of quantification of intracellular metabolites

Many different methods of quantification of intracellular metabolites are applied. For instance, mitochondrial proteomes are analysed by high-resolution two-dimensional gel electrophoresis. The first dimension (isoelectric focussing) separates proteins based on their pI, followed by the second dimension, an SDS-PAGE gel which separates the analytes based on their molecular weight. Spots of interest can be identified by nano-liquid chromatography/electron spray

ionisation-tandem mass spectrometry (nano-LC/ESI-MS/MS) and quantified by densitometry (optical density) [20]. In liquid chromatography, analytes in a liquid mobile phase interact with a solid immobile phase and are separated e. g. based on their polarity. Electro spray ionisation is a soft method of ionisation in which analytes are sent through a metal capillary and ionised by an electrical field between the tip of the metal capillary and a counter electrode. Mass spectrometry separates analytes based on their mass to charge ratio. Additional structural information may be obtained by selecting peaks of interest and recording a mass spectrum of these selected peaks [21].

For metabolic flux analysis, proteins or peptides may be labelled with stable isotopes, such as ^2H , ^{13}C , ^{15}N or ^{18}O and subsequently be analysed by one- or multidimensional LC-MS [22]. Another method of labelling is radioactive labelling, e. g. with ^{14}C followed by measurement on a scintillation counter.

These and other methods, e. g. Secondary Ion Mass Spectrometry (SIMS) or Magnetic Resonance Imaging (MRI) (based on nuclear magnetic resonance (NMR)) all have some limitations. Mass spectrometry, on one hand, cannot be performed in real-time and in live cells. MRI, on the other hand, is unable to depict subcellular processes [10].

One interesting method which is non-invasive and capable of subcellular resolution is Raman spectroscopy. With this method, certain rotational and vibrational modes in molecules are excited and statements about the strength of chemical bonds and chemical properties can be made. Monochromatic light is emitted. A photon excites a molecule from its ground state to a virtual energy state. The molecule returns to an a) higher-energetic or b) lower-energetic state, emitting a photon with an a) lower frequency (red-shift) or b) higher frequency (blue-shift). For biochemical applications, near-infrared (NIR) ($12500\text{-}4000\text{ cm}^{-1}$) is used. While mid-infrared (MIR) ranges from $4000\text{ to }400\text{ cm}^{-1}$ and excites fundamental vibrations, near-infrared excites overtones and combination vibrations. NIR can penetrate much farther into a sample than MIR because molar absorptivity is considerably lower [21]. With the help of this method, e.g. metabolites in urine have been quantified [23]. It is a non-invasive method which does not require sample pretreatment, is able to cover a wide dynamic range and requires small amounts of samples [23].

Finally, genetically encoded biosensors may be used for metabolite quantification. This method allows for in-vivo real-time quantification as well. Moreover, the detection limit is in the nano- to millimolar range compared with a detection limit of $50\text{ }\mu\text{M}$ for Raman spectroscopy [10]. Genetical encoding of biosensors is generally regarded as non-invasive. However, it has to be kept in mind that production of the biosensor might influence the host's metabolism.

1.4 Genetically encoded fluorescent/bioluminescent sensors

Biosensors are defined as molecules or cells that report analytes and processes in their environment. These sensors are genetically encoded in the organism of interest, produced by the organism and quantify metabolic processes. A variety of different types of genetically encoded

sensors can be seen in Fig.1.2.

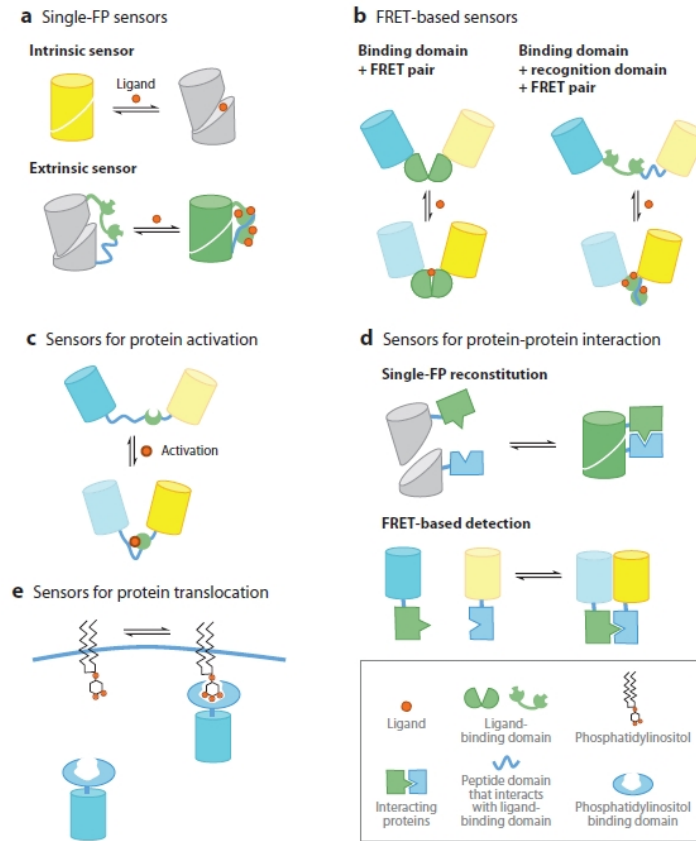


Figure 1.2: Schematic overview of various types of genetically encoded sensors ([10]). Single-FP sensors can report intrinsic or extrinsic mechanisms (a) or protein-protein interaction (d). FRET (Förster Resonance Energy Transfer)-based sensors may detect protein activation (c), protein-protein interaction (d) or intracellular metabolites (b). In sensors for protein translocation, a FP fused to the recognition domain is translocated near the cell wall upon addition of ligand (e).

Although genetically encoded fluorescent or bioluminescent sensors are widely researched, no publications regarding genetically encoded biosensors in *A. niger* were found except for a patent for a luminescent or fluorescent biosensor. The patent proposes a reporting system in which the analyte of interest is detected by binding to an inducible promoter sensitive to the analyte, which leads to expression of e. g. the Gaussia luciferase [24].

1.5 FRET sensors

1.5.1 General principle

Förster resonance energy transfer (FRET) biosensors present a promising method of determining metabolites of interest in vivo and in real-time. These biosensors are genetically encoded in organisms of interest. FRET biosensors are proteins consisting of two fluorophores (a so-called FRET pair consisting of a donor and an acceptor) and a binding domain which interacts with the analyte of interest. At small distances, energy transfer between the FRET donor and ac-

ceptor takes place. Binding of an analyte induces a conformational change in the biosensor, bringing the FRET donor and acceptor together or forcing them apart and causing a change in transfer of fluorescent energy. This process can be monitored with optical detection methods. Metabolites of interest can be quantified with the help of fluorescence microscopy.

FRET is a photophysical process involving a donor D and an acceptor A. Fluorescence occurs when a molecule D is excited to a higher quantum state D^* and emits a photon of light as it relaxes to its ground state. If the excited donor D^* is close enough to the ground state acceptor A, a non-radiative energy transfer from D^* to A can take place. The emission of the donor D decreases while the emission of the acceptor A^* increases.

The degree of FRET is quantified by the rate constant k_{ET} for dipole-dipole induced energy transfer. This rate constant is directly proportional to

- the orientation factor κ^2 which is assumed to be $2/3$ for random orientations
- the quantum yield Φ_D which is defined as the ratio of photons emitted and photons absorbed

and indirectly proportional to

- the fourth power of the refractive index n
- the fluorescence lifetime
- the sixth power of the distance between the two fluorophores R

It follows that the FRET rate diminishes very quickly over distance and only occurs in a range of up to 10 nm.

The transfer efficiency of FRET is defined as

$$E = \frac{1}{1 + (R/R_0)^6} \quad (1.1)$$

R_0 is the Förster critical transfer radius. At this distance, the transfer efficiency equals 50%.

The following prerequisites have to be met for FRET to occur:

- 1) The oscillation planes of donor and acceptor should be as parallel as possible [25].
- 2) The emission and absorption spectra of donor and acceptor need to overlap significantly [25].
- 3) The donor and acceptor have to be in close proximity to each other (in the range of R_0 , i. e. a few nm) [25].

To illustrate the principle of FRET, an example of a CFP (donor)-YFP (acceptor) FRET biosensor is given in Fig. 1.3 [10].

1.5.2 Fluorophores

The donor D (Fluorophore 1) and the acceptor A (Fluorophore 2) of the biosensor constitute a FRET pair. A good FRET pair should provide maximum overlap of donor emission and acceptor excitation as well as minimum direct excitation of the acceptor at the excitation maximum of the donor [26]. A broad variety of FRET pairs are currently used (Table 1.1 [27]).

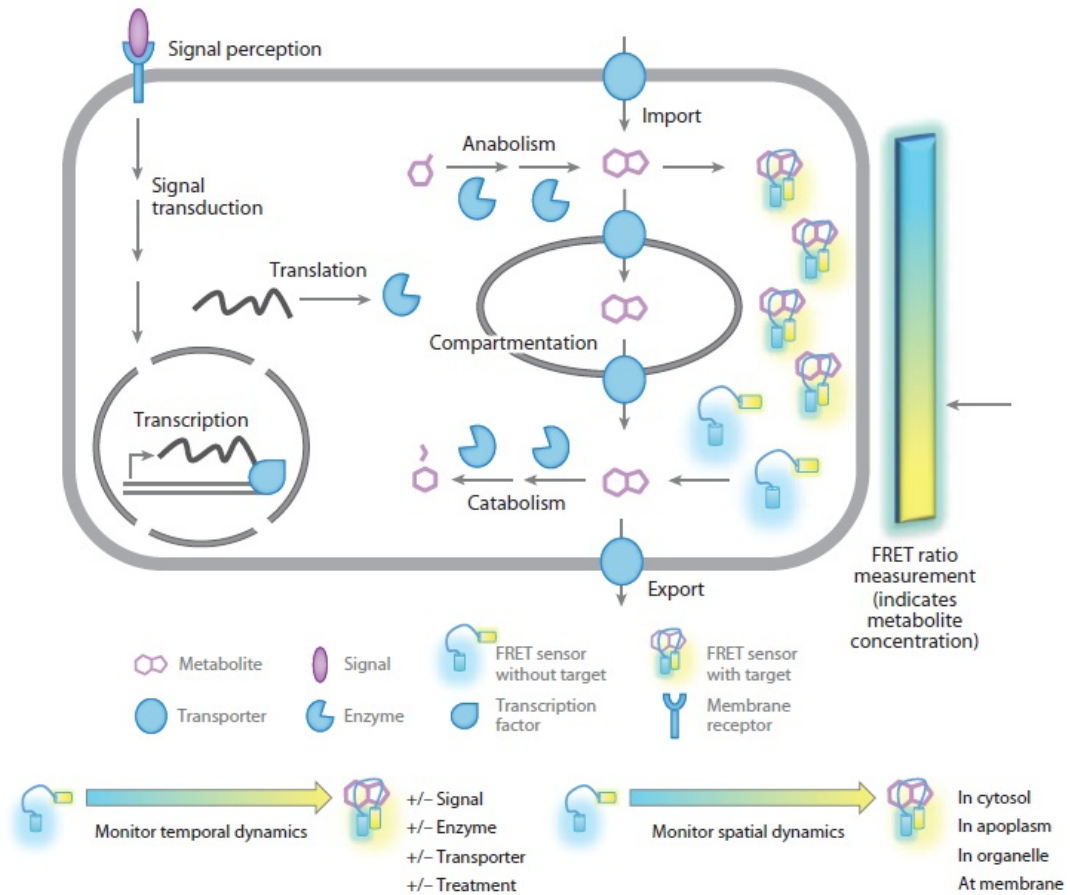


Figure 1.3: Example of a FRET biosensor [10]. The FRET pairs are apart from each other in the unbound state. The biosensor is excited at the excitation peak of CFP. In the unbound state, only CFP fluoresces.

The two fluorophores are connected by a binding domain which can bind the analyte of interest. Upon binding of the analyte, the biosensor undergoes a conformational change which brings the two fluorophores in close proximity to each other. Now, FRET takes place. This results in an increase of brightness in the acceptor (YFP) and decrease of brightness in the donor (CFP).

The overall colour changes from blue to green-yellow. By measuring the FRET ratio (Emission of YFP divided by emission of CFP), the metabolite concentration can be determined. A FRET sensor may report the presence of the analyte in any cellular compartment with high temporal and spatial resolution.

Table 1.1: Commonly used FRET pairs

FP FRET-Pair	R ₀
ECFP-EYFP	4.7
ECFP-Citrine	4.8
mCeruleanmCherry	4.8
ECFP-Venus	5
mCerulean-EYFP	5
CeruleanVenus	5.2
mCeruleanmVenus	5.3
SECFP-SEYFP	5.4
EGFP-mCherry	5.4
TagGFP-TagRFP	5.7
mTFP1-Citrine	5.7
mTFP1-mOrange	5.7
Citrine-mKate2	5.8
Clover-mCherry	5.8
mVenus-mCherry	5.8
mVenus-mOrange	5.8
mTurquoise1-SEYFP	5.8
mTurquoise2-SEYFP	5.9
Clover-mRuby2	6.3

The Förster distance and intensity of the fluorophores are indirectly proportionally related to each other. Therefore, a compromise between FRET range and intensity has to be made.

Some commonly used excitation and emission wavelengths are listed in table 1.2 [28].

Table 1.2: Excitation and emission wavelengths of widely used fluorophores

Fluorophore	Excitation wavelength [nm]	Emission wavelength [nm]
Wild Type GFP	396,475	508
GFP S65T	488	511
mCherry	587	610
eCFP	434	477
eYFP	514	527

1.5.3 GFP - an important FRET fluorophore

Properties of wild-type GFP

GFP was isolated from *Aequorea victoria*. It does not need external cofactors. The chromophore is a p-hydroxybenzylideneimidazolinone formed from residues 65-67. These residues are S-Y-G in the wild-type. Fig. 1.4 shows the mechanism for chromophore formation.

Nucleophilic attack of the amide of Gly67 on the carbonyl of Ser65 forms the imidazolinone, and dehydration takes place. Dehydrogenation of the α - β bond of Tyr66 by molecular oxygen puts its aromatic group into conjugation with the imidazolinone. This step gives the chromophore visible absorbance and fluorescence. It is presumed that hydrogen peroxide is released

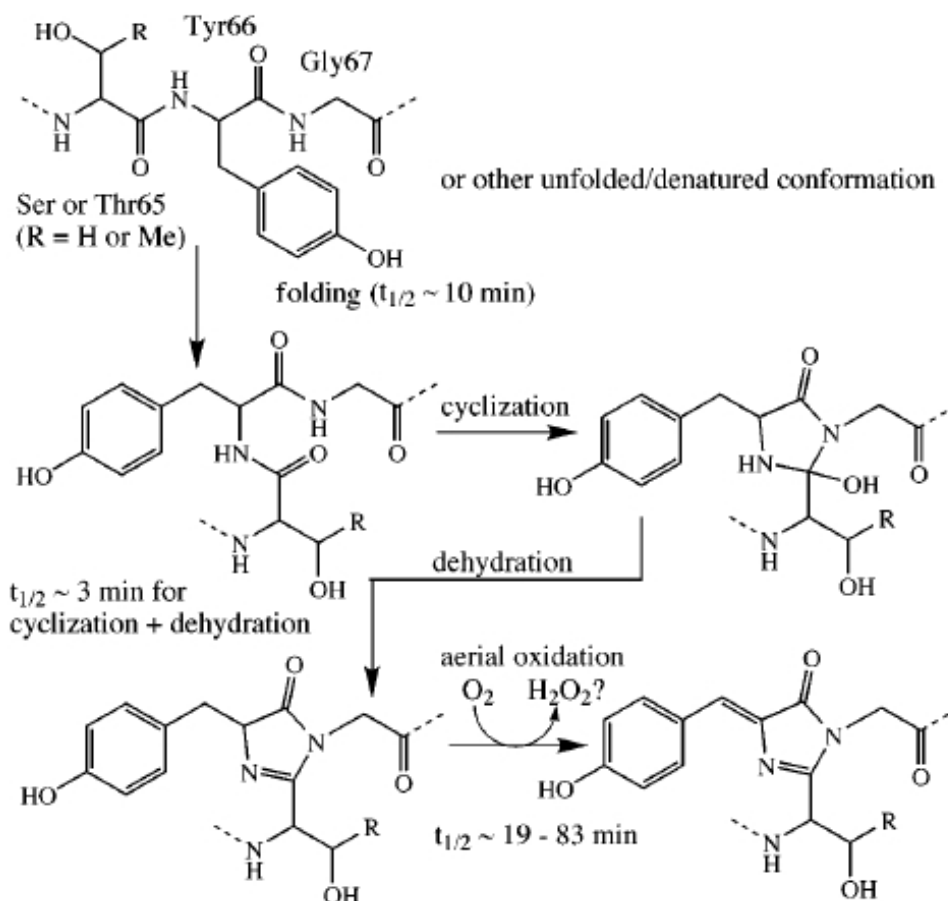


Figure 1.4: Intramolecular biosynthesis of the GFP chromophore [29].

in 1:1 stoichiometry with GFP [29].

GFP is an 11-stranded β -barrel threaded by an α -helix running up the axis of the cylinder. The chromophore is attached to the α -helix and located in the centre of the cylinder (Fig. 1.5). GFP can be dimeric or monomeric [29].

GFP variants may be classified by the distinctive component of their chromophores. Wild-type GFP from *Aequorea* belongs to Class 1 (wild-type mixture of neutral phenol and anionic phenolate). It has a major excitation peak at 395 nm which is about three times higher in amplitude than a minor peak at 475 nm. Excitation at 395 nm results in emission with a peak at 508 nm, whereas excitation at 475 nm gives a maximum at 503 nm. The 395 nm peak represents GFPs with protonated or neutral chromophores, whereas the 475 nm peak comes from deprotonated or anionic chromophores [29].

Mutations

Enhanced intensity and improved folding Class 2 GFP variants possess a phenolate anion in the chromophore. To cause ionisation of the phenol of the chromophore, Ser65 is replaced by Thr (**S65T**). The 395 nm excitation peak is suppressed and the 475 nm peak is enhanced five-to sixfold in amplitude and shifted to 490 nm. The oxidation to the mature fluorophore is fourfold faster compared to the wild-type [29].

The folding efficiency of wild-type GFP declines steeply at higher temperatures. In order to improve folding at 37°C, additional mutations were introduced. **F64L** and **V163A** are the

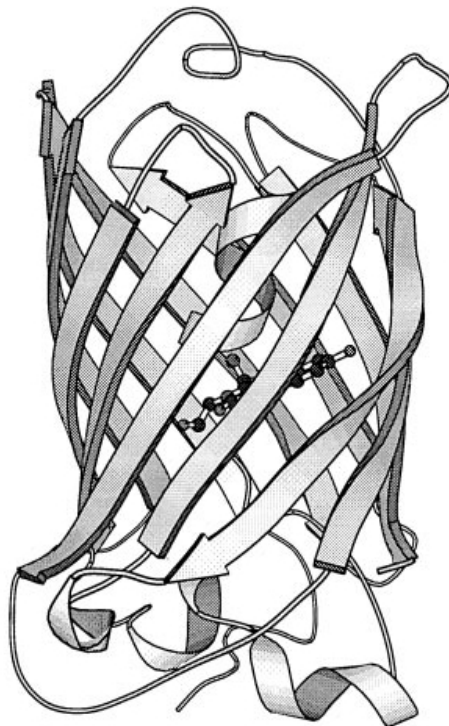


Figure 1.5: Secondary structure of GFP [29].

most commonly used replacements. These mutations only improve folding efficiency but do not increase the brightness of correctly folded molecules [29].

CFP In Class 5 GFP variants, the chromophore possesses an indole instead of a phenol or phenolate. This is achieved by mutating Tyr66 to Trp. The **Y66W** mutation turns GFP into CFP. Its excitation and emission wavelengths are 436 and 476 nm. Most cyan fluorescent proteins have double-humped excitation and emission peaks [29].

YFP This fluorophore can be obtained by creating a Class 4 GFP variant (phenolate anion with stacked π -electron system). In this class of GFP derivatives, an aromatic ring is stacked next to the phenolate anion of the chromophore, e.g. by introducing an aromatic residue at position 203. This leads to additional polarisability and π - π interaction which reduces the excited state energy. Therefore, excitation and emission wavelengths are increased by up to 20 nm. Of all aromatic residues at position 203, the **T203Y** mutation shows the highest shift. Excitation peaks at 516 nm and emission at 529 nm [29].

1.5.4 mCherry - an important FRET fluorophore

The fluorophore mCherry is a second-generation monomeric red fluorescent protein with improved brightness and photostability compared to its progenitor DsRed which was isolated from *Discosoma sp.*. Whereas GFP from *Aequorea* may dimerise, DsRed is always tetrameric. Since this is disadvantageous for a genetic fusion tag, a dimeric and a monomeric version (mRFP1) of DsRed were developed [30]. Although the DsRed chromophore bears resemblance to that of GFP, red-shifted fluorescent proteins undergo an additional reaction in chromophore maturation. The peptide bond immediately preceding the first amino acid in the chromophore triplet

X-Y-G is oxidized to an acylimine. The chromophore electron density is delocalised over the polypeptide backbone, which leads to an increase of excitation and emission maxima relative to GFP [31].

mCherry was derived from mRFP1. Its excitation and emission wavelengths are 587 and 610 nm. This red-shift compared to DsRed was obtained by substituting **K83** with a large nonpolar side chain **L**. Additionally, **E215** is hydrogen-bonded to the imidazolinone ring nitrogen and therefore protonated, which is not the case in DsRed. The chromophore environment of mCherry is more hydrophobic than in DsRed. While the five- and six-membered rings in naturally occurring fluorescent proteins such as GFP and DsRed are highly coplanar, the chromophore in mCherry is bent, which may explain its lower quantum yield compared to DsRed [31].

1.5.5 Binding domain

The recognition element of a FRET biosensor has to be chosen carefully. Any binding domain that undergoes a conformational change in the presence of the analyte of interest can be considered as a potential recognition element. This recognition element should possess some important intrinsic properties. The kinetics of association and dissociation of the analyte to the binding domain should be fast enough to be able to measure the dynamics of the analyte. The entire FRET biosensor should be able to withstand rapid changes of ionic strength and pH. The binding module should not interfere with other cellular proteins or pathways. Lastly, the binding domain should not affect the signaling and metabolic pathways of the analyte of interest [10].

For the present FRET biosensor, a C4-dicarboxylate binding domain that had already been published [1] was chosen. This protein, rcc03024 (DctP), originates from *Rhodobacter capsulatus*, a purple photosynthetic bacterium. The DctP protein is part of a TRAP-transporter SBP (solute binding protein). TRAP stands for tripartite ATP-independent periplasmic transporter. The *R. capsulatus* TRAP transporter consists of three components: 1) an extracytoplasmic solute receptor (ESR) (DctP), 2) a small membrane protein (DctQ) and 3) a big membrane protein (DctM). This class of transporters has only been discovered recently [32]. The transporter represents one of three big transporter protein families and is commonly found in many bacteria and archaea. All three transporter types are shown in Fig.1.6 [32].

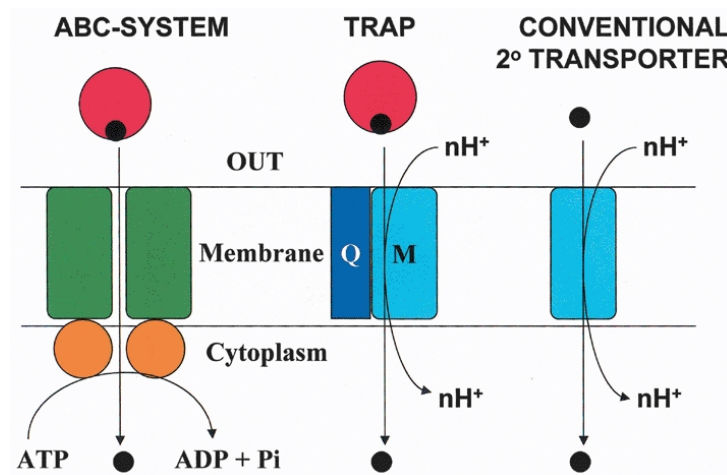


Figure 1.6: ABC, TRAP and secondary transporter [32]

The DctP ESR is able to bind four different C4-dicarboxylates: fumarate, succinate, malate and oxaloacetate [1].

1.5.6 Linkers

Linkers play an important role in the functionality of a biosensor. The connections between the recognition domain and the fluorophores need to have the right length to ensure sufficient flexibility [33] [34]. Likewise, the nature of the amino acids can have a big impact. If it is suspected that a FRET pair is too close together or too rigid, linkers may be prolonged with further amino acids. Alternatively, existing amino acids can be substituted with glycins [33]. Due to their tiny proton residue, glycins increase linker flexibility. Gly-Ser repeats are another commonly used linker [34].

In the present thesis, the linkers to build the FRET biosensor had to be adapted to make the construct Funbrick-compatible (see section 1.6). This added an element of uncertainty to the project. Even though the construct had already successfully been tested, it might not function properly with the modified linkers. The original amino acid sequence was modified as in Table 1.3.

Table 1.3: Linker adaptations

Linker	Fluorophore I-Core	Core-Fluorophore II
Published	GTTS	TSL
Funbrick-adapted	MHTS	TSEF

For better visualisation, the secondary structures of the published (a, b) and adapted sequences (c, d) for the Fluorophore I-Core (a, c) and Core-Fluorophore II (b, d) linkers are shown below (Fig. 1.7).

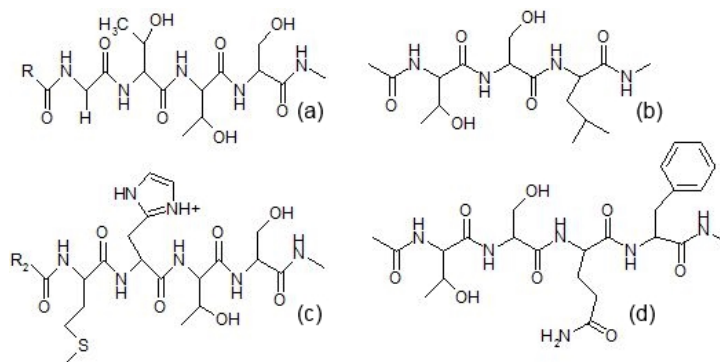


Figure 1.7: Published and modified linker structures.

In the first linker, G is replaced with the long amino acid M and the polar, uncharged amino acid T is replaced with the positively charged H. In the second linker, L is replaced with E. Although L is more hydrophobic, the amino acids are similar in length. At the end of the second linker, an additional amino acid is added. Phenylalanine is a big residue. All things considered, some substantial changes to the linkers were made.

1.6 The Funbrick system

The Funbrick system is a newly devised tool to facilitate transformation in *Aspergillus niger* (Laura van der Straat). This system uses a number of standardised restriction sites to build a variety of constructs. Many different types of Funbricks have been created. Fig. 1.8 shows the structure of a typical Funbrick similar to the Funbricks used in the present thesis.

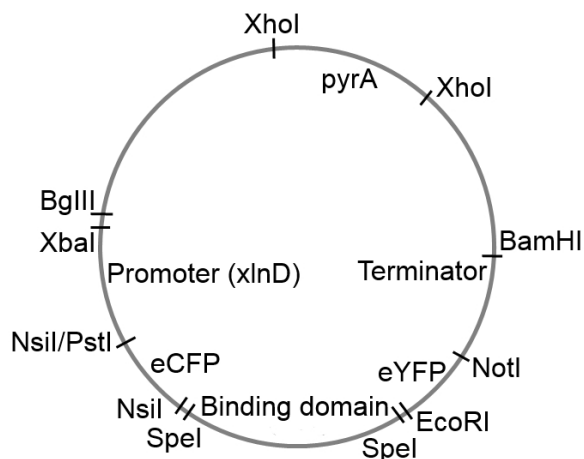


Figure 1.8: Schematic overview of a typical Funbrick

This scheme depicts a complete FRET biosensor construct in a Funbrick. The promoter enables transcription of the construct. eCFP is fused to the promoter with the NsiI/PstI scar, followed by the binding domain, the second fluorophore and the terminator. pyrA is inserted at the XhoI site as a selection marker.

The unique quality of the Funbrick system is the fact that, owing to usage of standardised restriction sites, almost any part of the construct can easily be replaced by another. For example, to insert another sensor core, the Funbrick would only need to be cut with e. g. NsiI and EcoRI, and the new sensor flanked by NsiI and EcoRI could be inserted. The only part which is not as flexible so easily is the first fluorophore because this part is fused to the promoter. However, it can be altered to e. g. GFP with the help of mutagenesis because changing from one colour to another often takes as little as one mutation.

If a part of the construct, e. g. the first fluorophore or a mitochondrial signal, should be fused to the promoter, this can be achieved by inserting a fragment cut with PstI and NsiI into a vector cut at the NsiI restriction site. The following illustration shows the schematic result of this ligation (Fig. 1.9).

The recognition sequence is depicted in orange for NsiI and in green for PstI. The fragment on the left represents the Funbrick backbone with the NsiI restriction site. The fragment on the right is the insert flanked by the PstI and NsiI restriction sites. The fragments are cut at the blue dents and the insert is introduced in the backbone. The restriction sites NsiI and PstI are compatible with each other, i. e. the PstI and NsiI ends can overlap and stick together.

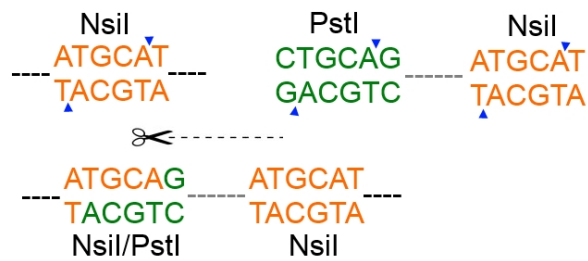


Figure 1.9: Schematic illustration of the NsiI/PstI scar

However, if they do so, the resulting sequence is a combination of the PstI and NsiI restriction sites. This sequence can neither be recognised by NsiI nor by PstI. As a consequence, inserts are permanently fused to the vector.

2 Aim and Approach

The aim of the thesis was to construct a FRET biosensor in two different versions (Fig. 2.1). Both versions respond to the same analytes of interest, but operate at different wavelengths. The idea behind using two different versions of a FRET biosensor is to monitor metabolites of interest in two different cellular compartments, the cytosol and the mitochondria, simultaneously. Furthermore, the sensor needed to be tested. Next, *A. niger* should be transformed with the sensor.

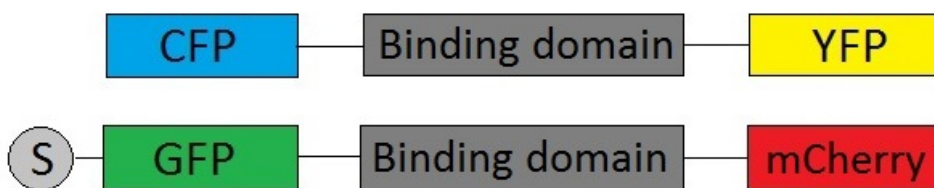


Figure 2.1: Schematic structure of constructs. One version of the sensor uses the GFP-mCherry FRET pair, whereas the other is based on the CFP-YFP FRET pair. The binding domain remains the same. One of the sensors should possess a mitochondrial signal at the N-terminus in order to get transported into the mitochondria. It is intended to use these two FRET pairs for simultaneous real-time in-vivo detection of C4-dicarboxylates in the cytosol and in the mitochondria.

As previously discussed, it was decided to build the Rcap C4 core FRET sensor in order to be able to quantify four different C4-dicarboxylic acids (malate, fumarate, succinate and oxaloacetate) due to their critical roles in the metabolism of *A. niger*.

The first goal was to improve the folding of enhanced GFP (eGFP) and to obtain the colours YFP and CFP from this improved version of GFP. The stop codon at the end of GFP needed to be removed in order to express the entire biosensor construct. This could be achieved by mutagenesis. Additionally, restriction sites had to be added to YFP by means of PCR to make the second fluorophore Funbrick-compatible.

The sensor binding domain Rcap C4 (in the Funbrick) and the mitochondrial signal (in pUC57) were used to build the sensor construct. Another goal was to insert the selection marker *pyrA* in the Funbrick (containing the Rcap C4 sensor) and to build the construct in the Funbrick.

The first major objective was to build the FRET biosensor in *E. coli* for protein purification with the help of affinity chromatography and subsequent sensor testing and calibration with the help of fluorescence spectroscopy. The construct was to be built with both FRET pairs. The second major objective was to build the sensor in the Funbrick for transformation of *A. niger*. These goals should be achieved with molecular cloning techniques.

3 Materials and Methods

All materials were properly autoclaved and disposed of.

3.1 Preparative work

3.1.1 Media preparation

1 M stocks of NaCl, KCl, $\text{MgSO}_4 \cdot 7\text{H}_2\text{O}$, $\text{MgCl}_2 \cdot 6\text{H}_2\text{O}$ and $\text{glucose} \cdot \text{H}_2\text{O}$ were prepared. Sterile water was prepared by autoclaving bottles of demi-water. SOB, SOC, liquid LB and LB plates were primed. Due to the observation that SOC gets infected very easily, only SOB was kept at room temperature. The amount of SOC required for transformations was made freshly on the day of transformations. Occasionally, LB agar was kept in a 60°C or 80°C stove overnight. LB^{Amp} plates were stored at 4°C prior to use.

3.1.2 Preparation of electrocompetent cells

Electrocompetent cells were prepared according to Protocol 23 (Section 8.4). On one occasion, the electrocompetent cells were contaminated with GFP-Lox in pET52 Rosetta colonies. The batch of electrocompetent cells was discarded and a new set of electrocompetent cells was prepared. After the contamination had occurred, pipettes were always cleaned with EtOH prior to preparation of electrocompetent cells as a safety precaution. In addition, freshly autoclaved pipette tips were used.

3.1.3 Preparation of protoplasts

Protoplasts for *A. niger* transformations were prepared according to Protocol 31 and 32 (Section 8.4). Two strains, 872.11 and N593, were grown. The first is unable to synthesise both arginine and uridine, while the latter cannot synthesise uridine. CM plates were inoculated and incubated in a Harstra incubator at 30°C for four days. Liquid cultures were grown at 30°C in a New Brunswick Scientific incubator.

3.1.4 Cultures

Three different strains of *E. coli* were used. XL 10-Gold ultracompetent cells were transformed with mutagenesis PCR products. These cells are tetracycline and chloramphenicol resistant. Most other transformations were performed with DH5- α . For protein production, a Rosetta 2 (DE3) strain was used. This strain harbours a pRARE plasmid for enhanced protein production which makes it chloramphenicol resistant.

Liquid cultures were inoculated by pipetting 1 μL of glycerol stock or scraping cell material from an agar plate with a pipette tip and dropping the pipette tip in the culture. Cells were grown in liquid LB with the required antibiotic(s) at the required concentration(s) and incubated at 37°C and 200-250 rpm in a New Brunswick Scientific innova 4000 Incubator Shaker overnight.

Plates were incubated upside down in a Jouan EB 170 S incubator at 37°C overnight or longer if colonies did not grow sufficiently overnight. All plates were stored in a cold room at 4°C.

20% Glycerol stocks were made from liquid cultures and stored at -80°C. A list of glycerol stocks of constructs is given in table 8.2.

3.1.5 DNA mini- and midiprep

Liquid cultures were harvested by centrifuging with a ThermoScientific Sorvall Legend XTR Centrifuge at 4800 g for 5 min.

Plasmid DNA was minipreped with the help of the ThermoScientific GeneJET Plasmid Miniprep Kit. Centrifugation steps were carried out with a 5415 D Eppendorf centrifuge at 13200 rpm or a 5417 R Eppendorf centrifuge at 10000 rcf. The samples were eluted with autoclaved demi water instead of elution buffer and stored at -20°C.

Cultures for DNA midiprep were grown in 50mL Falcon tubes or in up to 500 mL cultures in Erlenmeyer flasks overnight. Cultures were centrifuged at 4500 rpm for 20 min with the ThermoScientific Sorvall Legend XTR Centrifuge. DNA midiprep was performed with the Macherey-Nagel NucleoBond Xtra Midi Kit. Samples were dissolved in 150 μL demi-water and stored at -20°C.

3.1.6 Concentration measurements

DNA concentration was measured on a ThermoScientific Nanodrop ND-1000 Spectrophotometer. After blanking with MilliQ water, 1 μL of sample was measured using the NucleicAcid module and DNA-50 option. Absorbance was measured at 260 nm. Conversion into ng/ μL is based on the Beer-Lambert law (see formula 3.1).

$$A = E \cdot b \cdot c \quad (3.1)$$

This formula may be adapted for DNA as in formula 3.2:

$$c^* = \frac{A \cdot e}{b} \quad (3.2)$$

A	...	absorbance []
E	...	wavelength-dependent extinction coefficient [$L \cdot \text{mol}^{-1} \cdot \text{cm}^{-1}$]
e	...	wavelength-dependent extinction coefficient [$\text{ng} \cdot \text{cm} \cdot \mu\text{L}^{-1}$]
b	...	path length [cm]
c	...	analyte concentration [$\text{mol} \cdot L^{-1}$]
c*	...	analyte concentration [$\text{ng} \cdot \mu\text{L}^{-1}$]

For dsDNA, an extinction coefficient of $50 \text{ ng} \cdot \text{cm} \cdot \mu\text{L}^{-1}$ is assumed by the spectrophotometer software. The 0.2 mm pathlength is used for calculation and normalised to 1.0 cm on the display. The concentration range according to the manufacturer is 2-3700 ng/ μL with an uncertainty of $\pm 2 \text{ ng}/\mu\text{L}$ up to 100 ng/ μL and 2 % above 100 ng/ μL . Since only the range of the concentrations had to be determined, concentration measurements were only carried out once.

OD600 measurements were carried out on an Hitachi U-1100 Spectrophotometer.

3.1.7 Restriction digests

Restriction digests were performed with ThermoScientific FastDigest. 200 ng of DNA were used to perform restriction site checks. For preparative purposes, 5 μg of DNA were cut in 100 μL digest. The digests were prepared with autoclaved demi-water. Samples were incubated at the required temperature and time on an Eppendorf Thermomixer comfort thermoblock, vortexed with a Scientific Industries Vortex Genie 2 vortexer and spun down with a Qualitron Inc. DW-41 centrifuge.

3.1.8 Agarose gels

Agarose gels were prepared with agarose and TAE buffer and stained with 1 μL SybrSafe per 10 mL gel. All agarose gels were run at a voltage of 100V. The gels were run on a Mupid One electrophoresis system. Gel pictures were made with the Syngene GeneSys G:Box Chemi-XT4 gel reader. The Fisher BioReagents exACTGene 1 kb DNA Ladder and 50 bp Mini DNA Ladder were used as ladders. Samples from restriction digests were dyed by the restriction digest buffer. Samples without any dye were prepared with the ThermoScientific 6x DNA Loading Dye. Samples from Phusion and DreamTaq PCR were dyed by the PCR buffers.

3.1.9 Gel extraction

Bands were visualised on an invitrogen Safe Imager 2.0 plate, viewed with Bio-RAD XcitaBlue glasses and excised with sterile single-use scalpels. The fragments were extracted from gel using the Fermentas Gel Extraction Kit. For fragments smaller than 2 kb, the Freeze'n'Squeeze protocol (see section 8.4) was used as well. Fragments were eluted/dissolved with/in autoclaved demi-water and stored at -20°C .

3.2 Mutagenesis

Mutagenesis was performed with the help of the Agilent QuikChange Lightning Site-Directed Mutagenesis Kit. Due to financial reasons, the reaction scale was downsized to half of the total volume recommended in the protocol. Only one PCR tube per mutagenesis reaction was prepared. 25 or 50 ng of DNA template were used. The PCR tubes were vortexed and spun down prior to PCR. PCR was carried out in the BioRAD MyCycler version 1.065. The Dpn Digest was performed in a Jouan EB 170 S incubator with 1 μL DpnI. Competent cells were

heat-pulsed in a B. Braun 7P Thermomix MM water bath. After transformation, cells were incubated in the New Brunswick Scientific innova 4000 Incubator Shaker.

The following volumes of cells were plated: 250/125/75/30/10/1 μL

For all volumes below 100 μL , the desired volume was pipetted on top of 200 μL of NZY⁺ Broth to improve spreading.

For the control reactions, a ready-to-use 20 mg/mL X-gal solution was used and a 10 mM IPTG stock solution was freshly prepared.

Samples were diluted to 30-100 ng/ μL and sent to GATC for sequencing. Inserts in pJET were sequenced using standard pJET forward and reverse primers provided by GATC.

3.3 In silico tasks

All sequences are listed in 8.1.2.

3.3.1 Sequence verification

After each mutagenesis step, sequences had to be verified in order to ensure that the plasmid contains the desired mutation and that no undesired mutations were introduced. To this end, sequences were translated into their amino acid sequence with the help of EMBOSS Transeq [35]. Next, the amino acid sequences were aligned with NCBI Blast (blastp) [36].

3.3.2 Primer design

Primers for mutagenesis steps were designed by Laura van der Straat and Dorett Odoni. Further primers were designed based on the sequences of the fragments and recognition sites of restriction enzymes. Primer design was carried out with the help of the Sequence Editor [37]. The primers were ordered from Baseclear.

3.3.3 Molecular weight prediction

To analyse the SDS-PAGE gel, the molecular weight of the construct was predicted by translating its DNA sequence to its amino acid sequence using the EMBOSS Transeq tool [35] and entering the amino acid sequence in the ExPASy Mw/pI prediction tool [38].

3.4 PCR

3.4.1 PCR to add restriction sites to YFP

The restriction sites EcoRI and NotI were added to YFP with the help of Finnzymes Phusion High-Fidelity DNA Polymerase. The T_m temperature was calculated using the nearest-neighbour method of Breslauer et al. [39] and the calculator on the ThermoScientific website [40]. The lower T_m amounted to 81.4 °C. A medium temperature of 84.4°C was chosen for gradient PCR with eight different temperatures (see section 4.2.4).

By reducing stringency of PCR conditions, the PCR performance may be improved. The annealing temperature was lowered to span a range of 70.0 to 55.0°C. For determination of T_m in future PCRs by online programmes, the primers would be entered without restriction sites. Additionally, the extension time was increased to 30 seconds. The amount of template was increased from 3.2 to 10 ng/ μ L. The number of cycles was increased from 30 to 35 (see section 4.2.4).

3.4.2 ColonyPCR

Colony-PCR was performed using the ThermoScientific DreamTaq Polymerase. The PCR master mix was prepared on ice in a small excess to account for pipetting errors. The mix was divided in 25 μ L aliquots in ice-chilled PCR tubes. Transformants were hand-picked with sterile 1 μ L pipette tips, streaked on LB^{Amp} master plates and dipped in 25 μ L aliquots of the PCR master mix. Negative controls were always included. Positive controls were included if they existed. 1 μ L of positive control was pipetted to a 25 μ L aliquot of PCR mastermix. To check the results, 10 μ L of PCR product were loaded on an agarose gel in small slots.

3.4.3 Approaches to avoid ColonyPCR

Colony-PCR is a time-consuming technique to screen for transformants. For this reason, ways to avoid Colony-PCR were investigated.

GFP and CFP-Screening

GFP and CFP had to be inserted into pET52 in the correct orientation. The conventional approach would be based on two steps. First, Colony-PCR would have to be performed in order to identify transformants with the desired insert. Next, the positive transformants would need to be grown, miniprepmed and checked by restriction analysis to determine the orientation of the insert.

In the present thesis, another method to screen for positive GFP and CFP transformants was used. A Rosetta (DE3) strain was transformed with the construct. GFP transformants were induced with 0.02 mM IPTG and grown overnight. The plates were then photographed with the Syngene GeneSys G:Box Chemi-XT4 gel reader. Positive transformants showed a clear difference in brightness to the other colonies (see fig. 4.5 and 4.6). These transformants were picked, streaked on master plates and screened by Colony-PCR. With this approach, restriction analysis is not necessary because only the colonies with the insert in the right orientation will fluoresce.

Similarly, an alternative method to find positive CFP transformants was used. Colonies were streaked on master plates, grown in 1 mL LB^{Amp^{Chl}} in Eppendorf tubes, induced with 0.02 mM IPTG and scanned on a Molecular Devices SpectraMax M2 96 well-plate reader overnight. The excitation and emission wavelength were set to 430 and 475 nm respectively. Positive transformants showed a considerably higher emission over time. The presence of the insert was confirmed by Colony-PCR. As with the GFP screening method, the insert does not need to be checked for correct orientation by restriction digest. For protocols for both methods, see section 8.4.

Khanbrick: a proposed cloning tool

A second method of circumventing Colony-PCR was developed and started, but not pursued further because it was not of immediate use for building the FRET biosensor construct. A major problem regarding inserting a fragment at the NsiI restriction site is insertion of the fragment in the correct orientation. The present method is a potential way of eliminating the need to check for orientation of the insert.

Principle The construct was designed to be built in pET52, a plasmid with an Amp resistance gene that can be transformed into Rosetta for high protein production. The principle of the construct is shown in Fig. 3.1.

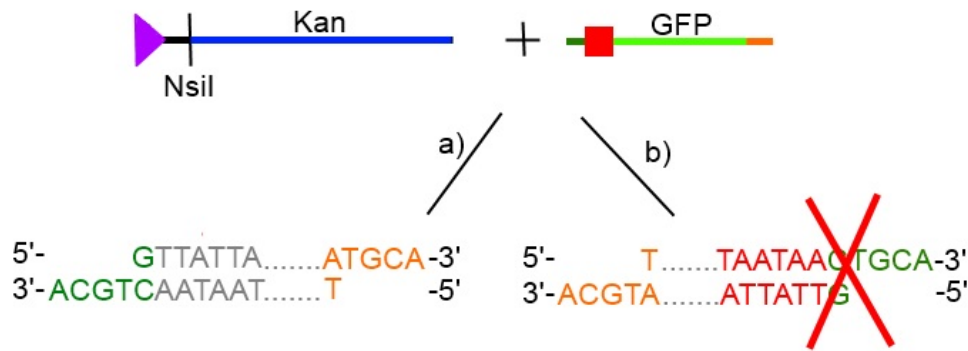


Figure 3.1: Principle of the Khanbrick cloning tool

The backbone features a promoter (purple) followed by a NsiI restriction site and a Kanamycin resistance gene (blue). The insert, in this case GFP noStop (lime green) flanked by PstI (dark green) and NsiI (orange), has a double antiparallel stop codon before the start of the actual GFP sequence (red). Two outcomes are possible:

a) If the insert goes in the backbone in the correct way, GFP and the Kanamycin resistance are expressed as a fusion protein. b) If the insert is in the wrong direction, the stop codon TAATAA prevents expression of the resistance gene.

Transformants are selected on LB^{Kan} plates. All transformants should have the insert in the correct orientation.

The Kan gene is flanked by a NotI restriction site on the 3' end. After successful insertion of the first fragment, the Kan gene may be cut out with NsiI and NotI and replaced by another NsiI/NotI fragment. Transformants could be selected on LB^{Amp}. This next building step should be less troublesome because the backbone and insert should only be able to reassemble in one way. The full project outline can be found in the appendix (Section 8.4).

3.5 Molecular cloning techniques

3.5.1 Overview

The following table gives an overview of the fragments and backbones used, their origin, building steps and the name of the resulting constructs (3.1) (bb... backbone, F... Fragments used for further constructs, f... failed, I... Insertion, M... Mutation, MS... mitochondrial signal). "Frog" is a GFP variant with the mutations F64L, S65T, Y66W and T203Y (see section 3.5.2).

Table 3.1: Building bricks for constructs

Template	Origin	Features	Insertions/Working steps	New constructs
pJET	Dorett Odoni	PstI-GFP-Nsil	M: F64L, GFP, CFP, YFP, No Stop, CFP Δ F64L; F: All colours	
pFB001	Baseclear	XhoI, EcoRI bb, NsiI-SpeI-Rcap C4-SpeI-EcoRI-NotI	I: pyrA (f); F: Rcap C4	pyrA-C4 "Leo"
pFB002	Mark van Veen	XhoI-pyrA-XhoI, Δ EcoRI bb, NsiI-SpeI-citA-SpeI-EcoRI-mCherry-NotI	I: GFP I: MS	GFP-citA-mCherry "Noël" MS-citA-mCherry "Liam"
pET52	Ruud Heshof	NsiI-Lox-NotI	I: CFP/GFP; C4-YFP (f)	GFP-Lox, CFP-Lox
pET52	Mark van Veen	GFP-citA-mCherry	I: Rcap C4	GFP-C4-mCherry "Freddie"
Freddie		GFP-C4-mCherry	I: YFP	GFP-C4-YFP "Montserratt"
Montserratt		GFP-C4-YFP	I: CFP (f), M: GFP to CFP, YFP to Frog, F: C4-YFP	CFP-C4-Frog "Michael"

3.5.2 Mutations to obtain desired fragments

Improved folding of GFP

GFP had previously been inserted into pJET with the restriction sites PstI and NsiI (see section 4.1.1) and was obtained from Dorett Odoni. GFP should be mutated to improve folding at 37°C with the primers **LS_GFP_F64L** and **LS_GFP_F64L_antisense**. 50 ng of GFP template were used. Two control reactions were performed to verify mutagenesis and transformation efficiency. Mutagenesis on the pWhitescript control plasmid enabled colonies to produce β -galactosidase. These colonies appeared blue on media containing IPTG and X-gal. If transformation of the pUC18 control plasmid was successful, these colonies exhibited the (β -gal⁺) phenotype as well. The control reactions were incubated for a total time of approximately 60 hours (see section 4.1.2).

GFP to CFP, YFP and GFP noStop

In the next round of mutations, three mutations were performed simultaneously:

- 1) GFP to CFP
- 2) GFP to YFP
- 3) GFP to GFP noStop (removal of stop codon at the end of GFP)

GFP was mutated to CFP by introducing the Y66W mutation with the primers **LS_GFP-Y66W** and **LS_GFP_Y66W_antisense**. Since the primer designs were based on the original GFP variant without improved folding, the F64L mutation was deleted. The change to YFP was obtained by introducing the T203Y mutation using the primers **LS_GFP_T203Y** and **LS_GFP_T203Y-antisense**. Finally, the stop codon at the end of GFP was removed with the primers **DO_pJetGFP-noStop_del78-80** and **DO_pJetGFP_noStop_del78-80_rev** (see section 4.1.2).

Prior to continuing working with YFP, the restriction sites EcoRI and NotI were added to YFP with the help of PCR using the primers **LS_EcoRI_YFP_F** and **LS_NotI_YFP_R**.

GFP to CFP and GFP noStop to CFP noStop

A further round of mutations was performed. GFP F64L should be mutated to CFP F64L without deleting the mutation that enhances the folding. Simultaneously, the same primers (**F64L_Y66W** and **F64L_Y66W_antisense**) were used to mutate GFP F64L noStop into CFP F64L noStop in order to be able to build the full sensor construct (see section 4.1.2).

GFP-C4-YFP to CFP-C4-Frog

Since C4-YFP could not be inserted in CFP-Lox (see section 3.5.3), another approach to build the second construct was tried. The construct Montserrat was used as a template. GFP F64L nS should be mutated to CFP F64L with the primers **F64L_Y66W** and **F64L_Y66W_antisense**. Due to the high similarity of the sequences, the Y66W mutation was not only introduced in GFP, but in YFP as well, creating a new GFP variant with the mutations F64L, S65T, Y66W and T203Y ("Frog") (see section 4.5.3).

3.5.3 Fragments and constructs

Rcap C4 binding domain and mitochondrial signal

The binding domain Rcap C4 in pFB001 and the mitochondrial signal in pUC57 had been ordered from Baseclear. pFB001 is a Funbrick with the standard Funbrick restriction sites (XhoI for pyrA insertion, NsiI, SpeI, EcoRI, NotI). DH5- α was transformed with the plasmids in order to grow a large quantity of plasmids via midiprep. Both plasmids were transformed with electrotransformation (see section 4.2.1).

Prior to continuing working with the Rcap C4 sensor and YFP, a check to see whether the restriction sites of YFP and the binding domain were functional was performed. Fig. 3.2 is a scheme of the various restriction sites.

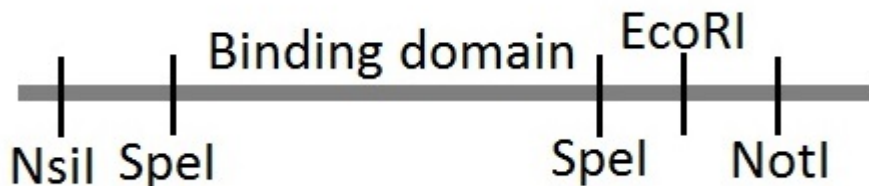


Figure 3.2: Schematic overview of binding domain restriction sites

The sensor was cut with SpeI, NsiI, NotI and EcoRI in various combinations (see section 4.2.2). The Rcap C4 fragment was cut out from the Funbrick in order to build the construct in pET52 in *E. coli*.

pyrA gene

The pyrA gene is used as a selection marker because it enables uridine biosynthesis in *A. niger*. An *A. niger* strain with a uridine auxotrophy is transformed with a vector containing the pyrA gene. Only positive transformants are able to synthesise uridine, which is essential for the fungus. This gene should later be inserted in the Funbrick pFB001. For this purpose, the plasmid pWA423 was obtained from Jasper Sloothak and the pyrA gene on pWA423 was midipreped. The mitochondrial signal and pyrA should be extracted from agarose gel. For a test run, the mitochondrial signal was diluted 1:8 and pyrA was diluted 1:6. The agarose content was changed to 2% for the mitochondrial signal (see section 4.2.3).

Insertion of GFP and CFP in pET52-Lox

The pET52 plasmid with the Lox insert was obtained from Ruud Heshof. GFP and CFP were inserted at the NsiI site. It was first attempted to transform the pET52 plasmid in DH5- α (see section 4.3.1).

The transformation to insert GFP and CFP in pET52 was repeated (see section 4.3). SOC was pre-heated to 37°C. The insert:vector ratio was increased from 10 to 50 minutes. The transformation was carried out in Rosetta. Prior to plating the transformants, IPTG was spread on

the plates to induce protein production. Ideally, both GFP and CFP should then be visible in the colonies with the insert in the right direction.

10 μL of transformants were spread on plates with varying concentrations of IPTG. To calculate the required amount of IPTG on the plates, it was assumed that each plate contained approximately 20 mL of agar. Before adding IPTG, 20 μL of a 1000x chloramphenicol stock solution was spread on all LB^{Amp} plates. Five concentrations of IPTG were tested (Table 3.2).

Table 3.2: IPTG concentrations

Concentration [mM]	10 mM IPTG stock [μL]
1	2000
0.5	1000
0.1	200
0.05	100
0.02	40

It was observed that a volume of 1 mL was too big for plating. The 1 mM and 0.5 mM IPTG plates did not dry. Therefore, cells were plated on the liquid, which might have inhibited their growth. The 1 mM and 0.5 mM IPTG plates were not turned upside down for incubating.

95 CFP transformants were grown in 1 mL LB^{AmpChl} cultures for one hour, induced and screened with the help of the Molecular Devices SpectraMax M2 reader overnight. The most promising transformants could be identified by plotting the emission over time and comparing the slopes to the negative control (LB medium). If the slope was 2.6 times higher than in the negative control, potential transformants were found. Colony-PCR of CFP was carried out in order to evaluate the optical screening method (see section 4.3). All transformants with promising slopes (especially Colony 3 and 23), one transformant with an average slope and one transformant with a poor slope were screened (Table 3.3). CFP noStop was used as a positive control. 1 μL of each colony was pipetted into 25 μL aliquots of the PCR mastermix.

Table 3.3: Colonies for CFP Colony-PCR

Slope	Colonies
Promising	1, 2, 3, 8, 23, 24, 32, 56, 64
Average	4
Poor	13, 42, 84

Insertion of Rcap C4 binding domain

Insertion of Rcap C4 in GFP-pET52 and CFP-pET52 It was attempted to build the construct with the help of triple-point ligation. The Rcap C4 fragment and the second fluorophore should be inserted at the same time. Since the three fragments possess complementary ends, the vector should only reassemble and be transformed if all three fragments are correct. Triple-point

ligation was performed analogously to normal ligation except for a higher molar vector to insert ratio (1:6). The ligation mix was simultaneously transformed into Rosetta and DH5- α (see section 4.4.1).

Since this approach did not work, the construct should be completed with two "traditional" ligations. First, the sensor should be inserted as a NsiI-NotI fragment. Second, the second fluorophore should be inserted as an EcoRI-NotI fragment. To this end, the sensor was cut with NotI and NsiI and extracted from gel (see section 4.4.1). The sensor was inserted in the GFP- and CFP-pET52 backbone, but the negative control was positive. Two explanations seemed most probable. Either cells could grow on the plate because the ampicillin had already degraded, or the electrocompetent cells had been contaminated with Amp-resistant colonies. To find out, an aliquot of electrocompetent cells was plated on a fresh LB^{Amp} agar plate from another source and on an agar plate of the same batch. The negative control and the transformants were induced with 0.05 mM IPTG to screen optically for GFP-containing transformants. The insertion of Rcap C4 in GFP-pET52 and CFP-pET52 was repeated (see section 4.4.1).

The ligation mix had been stored at -20°C. The transformation was repeated in parallel with Laura van der Straat to make sure that no mistakes had been made in the transformation procedure (see section 4.4.1).

The ligation should be repeated. In the next ligation, the incubation time would be increased from 10 minutes to one hour, and the T4 ligase would be heat-deactivated after incubation. The ligation mixes were prepared without addition of ligase, but stored at -20°C because a shorter way to build the construct was found.

Insertion of Rcap C4 in GFP-citA-mCherry The plasmid pET52 with the GFP-citA-mCherry construct was cut with NsiI and EcoRI. The Rcap C4 fragment was inserted (see section 4.4.2).

In a second attempt, some modifications were made. More DNA (both of insert and vector) were used. The amount of ligase used was increased to 1 μ L. The incubation time was changed to one hour and the ligase was heat-deactivated after ligation. Extra care was taken that the buffer was properly mixed before it was added to the ligation mix and that the ligation mix was well homogenised before adding the ligase. In addition, the danger of losing some of the ligation mix by purification was eliminated by transforming into chemically competent cells instead of electrocompetent cells (see section 8.4).

Insertion of YFP in GFP-C4-mCherry The second construct with the same core domain but different fluorophores should be built as well. To this end, mCherry of the first construct should be replaced by YFP. mCherry was cut out from Freddie and the backbone was extracted from gel. The fragments were ligated and transformed into chemically competent cells (see section 4.5). In addition to incubation overnight, transformants were incubated for 6.5 hours and screened with Colony-PCR. **C4_F** and **LS_NotI_YFP_R** were used as primers.

To improve gel extraction yields, it was attempted to cut closer to the DNA bands. The empty column was centrifuged for 5 min. Elution water was pre-heated to 55°C prior to elution. Between 30 and 20 μ L of water were used for elution.

Insertion of C4-YFP in CFP-Lox The C4-YFP fragment should be cut out and inserted into CFP-Lox. The extraction of C4-YFP had to be repeated due to low yields. It was attempted to optimise the gel extraction procedure further. Double combs were used in order to cut out less gel. Furthermore, the Squeeze'n'Freeze protocol for gel extraction was tested (see section 8.4). C4-YFP was inserted in pET52-CFP (see section 4.5.2).

The ligation to insert C4-YFP in pET52-CFP was repeated. Simultaneously, the first part of the construct in the Funbrick should be built. To this end, GFP nS for the cytosolic signal and the mitochondrial signal for the CFP-YFP mitochondrial signal should be inserted in FB002. The Funbrick was digested and dephosphorylated before ligation (see section 4.5.2).

3.5.4 Ligation

The amount of insert and vector required for the ligation mix was calculated according to the following example (Table 3.4).

Table 3.4: Calculation of ligation mix

Compound	Name	Size [bp]	Ratio	Amount 1:1 [ng]	Amount 1:3 [ng]
Vector	pJET	2782		100	100
Insert	EcoRI-YFP-NotI	3.9	25.9	77.6	

First, the sizes of the vector and insert in basepairs are determined. Next, their ratio is calculated. This method of calculating ratios is based on the assumption that AT/GC content of DNA fragments is approximately the same. Therefore, the molecular weight of the constitutional repeating unit of the vector and insert should be roughly the same. 100 ng of vector are used for ligations. This amount divided by the ratio gives the equimolar amount of insert. However, the insert to vector ratio should preferably be greater than one. By adding an excess of insert, reaction equilibrium should be shifted towards insert uptake. Therefore, the calculated amount is multiplied by a factor $1 \leq n \leq 5$. Molar ratios ranging between 1:1 to 5:1 insert:vector are commonly used.

If a vector is cut only once, the probability of re-ligation is pretty high. To lower this probability, the vector was dephosphorylated with the Fermentas FastAP Thermosensitive Alkaline Phosphatase.

All ligation mixtures for electrotransformations had to be purified from buffer salts with the help of the ThermoScientific GeneJET PCR Purification Kit. 2 μ L of ligation mix were used per 50 μ L aliquot of competent cells.

pJET

Cloning into pJET was performed using the ThermoScientific CloneJET PCR Cloning Kit. EcoRI-YFP-NotI was inserted using the Blunt-End Cloning Protocol.

T4 DNA Ligase

For all other ligations, the ThermoScientific T4 DNA Ligase was used, following the Sticky-end ligation protocol.

Ligation to clone YFP into pJET

YFP was cloned into pJET in order to confirm the functionality of the restriction sites by restriction digestion (see section 4.2.5).

Ligation to insert pyrA into the Funbrick

pyrA should be inserted in the Funbrick. The ligation mixes were prepared. Linearisation of the Funbrick was checked by digesting the Funbrick with XhoI and running the product on gel. 1 μ g of Funbrick was linearised and purified with the PCR purification kit (see section 4.2.6). Due to the low success rate, it was decided to screen a larger amount of transformants for the insert with the help of Colony-PCR. To this end, primers were designed to screen for the pyrA insert in the Funbrick. At the same time, primers to check for the mitochondrial signal, G/CFP and mCherry were designed. The primers are based on the sequences and their adjunct restriction sites. The C4core forward primer was designed by Dorett Odoni.

To prevent pipetting errors from happening in the future, all further ColonyPCRs were pipetted in a scheme like this: NC - PC - Ladder - 1 - 2 - 3 - 4 - 5 - Empty lane - 6 - 7 - 8 - 9 - 10 - Ladder etc. For further building of constructs, a different Funbrick (FB002) was used. This Funbrick had been built by Mark van Veen. In this vector, the pyrA gene had successfully been inserted and the EcoRI restriction site in the backbone had been deleted by mutagenesis. Moreover, the plasmid already contained the second fluorophore mCherry and was equipped with all required Funbrick-compatible restriction sites. This Funbrick was transformed in DH5- α to grow more plasmid.

3.5.5 Transformation

Electrotransformation

Electrotransformation was performed according to Prt. 09 - Electrotransformation of E.coli cells (see section 8.4). Cells were pulsed with the Bio-RAD Gene Pulser II and Pulse Controller Plus. A negative control was always included. For ligation mixtures, a positive control was included as well.

Heat-shock transformation

Heat-shock transformation was performed according to the Heat-shock transformation protocol (see section 8.4). Cells were heat-pulsed in a B. Braun 7P Thermomix MM water bath.

3.6 Preparation and quantification of sensor

Freddie was transformed into Rosetta and grown in 500 mL LB^{Amp^rChl}. To make sure that the transformants were positive, three transformants were first grown in 6 mL LB^{Amp^rChl} each and an aliquot of 1 mL per transformant was induced with 0.02 mM IPTG for one hour (Fig. 3.3).

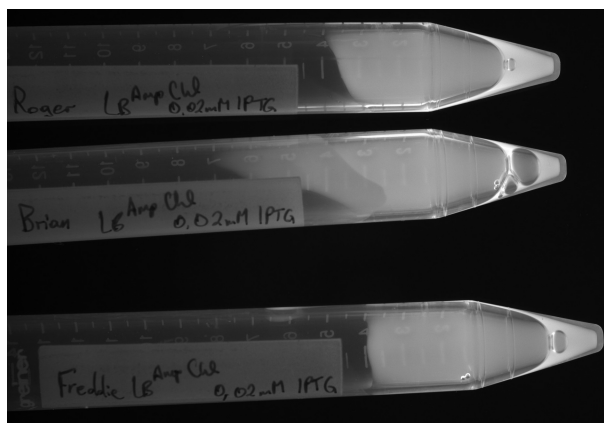


Figure 3.3: Screening for expression of FRET biosensor

All three transformants had taken up the plasmid. Freddie was chosen for inoculation of the big culture.

Cell pellets were washed with 50 mL of washing buffer. The resuspension was centrifuged at 4700 rpm for 5 min. The pellets were resuspended in 10 mL washing buffer and the cell-free extract was prepared with the help of the French Press. The lysing process was repeated once with the lysate. The cell-free extract was stored on ice and centrifuged at 4700 rpm for 10 min. The supernatant was transferred to a small Falcon tube. The resin of a StrepTactin column was poured into the tube to bind the protein overnight. The process was carried out at 4°C and supported by mild shaking at 20 rpm. The column without resin was washed with 1 CV (1 mL; equivalent to the volume of resin) and stored in wash buffer at 4°C overnight.

3.6.1 Cell lysis

Cells were lysed with the help of an American Instrument Co. French Pressure Cell Press. Cells were lysed at a pressure of 7000 to 10000 psi (480 to 690 bar). A medium cell was used for small volumes and a big cell for large volumes. For the big cell, the value at the handle was always set to 1000. All parts were cleaned with EtOH after use.

3.6.2 pH measurements

The pH of the induced and non-induced culture was measured with a pH-meter. The glass electrode was stored in a 3M KCl solution and thoroughly rinsed with deionised water before and after use. Before use, the accuracy of the pH-meter was checked by measuring calibration solutions.

3.6.3 Strep-tag protein purification

Purification of the FRET biosensor was carried out according to the IBA Strep-tag Purification protocol. The FRET biosensor was expressed with a Strep-tag and could be purified with the help of Strep-tactin affinity chromatography.

For analysis and in vitro characterisation, the biosensor was purified and the FRET activity of the purified protein was measured. For this purpose, Freddie (GFP noStop-Rcap C4-mCherry) was grown. The culture should be grown until the OD was 0.6, but was accidentally grown until the OD was 1.27 and induced for three hours. It was divided in big 50 mL Falcons and centrifuged at 4000 rpm for 5 min. The supernatant was discarded and the pellets were stored at -20°C over the weekend (see section 4.6.2).

The supernatant was centrifuged at 4700 rpm for 5 min. The resin was resuspended with some washing buffer and poured in the column. The tube was rinsed with 1 mL washing buffer (fraction Wash 1). The column was washed until the eluate was no longer pink. Next, the protein was eluted with elution buffer. The resin had a strong pink colour. Eluted fractions were collected until the resin was no longer pink. The column was washed with 3 CV of regeneration buffer and stored in the regeneration buffer at 4°C. All fractions were stored at 4°C.

3.6.4 SDS-PAGE

SDS-PAGE was carried out using pre-cast ThermoScientific 12% Precise Protein gels and HEPES running buffer. Samples were prepared by adding 10 μ L of loading dye containing SDS and 2-mercaptoethanol to 30 μ L of sample. The mixture was heated to 98°C for 5 minutes on a heatblock under a fumecage.

20 μ L of the mixture were loaded on gel. The PrecisionPlus Protein Standards Unstained Ladder was used as ladder. Gels were run with the BioRAD PowerPac Basic at 80V for 70 min.

The gels were taken out of the chamber, put in a box with some demi-water and microwaved for 30 s at 750W. This step was repeated twice. Gels were stained with a Coomassie Brilliant Blue staining solution (0.025% Coomassie Brilliant Blue in 40% MeOH, 10% Ice acetic acid, 50% demi H₂O) and destained with a destaining solution (250 mL ice acetic acid, 625 mL MeOH, 1625 mL demi H₂O).

3.6.5 BCA Assay

The bicinchoninic acid assay is a method of protein quantification. Peptide bonds in proteins reduce Cu²⁺ to Cu⁺. Each Cu⁺ ion then forms a chelate complex with two molecules of bicinchoninic acid. Samples are measured at a wavelength of 562 nm.

The measurements were carried out with the ThermoScientific Pierce BCA Protein Assay. A standard curve was recorded with bovine serum albumine. Ideally, the protein used for the standard curve should be identical to the analyte. If that is not possible, it is preferable to have a protein with properties and structure of great similarity. BSA is globular whereas GFP and its variants possess a beta barrel structure. A standard curve was recorded using the following bovine serum albumine concentrations:

Table 3.5: BSA Standards

Sample	Concentration [$\mu\text{g/mL}$]
A	2000
B	1500
C	1000
D	750
E	500
F	250
G	125
H	25
I	0

The assay was first used with already prepared BSA dilutions. However, since the calibration curve was unsatisfactory (rather high deviations compared to sample measurements), the assay was repeated with freshly prepared standards. The new standards were prepared using Buffer E from the Strep-tactin protocol as eluent to minimise matrix effects.

Since the assay was measured on a Nanodrop Spectrophotometer, a very small amount of sample was needed. For this reason, the assay was downscaled. 5 μL of sample were mixed with 100 μL of working reagent. Despite the downscaling, reproducible results could be obtained.

Protein content was measured with the help of the BCA Assay (see section 4.6.2). For the standard curve, the highest concentrated standard was not used (Fig. 3.4).

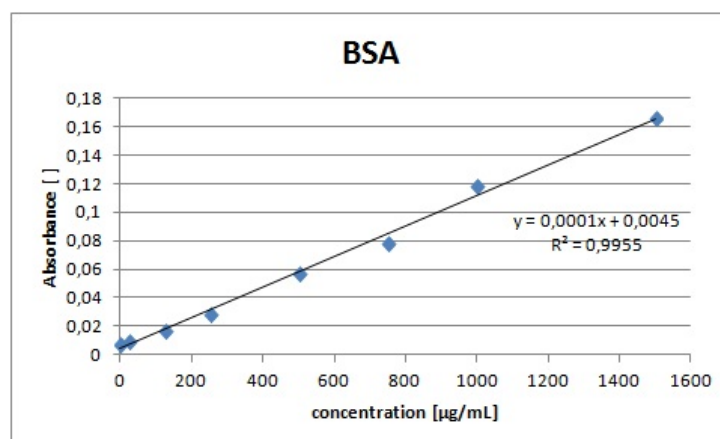


Figure 3.4: BCA Assay Calibration Curve

3.7 Testing of sensor

3.7.1 96 well-plate reader

Fluorescence measurements were carried out on the Molecular Devices SpectraMax M2 96 well-plate reader using a black 96 well-plate. The data was analysed with the help of the software DataLab.

The FRET properties of the GFP-Rcap C4-mCherry sensor were measured. For first measurements, Freddie was grown in 5 mL LB^{Amp}, induced with 0.02 mM IPTG for three hours, and the cell-free extract was prepared. The cell-free extract was measured in a black well-plate in the 96 well-plate reader. For a first test, the following dilution series of fumarate and succinate were prepared:

Table 3.6: Fumarate and succinate dilutions for sensor testing

Substance	Dilutions [M]									
Fumarate	$5 \cdot 10^{-10}$	$5 \cdot 10^{-9}$	$5 \cdot 10^{-8}$	$5 \cdot 10^{-7}$	$5 \cdot 10^{-6}$	$5 \cdot 10^{-5}$	$5 \cdot 10^{-4}$	$5 \cdot 10^{-3}$		
Succinate	$5 \cdot 10^{-10}$	$5 \cdot 10^{-9}$	$5 \cdot 10^{-8}$	$5 \cdot 10^{-7}$	$5 \cdot 10^{-6}$	$5 \cdot 10^{-5}$	$5 \cdot 10^{-4}$	$5 \cdot 10^{-3}$	$5 \cdot 10^{-2}$	

49 μ L of cell-free extract were aliquoted into the wells. To each aliquot, 1 μ L of substrate was added. Each concentration was measured in duplicates in the well-plate reader. The fumarate and succinate solutions were not prepared in duplicates.

In a GFP-mCherry sensor, the quantum yield is a lot lower for mCherry than for GFP, so the tiny peak will likely be overshadowed by GFP. Therefore, instead of measuring FRET ratios, the sensor can also be tested by measuring the emission of GFP and comparing the intensity of GFP emission for different substrate concentrations. According to [1], the FRET ratio (emission of acceptor divided by emission of donor) should decrease with addition of substrate. This means that the FRET pair should be together at low concentrations and move apart upon substrate addition, i. e. the emission of GFP should increase with substrate addition.

The sensor was excited at different wavelengths from 300 to 485 nm in intervals of 5 nm. Emission was measured at 510 nm (see section 4.6.1).

The values for the different fumarate and succinate concentrations were plotted for different wavelengths. Linear regression was performed and the slopes of the regression lines were compared. The highest slopes were found around 355 nm, which supports the finding that the present GFP mutation has its highest excitation peak at that wavelength. The relationship between substrate and GFP emission was investigated at the excitation wavelength with the highest slopes (355 nm for fumarate and 360 nm for succinate). Emission was plotted against molarity of the substrate, and linear regression was performed.

Prerequisites for linear regression are:

- 1) x and y values should be normally distributed.
- 2) Linearity of the relationship.
- 3) Homoscedascity. This means that variance should not increase with increasing values.
- 4) Independence of values.

1) was checked by making histograms. 2) and 3) were checked on a scatter plot. A popular test to check for 4) (correlation of residues) is the Durbin-Watson coefficient (see section 4.6.1).

Linear regression for succinate and fumarate was performed. It was tested whether the correlation coefficient is significantly different from zero. The null hypothesis H_0 is that the correlation coefficient is equivalent to zero. Tests for equality are always two-sided. Here, a two-sided t-test was performed (Table 4.1). A significance level of $\alpha=0.05$ was chosen for the test. If the t-statistic is bigger than the critical value of $t_{\alpha/2}$, H_0 has to be rejected, i. e., the regression coefficient is significantly different from zero (see section 4.6.1).

3.7.2 Varian Cary Eclipse Fluorescence Spectrophotometer

Further fluorescence measurements were performed with a Varian Cary Eclipse Fluorescence Spectrophotometer using the Scan option.

The purified protein was measured on the Varian Cary Fluorimeter. The purified sensor and the cell-free extract were excited at 480 nm (GFP) and at 587 nm (mCherry) since the new excitation maximum as shown before had not yet been discovered. Therefore, the measurement conditions might not be ideal. The emission was scanned from 490 to 600 nm (see section 4.6.2).

Since both GFP and mCherry were present in the cell-free extract, it was attempted to measure FRET behaviour by subsequently adding various amounts of substrate to the cell-free extract as follows (Table 3.7). To even out dilution effects, the same volume of demi-water was added to an analogously prepared cuvette. The sensor was excited at 480 nm and emission was measured from 490 to 750 nm (see section 4.6.2).

Table 3.7: Measurement of fluorescence

Sample	Added substrate ($5 \cdot 10^{-2}$ M succinate)
Initial sample (1000 μ L extract)	Amount[μ L]
2	10
3	100
4	200
5	250

4 Results and Discussion

4.1 Mutations

4.1.1 Analysis of GFP insert

A restriction digest was performed to determine the orientation of GFP in pJET. Since the first experiment was not conclusive enough because DNA concentration was too low, the restriction digest was repeated (Figure 8.1).

As can be seen from lane 1, PstI cuts the backbone twice. However, since the plasmid was only used to isolate PstI-GFP-NsiI from gel and there was sufficient space between the GFP band at approx. 700 bp and the other bands, this did not pose a problem. The finding that PstI cuts the backbone twice is confirmed by lane 3. The faint band at 5500 bp in lane 4 and 5 is assumed to be an artefact. The lane with PstI and BseRI shows the same pattern as the PstI lane. This is plausible because the restriction site for BseRI is only 40 bp away from the site for PstI. Cutting the insert with XhoI and NsiI produces a single band at around 3600 bp. Therefore, it can be concluded that the restriction site for NsiI is located close to XhoI (the short fragment between XhoI and NsiI cannot be seen). Cutting with XbaI and NsiI results in three bands of approx. 3600, 3000 and 800 bp: the backbone of 3000 bp and the approximate size of the insert of 800 bp. It is assumed that the band at 3600 bp shows the linearised plasmid cut only once. This also indicates that NsiI is located at position 1 in 4.1.

In order to find out the orientation of the GFP insert, the plasmid was also cut with XhoI/NsiI and XbaI/NsiI. Fig. 4.1 shows a sketch of the multiple cloning site.



Figure 4.1: Multiple cloning site region

Consequently, if NsiI is located at the N-terminal region of the multiple cloning site, it follows that PstI is at the C-terminal region (position 2 in 4.1). Since GFP was inserted as PstI-GFP-NsiI, it can therefore be concluded that GFP was inserted in the inverted orientation.

4.1.2 Improved folding of GFP

Figure 4.2 shows the mutagenesis (left) and transformation controls (right).

The control mutagenesis was successful. However, not all colonies had the blue phenotype.

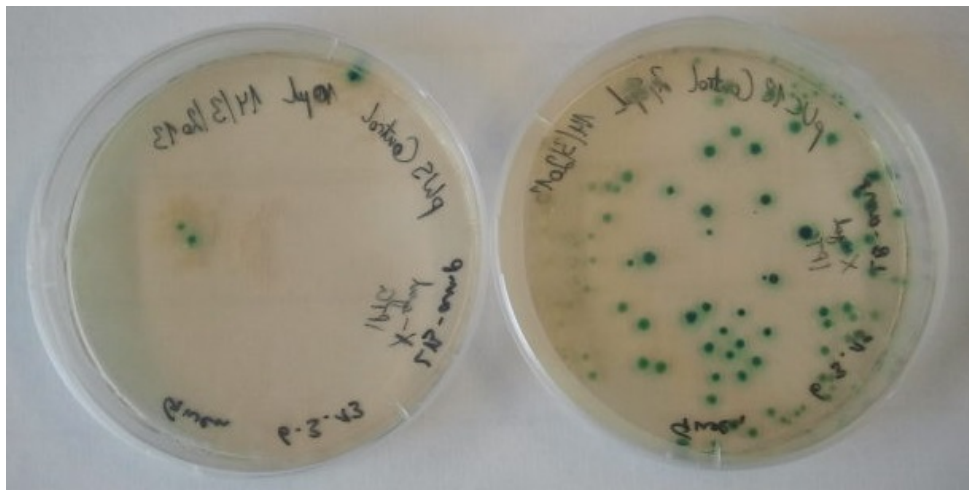


Figure 4.2: Mutagenesis and transformation control

This may be explained by the fact that the PCR conditions were not optimised for the control plasmid since the elongation time was adjusted to the size of the GFP-pJET plasmid. Transformation was successful as well. The colour gradient in the colonies is most likely caused by a concentration gradient in X-gal and/or IPTG. It can be assumed that transformation was successful in nearly all colonies.

Since the control reactions worked well, they were not repeated in further experiments.

Four colonies (I, III, V and VI) were sent to sequencing and analysed. All colonies contain the desired mutation. Fig. 4.3 shows a screenshot of the alignment tool.

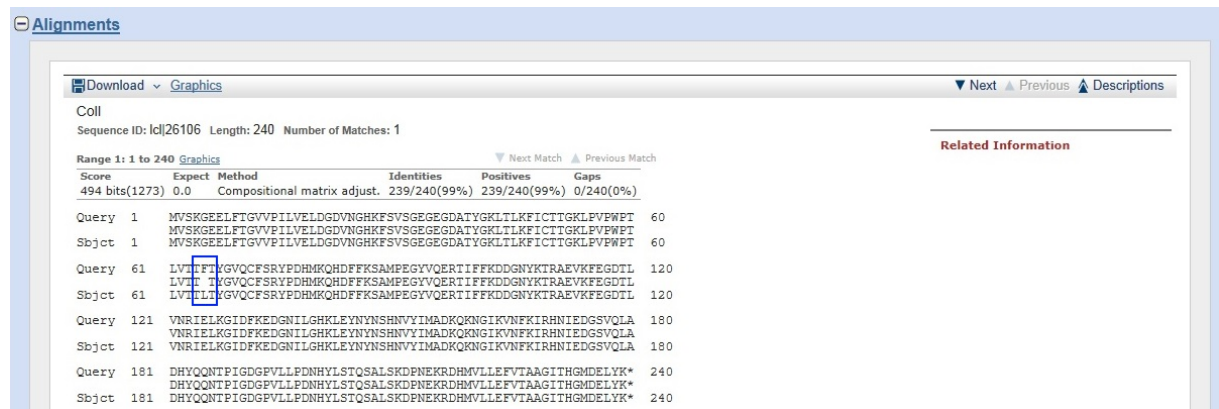


Figure 4.3: Alignment of sequences. The F64L mutation was manually highlighted.

GFP to CFP, YFP and GFP noStop

From each mutagenesis, four transformants were grown, miniprepped and sent to sequencing (Col. 1A, 1B, 1C, 1D; Col. 2A, 2B, 2C, 2D; Col. 3A, 3B, 3C, 3D). All colonies except 2D contained the desired mutations.

The primers to mutate GFP into CFP had been designed based on the original GFP sequence. The mutation F64L for enhanced folding had not been taken into account. Therefore, the plasmid was mutated to CFP, but the amino acid 65 was mutated back to F. While this was not

desired, the present mutation may be used for comparison with CFP F64L to assess the effect of the F64L mutation on better folding.

GFP to CFP and GFP noStop to CFP noStop

Four colonies per mutation were grown, minipreped and sent to sequencing. All colonies of CFP F64L contain the desired mutation. Colony V and VII of CFP F64L noStop contain the desired mutation. The sequences from colonies VI and VIII show different results. There appears to be a random insertion of nucleotides between NT 210 and 250. The sequences were aligned with ClustalX 2.1 (Figure 4.4).

Colony V shows the desired sequence. Both Colony VI and VIII appear to have a random in-



Figure 4.4: Alignment of CFP noStop colonies. Here, GFP and three colonies are aligned.

sertion. The insertions are almost exactly the same. The reason for these insertions is unknown. There could have been an error in the sequencing process. It could also be that these insertions can randomly appear. If this can happen in the sequence of the insert, it is possible that it happens in the plasmid backbone as well. This would pose undesired difficulties in working with mutagenesis.

Colony V was midipreped for further working steps.

4.2 Insertion of *pyrA* and YFP

4.2.1 Transformation of DH5 – α with Rcap C4 binding domain and mitochondrial signal

The transformations were successful.

4.2.2 Restriction site check of YFP and Rcap C4 binding domain

Fig. 8.2 shows the resulting agarose gel. Lane 1 shows that the restriction sites in YFP are functional. All binding domain restriction digests should yield fragments of approximately the same size. The gel confirms that all restriction sites work. However, there is an additional fragment of approx. 1400 bp in the last lane. This means that EcoRI cuts the plasmid twice. Since there is only one EcoRI restriction site in the binding domain region, this signifies that EcoRI cuts the Funbrick backbone.

The fact that EcoRI cuts the Funbrick backbone is disadvantageous because it makes the Funbrick system less interchangeable. If the plasmid was cut apart every time an EcoRI-NotI (fluorophore II) fragment is supposed to be exchanged, that exchange step would be unsuccessful. For this reason, it was decided to mutate the backbone in order to delete the EcoRI restriction site.

4.2.3 Extraction of mitochondrial signal and *pyrA* from gel

Both fragments were successfully extracted from gel.

4.2.4 Addition of restriction sites to YFP by PCR

No bands were visible except for very faint bands of primer dimers. Therefore, the PCR was repeated with some altered parameters.

YFP was amplified very well with every annealing temperature. The fragment was extracted from gel.

4.2.5 Cloning of YFP into pJET

A YFP-pJET colony was grown, minipreped and checked by restriction digest. Fig. 8.3 depicts the result of the restriction digest of Colony κ . As becomes apparent from this gel, both restriction sites are functional. The insert YFP cut out by EcoRI and NotI can be seen around 700 bp. In the neighbouring lanes, the linearised plasmid can be seen and compared to the uncut plasmid in the last lane. To ensure that no mutations had been introduced to Colony κ during PhusionPCR, the colony was sent to sequencing. The sequence of the insert was correct. Therefore, the colony could be used for further work. Colony κ was midipreped.

4.2.6 Insertion of *pyrA* in Funbrick

A *pyrA* transformant was grown, minipreped and checked by restriction digest. However, no *pyrA* band could be seen. In order to find a positive transformant, twelve transformants were grown, minipreped and checked by restriction digest. Again, no *pyrA* band could be seen. This could be due to various reasons. The Funbrick had been cut only once at the NsiI restriction site. Therefore, the vector could easily re-ligate. As there is no selection advantage in taking up the *pyrA* insert, the majority of the screened transformants probably took up the re-ligated Funbrick without the *pyrA* insert. However, it could also be that the XhoI restriction enzyme was not working properly. An agarose gel with the pWA 423 *pyrA*-containing plasmid, Colony α from the transformants, the Funbrick without any insert and the uncut Colony α was run to rule out this possibility. All samples except the uncut Colony α were cut with XhoI.

The digest of the pWA 423 plasmid proves that the XhoI restriction enzyme is working properly. A band at around 2500 bp can be attributed to the *pyrA* fragment (2351 bp). Colony α and the Funbrick without *pyrA* are linearised and their backbones display the same sizes. No bands at around 2500 bp are visible. From this gel, it can be concluded that these transformants had not taken up the *pyrA* fragment. Vectors with compatible ends are normally dephosphorylated to prevent re-ligation. In the present ligation, this step had not been carried out, which could explain the low rate of transformants with the desired insert.

69 transformants were screened with the help of Colony-PCR. Six positive transformants were found. Four of the positive transformants were grown and minipreped. Colony 59 is interesting because there seem to be multiple bands. Colony 68 (Leo) was used for further work because it showed the brightest band. Colonies 50, 53 and 57 (Laura, Dorett, Tom) were grown as backups.

For reasons discussed previously, the EcoRI restriction site in Leo should be eliminated by mutagenesis. This step was performed by Wen Ying Wu. Seven transformants were grown and checked for elimination of the EcoRI restriction site in the backbone by restriction digest. From this digest, it can be concluded that mutagenesis was successful in all seven transformants since only the linearised plasmid can be seen.

To make sure that all restriction sites are functional, a more detailed restriction digest of mutated Leo Colony α was performed. From this gel, it can be concluded that *pyrA* is not present.

To rule out the possibility that the insert was eliminated by mutagenesis, a restriction digest of Leo, Laura, Dorett and Tom without the mutation was made. All samples were cut with XhoI. The gel shows that none of the transformants have the insert.

If only one transformant did not have the insert despite a positive PCR result, this could be due to a positive and a negative colony growing very closely together. One colony would be amplified in PCR, but overgrown by the negative colony in the liquid culture. However, it is rather unlikely that this happened to all four transformants. The most probable explanation for this occurrence is that an error in pipetting was made and thus the wrong transformants were grown.

4.3 Insertion of first fluorophore

All the colour fragments - YFP, CFP, GFP and mCherry - as well as the Rcap C4 binding domain were cut out from the plasmids, run on gels and extracted.

4.3.1 Insertion of CFP and GFP in pET52

Transformants were small after incubation overnight and were incubated for another 60 hours. 40 transformants per colour were screened for the insert with the help of Colony-PCR. The positive and negative control were successful. There were no amplicons from GFP, but two positive CFP transformants. It is assumed that the reason for this low success rate is that the competent cells were incubated with the ligation mix on ice too long.

Colony 32 and 38 showed a band around 700 bp. These two colonies were minipreped and analysed with a restriction digest to check whether the insert has the right orientation. GFP noStop in pJET was digested with PstI and NsiI and used as a positive control. CFP Colony 32 and 38 were cut with NotI and NsiI. If CFP is inserted in the correct orientation, a digest with NsiI and NotI should cut out the *Lox* gene (1815 bp). However, both colonies showed bands

at approximately 2600 bp. If CFP is inserted in the wrong orientation, CFP-Lox (2544 bp) is cut from the plasmid. It can be concluded that the insert was in the wrong direction in both colonies. For this reason, the transformation was repeated with some modifications (see section 3.5.3).

Colonies grew best on the 0.05 and 0.02 mM IPTG plates. The colonies did not show any colours. It was attempted to visualise a colony by streaking on the masterplate and on an object slide and looking at the colony under an Olympus BX41 fluorescence microscope. Nothing could be seen under the fluorescence microscope.

Since the Syngene GeneSys G:Box Chemi-XT4 gel reader has an option to excite eGFP, pictures of the GFP-Lox transformants were taken on the GelReader (Fig. 4.5 and 4.6). The fluorescent colonies were circled in red for easier visibility.

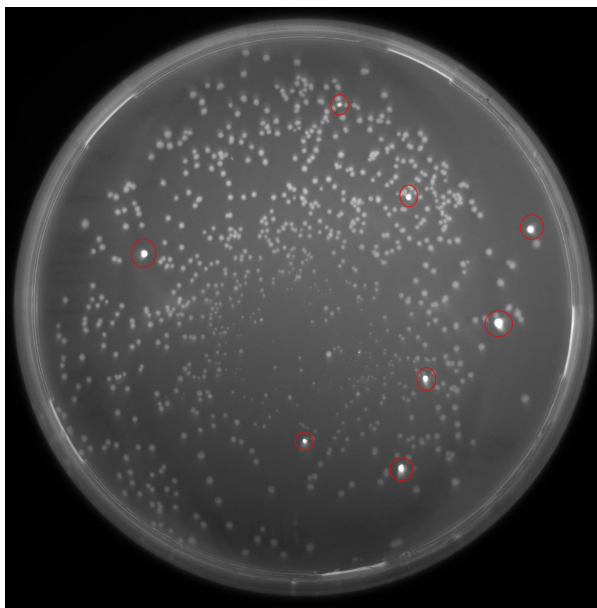


Figure 4.5: GFP 0.02 mM IPTG

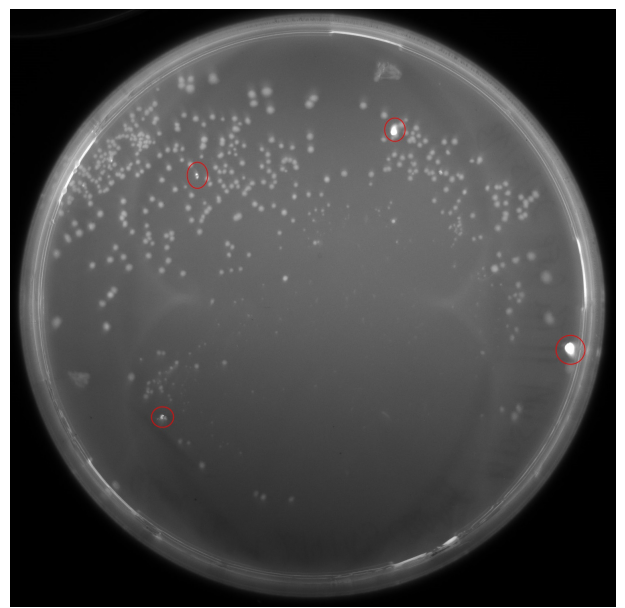


Figure 4.6: GFP 0.05 mM IPTG

By taking pictures of the plates in different angles and with a negative control (normal colonies), it was ensured that the brightness of the transformants was not caused by optical effects (not shown). Positive transformants were identified with the help of Fig. 4.5 and 4.6 and marked on the plates. Colony-PCR to screen for GFP was performed for 13 transformants to confirm the image. Of the 15 transformants screened, 13 were positive. The brightest transformants (1, 5, 10 and 12) were grown and used for further work.

It was confirmed by gel that colonies 3 and 23 have the CFP insert. These transformants have a slope 2.8 times higher than the negative control in the 96 well-plate reader screening. Therefore, it can be assumed that if transformants have a slope 2.8 times higher than the negative control, these transformants have the CFP insert.

CFP Colonies 3, 23, 8 and 56 were checked by a restriction digest with NotI and NsiI (Fig. 8.4). In this gel, there was a smear in all lanes. This indicated that there was some DNA degradation. Colony 23 was particularly badly affected - instead of any bands, there was just a

big smear. Since Colony 3 appeared to be OK, it was decided to continue working with Colony 3 only. In the lane with the uncut Colony 3, four bands were visible. This could be explained by the fact that plasmid DNA can exist in many different forms, e. g. circular and supercoiled. An additional problem concerning fragment isolation from gel is the fact that the Rosetta strain used also possesses a pRARE plasmid for enhanced protein production. Bands from this plasmid might overlap or interfere with bands from the pET52 plasmid.

One possible cause for DNA degradation is overly long incubation. Samples had been incubated with NotI for 30 minutes. Restriction digests with a NotI incubation time of 10 and 15 minutes (and NsiI of 5 minutes) were tested to see if there was less DNA degradation (Fig. 8.5).

It can be stated that DNA degradation is worse in the GFP-Lox plasmids than in the CFP-Lox plasmids. All colonies show the Lox gene at around 1800 bp. The bands at approximately 5000 bp show the pRARE plasmid (4694 bp). This plasmid can be seen as the lower plasmid in the uncut CFP colony, whereas the upper plasmid is the pET52 CFP-Lox construct. The band above the pRARE band in CFP Col. 3 is the pET52 plasmid with CFP (5897 bp). The same fragment size can be seen in GFP Col. 10 after 10 minutes - this is the GFP-pET52 backbone. A fragment at around 5000 bp very close to the pRARE band can be seen in CFP Col. 8: the pET52 backbone without the CFP insert. The size difference between the backbone with and without the insert is clearly visible. The gel shows that an incubation time of 15 minutes is OK for CFP-Lox and that GFP-Lox should not be incubated longer than 10 minutes.

GFP-Lox and CFP-Lox in Rosetta were grown in LB^{Amp} to make the colonies lose the pRARE plasmid with the chloramphenicol resistance and miniprep. An agarose gel showed that the colonies had lost the pRARE plasmid. These Amp-grown colonies were miniprep, digested and extracted from gel. The incubation time for NotI was shortened to 10 minutes.

4.4 Construction of the first FRET biosensor

4.4.1 Insertion of Rcap C4 in GFP-pET52 and CFP-pET52

Some transformants could be grown. These transformants were screened with Colony-PCR using the **GCFP_F** forward primer and **mCherry_R/LS_NotI_YFP_R** reverse primers.

Since C/GFP and Cherry/YFP are rather similar to each other, the reverse primers of the second fluorophore can also anneal to the first fluorophore. Many fragments of approx. 700 bp could be amplified. However, no positive band of the size of the whole construct could be seen. This could mean that none of the transformants have the construct. Another possible explanation is that only the small fragments were amplified or that perhaps amplification of the entire construct was inhibited for some reason. Therefore, all of the transformants which had positive bands of the size of a fluorophore (around 700 bp) were screened with different primers. This time, the **C4_F** primer was used instead of the **GCFP_F** primer while the reverse primer remained the same. Again, nothing could be amplified except for the positive control. pET52-Lox, GFP-Lox, CFP-Lox, CFP Colonies 49, 91 and 62 and GFP Colonies 20, 33 and 34 were

grown overnight to perform a third check by restriction digest analysis. However, the results were inconclusive. For this reason, the whole restriction digest was repeated by cutting all transformants with a) NsiI/NotI, b) NotI and c) NsiI (Fig. 8.6).

M. stands for Mark, the Funbrick FB002. The Mark lanes demonstrate that all restriction sites are working: Cutting Mark with NotI and NsiI results in the bright backbone band and a fragment of the sensor and mCherry, and cutting with either NsiI or NotI linearises the vector. All the other lanes show strange results because every sample has the same pattern regardless of which enzymes it was digested with. No conclusions could be drawn from this gel. Since Colony-PCR results were negative as well, it can be assumed that the triple point ligation did not work.

The sensor was inserted in the GFP- and CFP-pET52 backbone. In this transformation, the negative control was positive. It was discovered that some of the cells on the negative control plate were fluorescing. This means that the electrocompetent cells were contaminated, probably with GFP-Lox in pET52 *E. coli* cells. All aliquots of electrocompetent cells were discarded and fresh electrocompetent cells were prepared.

The transformation was successful. However, the transformants were rather small and incubated for a longer time. The colonies could not be picked for Colony-PCR, so it was attempted to streak them on a new plate to get single colonies. The colonies on the new plate did not grow well.

In a second attempt to transform the cells with the same ligation mix, no transformants grew.

4.4.2 Insertion of Rcap C4 in GFP-citA-mCherry

No transformants grew. The positive control was positive. Therefore, it can be assumed that the ligation did not work.

The second time, approximately 24 transformants had grown. They were screened with Colony-PCR. In total, 19 out of 24 transformants had the Rcap C4 insert. The FRET biosensor in pET52 ("Freddie") had successfully been constructed. Four transformants (Col. 6-9 - Freddie, Brian, Roger and John) were grown, miniprepmed and analysed by restriction digest. All colonies were cut with EcoRI and NsiI. Although the bands are rather faint, a band at around 1000 bp is visible in every lane, confirming the insertion of the binding domain (959 bp).

4.5 Construction of the second FRET biosensor

4.5.1 Insertion of YFP in GFP-Rcap C4-mCherry

Transformants were rather small. Only 5 transformants were visible. No amplicons could be seen on gel. Therefore, it was decided to repeat the transformation. Perhaps the transformation

did not work because DNA concentrations of the gel extracts were too low. As a safety precaution, all fragments were freshly isolated from gel for the repetition of the transformation.

Isolation of the required fragments from gel resulted in very low yields of approximately 10 ng/ μ L. This concentration is so low that ligations are less likely to succeed. For this reason, some modifications to the protocol were made (see section 3.5.3). With these measures, yields could be improved to around 15 ng/ μ L.

The transformation of YFP into pET52-GFP-Rcap C4 was repeated with the newly excised gel fragments in the same manner. The transformation was successful. 19 transformants were screened with Colony-PCR. Many transformants have the insert. Colony 14, 5 and 3 (Montserrat, Barnabé and Martí) were grown and used for further work.

4.5.2 Insertion of C4-YFP in CFP-Lox

No transformants grew. The positive and negative control worked. This means that the ligation did not work.

The repeated transformation to insert C4-YFP in pET52-CFP did not work. The transformations to insert GFP nS and the mitochondrial signal in the Funbrick seemed to have worked. Some transformants had grown in both experiments. The colonies were stored at 4°C. Due to time limitations, the transformants have yet to be screened for the insert by Colony-PCR.

4.5.3 Mutation of GFP-C4-YFP to CFP-C4-YFP

The first sequencing results did not cover the first fluorophore. Therefore, the sequences were re-sent to sequencing, using another primer. The translated nucleotide sequences were aligned with the translated nucleotide sequence of the entire construct. The first sequences covered the binding domain. The second time, YFP was sequenced. Therefore, no conclusions concerning the presence of the Y66W mutation in the first fluorophore can be drawn. An aspect that was not considered prior to performing the experiment was that YFP possesses a 100% identical "homolog" to the region of the GFP sequence in which the mutation to CFP should be introduced. Since the nucleotide sequence of YFP in the annealing region of the mutation-introducing primer is exactly the same as in GFP, the mutation Y66W was introduced to YFP as well. This mutation is present in Michael, Jermaine, Paris and Janet, although Janet has a spontaneous insertion of unknown origin shortly after the Y66W mutation. As this was the second time that this phenomenon occurred, these spontaneous DNA insertions seem to pose a critical problem for mutagenesis.

It is unknown how the Y66W mutation affects the YFP fluorophore. However, since this mutation was used to change GFP to CFP, it can be speculated that YFP will change its colour. A new GFP derivative with the mutations F64L, S65T, Y66W and T203Y (Frog) was created. Although the combination CFP-Frog might not work as a FRET pair, perhaps Frog turns out to be useful as a new acceptor molecule.

4.6 Characterisation of the FRET biosensor

4.6.1 Sensor measurement in the cell-free extract

Determination of GFP F64L S65T properties

First, the excitation maximum of GFP was determined (Fig. 4.7).

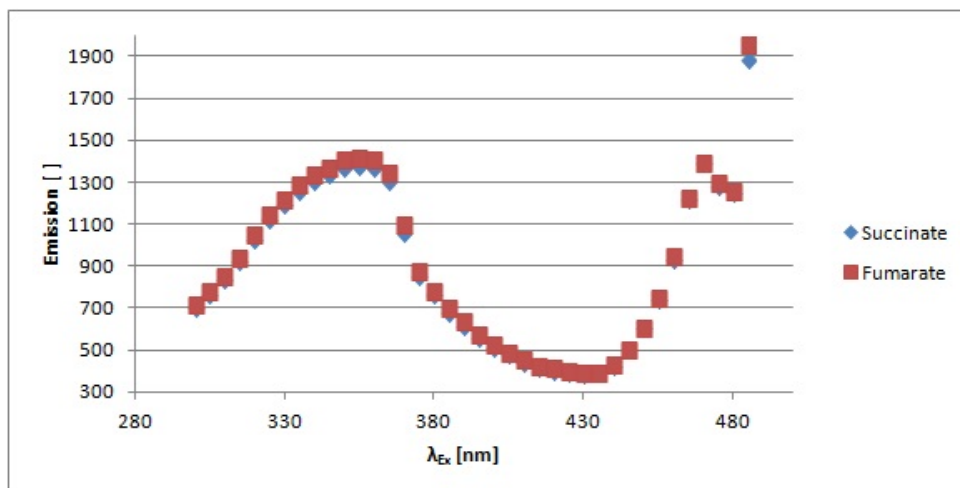


Figure 4.7: Determination of excitation. The emission of the fumarate and succinate blanks (induced cultures without any substrate) was plotted against the excitation wavelengths.

The data at longer wavelengths from 465 nm on may not be regarded as reliable because the 96 well-plate reader has a strong measurement bias at the end of a spectral scan. In the negative control, a sudden increase in emission is seen at 465 nm.

In the present experiment, GFP has an excitation maximum around 355 nm. This is an interesting discovery because GFP with the S65T mutation that was used as the template for improving the GFP folding (F64L) has an excitation peak at 488 nm. However, there is also a GFP variant with a mutation in the same region (Y66F) which shifts the excitation peak to 360 nm whereas the emission peak stays at 510 nm [28]. Fig. 4.8 shows the secondary structures of the three GFP variants.

Structure-wise, all three variants are very similar to each other. The amino acid at position 66 remains aromatic for all three variants. F at position 64 is replaced by L in the GFP F64L variant. Phenylalanine is rather apolar and hydrophobic, as is leucine. It is easy to imagine that this substitution improves folding at higher temperatures due to decreased steric hindrance. Both serine and threonine are polar and possess an OH group - again, the substituent shows strong similarity. The theoretical pI of all three combinations (F-T-Y, L-T-Y and F-S-F) is 5.52 (computed with the ExPASy Compute pI/Mw tool [38]). Since the structures are very similar to each other, it is plausible that the present construct has the same excitation peak as the Y66F variant. However, it is important to note that this blue-shift is not confirmed by literature.

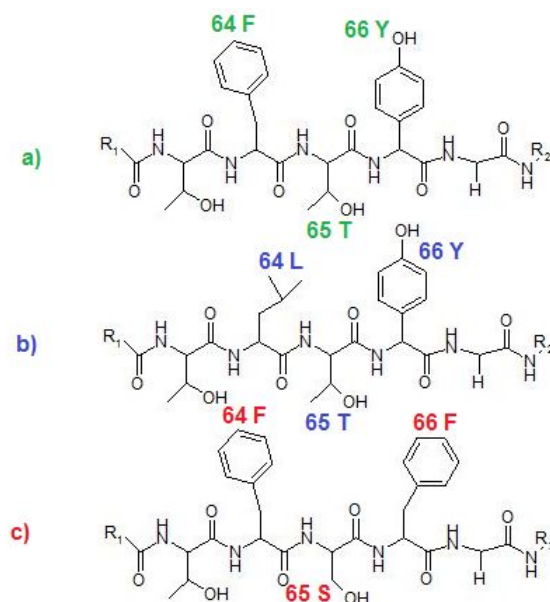


Figure 4.8: Molecular structure of GFP variants: a) GFP S65T (green), b) GFP F64L S65T (blue) as used in the construct, c) GFP Y66F (red).

GFP with F64L and S65T has two absorption peaks at around 395 and around 490 nm [41] [42]. Since the F64L mutation should not affect the excitation and emission properties of the chromophore, there seems to be no substantial difference in the GFP S65T and the GFP F64L S65T variants that would offer a sound explanation for this blue-shift. It can be speculated that other factors are responsible for this observation. Since the analyte was measured in the cell-free extract, dipole-dipole interactions and hydrogen bonding with other substances present in this extract may have led to solvatochromic effects.

Measurement of FRET activity

Linear regression The Durbin-Watson test showed that there seems to be no correlation. However, unlike the residues for succinate, the residues for fumarate are not normally distributed. The emission values for fumarate and succinate were averaged from two measurements. This could possibly be an explanation for the non-normal distribution of the fumarate residues. The fact that this prerequisite for linear regression is not fulfilled for fumarate has to be kept in mind for further statistical analysis. However, by looking at the scatter plots, it seems that there is at least one outlier in both fumarate and succinate, which could also skew the results for the residues (Fig. 4.9 and 4.10). Additionally, the fact that the solubility of fumarate is considerably low (4.9 g/L at 20 °C [43]) might come into play.

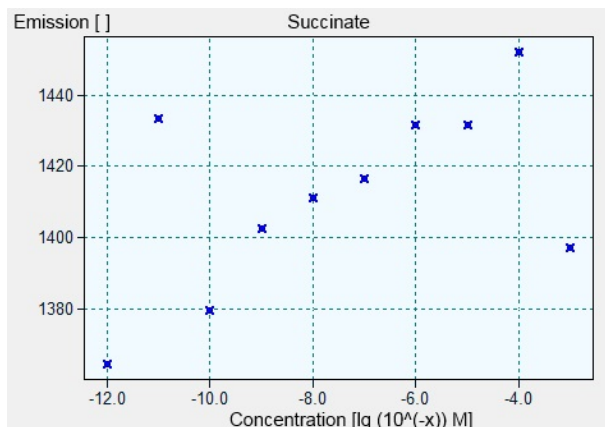


Figure 4.9: Emission/succinate concentration

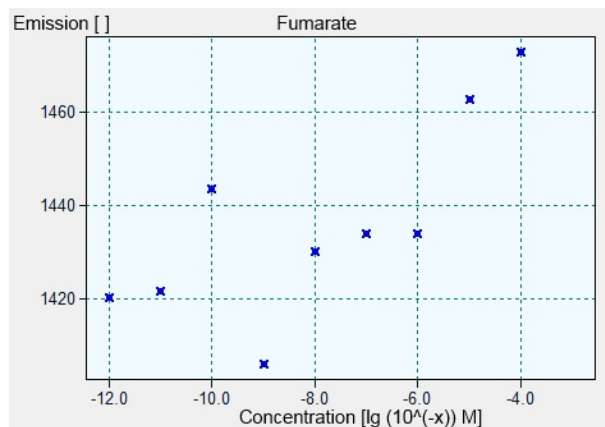


Figure 4.10: Emission/fumarate concentration

Visual inspection of the graphs suggests that there are two outliers for both fumarate and succinate. This can most likely be explained by pipetting or preparation errors, e. g. not enough homogenisation prior to measuring or making dilutions. Another factor that has to be taken into account is possible inhomogeneities or interfering substances in the cell-free extract - all components of the culture broth were still present.

Table 4.1: Test for significance of correlation coefficient

Substance	t-statistic	critical value $t_{\alpha/2}$	Result
Fumarate	2.9476	2.3646	H_0 rejected
Succinate	1.7705	2.3060	H_0 accepted
Succinate without 10^{-11}	2.8703	2.3646	H_0 rejected
Succinate without 10^{-3}	3.0583	2.3646	H_0 rejected
Succinate without both outliers	13.9748	2.4469	H_0 rejected

Correlation of succinate/fumarate concentration and GFP emission For fumarate, the correlation coefficient is significantly different from zero. This is not the case with succinate if all data points are considered. However, if the outlier at 10^{-11} or the outlier at 10^{-3} or both outliers are eliminated, the correlation coefficient has a significant difference from zero.

From this experiment, it can be concluded that the FRET biosensor is functioning. However, this is just a measurement of a trend.

4.6.2 Sensor purification and analysis

Purification and SDS-PAGE

The supernatant turned intense pink overnight.

The protein purification process was analysed with SDS-PAGE (Fig. 4.11 and Fig. 4.12). Aliquots of the following fractions were kept (a 10-fold dilution for SDS-PAGE analysis is marked by *):

- 4 Supernatant of culture
- 3 Pellet of cell-free extract
- 2 Supernatant of cell-free extract*
- 1 Supernatant after binding*
- 0 Washing buffer without sample added
- 0.5 Washing buffer - resin suspension - addition of sample*
- 1 Wash 1*
- 2 Wash 2*
- 3 Wash 3
- 4 Wash 4
- 5 Wash 5
- 5a Wash 6
- 6 Elution 1
- 7 Elution 2*
- 8 Elution 3
- 9 Elution 4
- 10 Elution 5
- 11 Elution 6
- 12 Elution 7

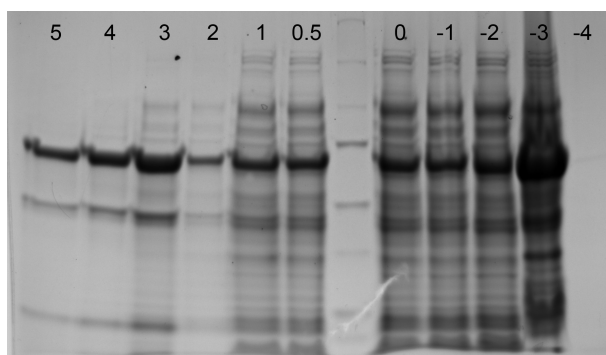


Figure 4.11: Polyacrylamide gel 1

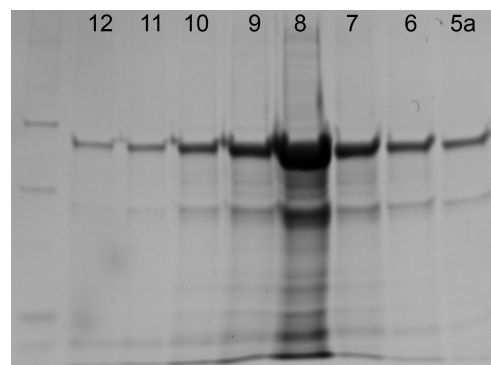


Figure 4.12: Polyacrylamide gel 2

The gel is largely inconclusive. The biggest band is around 70 kDa. Fairly large bands can also be observed at 45 kDa and 20 kDa. There are many byproducts, even in the eluted fractions. Sample 0 is the washing buffer without any sample added. However, the sample shows the same pattern on gel as the other fractions. This could indicate that the to be purified protein was heavily contaminated. The columns had been used before. It could be that the regeneration procedure as recommended in the StrepTactin protocol is not thorough enough. The supernatant of the cell culture was not concentrated enough to see anything on gel. The molecular weight of GFP, the whole construct and C4 core-mCherry were calculated using the DNA sequence, the EMBOSS Transeq and ExPASy Mw/pI calculation tool. The entire construct should have a molecular weight of 88 kDa, whereas GFP has a molecular weight of 27 kDa and C4 core-mCherry 61 kDa. The biggest band on the gel has around 70 kDa. There is a faint band at around 80 kDa. The progress of protein purification could be monitored by observing the colour of the column. Some of the protein was bound to the column, but it could be that residual protein from the previous purifications interfered with the purification process.

Protein content

Table 4.2: Purified sensor concentrations

Fraction	Concentration [$\mu\text{g/mL}$]	Absorbance 1 []	Absorbance 2 []	Average []
6	191	0,025	0,026	0,0255
7*	2839	0,035	0,036	0,0355
8*	608	0,011	0,013	0,012
9	340	0,041	0,044	0,0425
10	144	0,02	0,021	0,0205
11	117	0,017	0,02	0,0185
12	79	0,013	0,011	0,012
8	991	0,111	0,118	0,1145

Fraction 8 was measured pure and 10-fold diluted. The measurement of the pure fraction is considered to be more reliable because the 10-fold dilution value is rather low (between the first and second protein standard) and linear regression works best in the middle of the calibration range. As indicated by the colour of the fractions, 7 and 8 showed the highest concentration.

Further biosensor properties

Freddie was grown in a small volume of $\text{LB}^{\text{Amp}^{\text{Chl}}}$ to look at some properties of the culture. Part of the culture was induced with 0.02 mM IPTG for three hours while the other part was not induced. LB medium was used as a blank. All three tubes were checked with the GeneSys Gel Reader (Fig. 4.13).

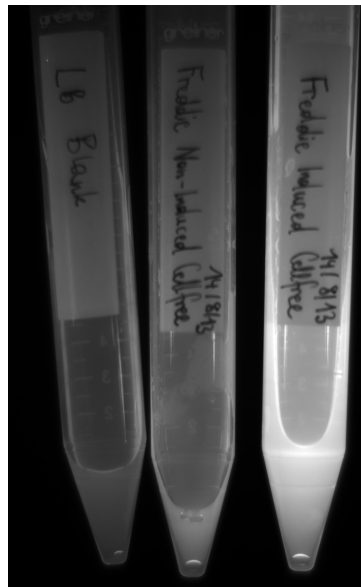


Figure 4.13: Comparison of FRET construct cultures

A clear difference between the LB blank (left) and the non-induced Freddie culture (middle) can be observed. The promoter for the construct is somewhat leaky. There is also a clear difference between the non-induced and induced (right) Freddie culture. The induced culture is visibly brighter.

The pH of Buffer E of the Strep-tactin protocol, the non-induced and induced cultures was measured (Table 4.3).

Table 4.3: pH measurements

Sample	pH
Buffer E	8.25
Freddie induced	7.22
Freddie not induced	7.16

The pH was measured because it may affect FRET. The pH of the induced and the non-induced culture is almost identical.

Fluorimeter measurements of purified biosensor

In the purified sensor, only mCherry could be excited. Excitation at 480 nm led to a small emission peak of mCherry which was attributed to spectral bleed-through. In the cell-free extract, both GFP and mCherry were present. Various hints suggest that GFP may have been cleaved off the construct at some point in the process of protein purification.

- Inconclusive SDS-PAGE gel. The biggest band (which should be the FRET biosensor) does not correspond to the theoretical molecular weight of the construct.
- After binding to the resin, the sensor turned intense pink overnight. The fact that the purified protein was so intensely pink could indicate the absence of GFP.
- GFP could not be excited in the purified protein fraction.
- Samples for SDS-PAGE were checked under the GelReader. Of these, only the supernatant of the cell culture fluoresces when excited at the GFP-specific wavelength.
- Restriction digests of plasmids from Rosetta resulted in unusually high degrees of DNA degradation. This could indicate high DNase and protease activities.

If GFP was cleaved off, it must have occurred at a timepoint between induction of the cells and binding of the cell-free extract to the resin. However, the strep-tag used for purification of the biosensor is located at the N-terminus of the protein and the protein could successfully be purified. Therefore, the strep-tag was most likely present in the construct and interacting with the column. If the strep-tag was present, then it follows that GFP was present as well, just not folded properly or impaired in functionality in another way.

When measuring the cell-free extract, the intensity of GFP for succinate and the diluted blank control remained the same for all concentrations. The emission of GFP for succinate was slightly lower than for the diluted blank. This difference could be explained with the noise of the measurement or slight pipetting errors.

It can be concluded that the FRET sensor in the cell-free extract in Rosetta did not work. This could be the case if GFP was not folded properly or cleaved off. However, GFP was still present in the solution, so FRET could happen if GFP was in close proximity to mCherry, but

would remain constant. Many components are present in the cell-free extract, including C4-dicarboxylic acids. These could block the binding domain, which would constantly force GFP and mCherry apart and prevent the construct from any FRETting. The latter theory seems less likely because the sensor was functioning well in the cell-free extract of DH5- α . Further research would be needed to discover the reason for this behaviour of the sensor.

5 Conclusions

All mutations to get the required fluorophores could be performed. *pyrA* could be inserted into the Funbrick, but the wrong transformants were grown. To avoid similar mistakes in the future, a reliable pipetting method for loading large numbers of transformants on gel was assumed. It was discovered that *EcoRI* cut the Funbrick backbone. The restriction site could successfully be deleted.

A functional FRET biosensor was constructed.

In the process of constructing the biosensor with the CFP-YFP FRET pair, a GFP derivative with a new combination of mutations (Frog) was created. For the biosensor with the CFP-YFP FRET pair, the C4-YFP fragment and the pET52-CFP backbone were created. However, the final ligation and transformation still have to be performed.

Purification of the biosensor was unsuccessful. This was unexpected because a similar Funbrick-compatible sensor was successfully purified by Mark van Veen. The only difference between the tested construct and the purified construct was the *E. coli* strain used - DH5- α and Rosetta. GFP was functional in DH5- α and visibly expressed in the Rosetta culture broth, but not functional in the cell-free extract and protein purified from Rosetta.

If the present FRET biosensor is built in the Funbrick system and if *Aspergillus niger* is transformed with the sensor, this could be the first genetically encoded FRET biosensor in *A. niger* and lead to a much better understanding of the host's metabolic pathways.

6 Recommendations

At first, many transformation steps were planned. However, since ligations can easily fail, transformations are highly time-consuming. If possible, it is wiser to minimise the number of transformation steps or to consider alternative ways of building a construct, e. g. mutating GFP to CFP instead of cutting it out and replacing it with CFP via ligation. The danger, however, is that every PCR step instead of ligation is prone to introduce unwanted mutations in the construct. Therefore, the construct always has to be checked by sequencing. Two occurrences of random DNA insertions in transformants underline the importance of this measure.

A major problem regarding preparation of fragments for ligations is the low yield of agarose gel extraction. Typically, preparation of 5 μg plasmid results in 400 ng of extracted DNA. Therefore, existing methods to purify fragments from gel should be optimised, or alternative methods to do so should be investigated. Perhaps even a different separation method (such as dialysis) could be considered.

It could be observed that ligations often failed. It would be advisable to optimise present ligation methods. This could be done by testing different ligation mixes, minimising the volume of the ligation mix to 5 μL , incubating the ligation mix at lower temperatures (16 to 20°C) overnight or testing other experimental parameters.

Since the FRET biosensor purified from Rosetta was not functional and DNA isolated from Rosetta colonies was subject to degradation, it is advised not to purify the FRET biosensor from Rosetta or to build a construct in Rosetta. The Rosetta pRARE plasmid would contaminate DNA miniprep.

The purified FRET biosensor should be tested. It is advised to follow Jan Willem Borst's method of protein production: Cells are grown at 37°C until OD600 reaches 0.6, then induced and grown at 20°C overnight and with plenty of aeration to ensure high protein production and good aeration for fluorophore maturation. The construct should be transformed in a strain with a low amount of proteases.

An experiment should be designed to find out why GFP was not functional in the purified FRET biosensor. The growth of the biosensor could be repeated in the same way. Perhaps samples could be analysed with HPLC-MS if the sensitivity of the measurement is sufficient and the analyte matrix has no interfering effect. Cell lysis could be carried out only once instead of twice to make sure that the purified protein is not affected by the high homogenisation pressures.

The newly created GFP derivative "Frog" with the combination of mutations F64L, S65T,

Y66W and T203Y should be tested for its qualities as a potential FRET fluorophore. It could be excised from Michael and grown e.g. in pET52 in DH5- α . If its excitation and emission properties are characterised, it could be tested in combination with a fluorophore that meets the formal requirements for being a FRET partner.

The reason for rapid DNA degradation of CFP-pET52-Lox and similar constructs should be found out and ideally eliminated or avoided. The digestion of CFP-pET52 and extraction from gel should be optimised. At present, there are two correlated problems with the digest. First, not the entire plasmid is completely cut due to the short incubation time, which results in loss of fragment. Second, this occurrence leads to two close bands on an agarose gel. To separate them enough to be able to cut out the relevant band, the gel has to be run for a longer time (60 minutes). The long running time causes the bands to thin out and leads to further loss of DNA. If the reason for rapid DNA degradation is found, the incubation time of the digest can be increased. Alternatively, the pET52-CFP-Lox plasmid could be transformed into DH5- α for further work.

Since there is an indication that the FRET sensor is functional, it makes sense to build the construct in the Funbrick. The putative Funbrick-GFP-citA-mCherry ("Noël") and Funbrick-Mito signal-citA-mCherry ("Liam") transformants should be screened for their respective inserts by Colony-PCR. The functionality of the mitochondrial signal could be checked by transforming Liam into *A. niger* and performing fluorescence microscopy at an excitation wavelength of 587 nm (mCherry). The Funbrick-Mito signal-CFP-C4-YFP ("Matthew") and Funbrick-GFP-C4-mCherry ("Felix") could be built. The two systems could even be combined with the BamHI/BgIII system. The complete GFP-C4-mCherry construct (including promoter) could be cut out from Felix with BamHI and BgIII and inserted into Matthew at Matthew's BamHI restriction site. The insert would leave the BamHI restriction site intact on one side and form a BamHI/BgIII scar on the other side. The resulting Funbrick ("Robbie") would have both constructs. Both FRET sensors could be transformed into *A. niger* in one go. However, there might be practical problems due to the large size of this "final" Funbrick.

7 Abbreviations

Amp	Ampicillin
AP	Alkaline phosphatase
bp	basepairs
Ch	Chloramphenicol
CFP	Cyano fluorescent protein
CM	Complete medium
CV	column volume
DNA	Deoxyribonucleic acid
EDTA	Ethylenediaminetetraacetic acid
EtOH	Ethanol
ESR	Extracytoplasmic solute receptor
FD	FastDigest
FDGB	FastDigest GreenBuffer
FP	Fluorescent protein
FRET	Förster resonance energy transfer
eGFP	enhanced green fluorescent protein
GFP	Green fluorescent protein
HEPES	2-[4-(2-hydroxyethyl)piperazin-1-yl]ethanesulfonic acid
iPrOH	Isopropanol
MeOH	Methanol
NC	Negative control
nS	noStop
NT	nucleotide
PC	Positive control
PCR	Polymerase Chain Reaction
Rcap	<i>Rhodobacter capsulatus</i>
SDS-PAGE	Sodium dodecyl sulfate polyacrylamide gel electrophoresis
TAE	Tris, acetic acid, EDTA
TCA	Tricarboxylic acid cycle
TRAP	Tripartite ATP-independent periplasmic transporter
Tris	Tris(hydroxymethyl)aminomethane
YFP	Yellow fluorescent protein

References

- [1] Alexandre Bourds, Steven Rudder, Alison K. East, and Philip S. Poole. Mining the sinorhizobium meliloti transportome to develop fret biosensors for sugars, dicarboxylates and cyclic polyols. *PLOS ONE*, 7, 2012.
- [2] P. Vasantham and S. M. Muthukkaruppan. The production of citric acid on industrial scale by aspergillus niger. *Advances in Plant Sciences*, 25, 2012.
- [3] Ying Yang, Depei Wang, and Nianfa Gao. Changes of -glucosidase and glucoamylase from aspergillus niger in citric acid fermentation. *Zhongguo Niangzao*, 32, 2013.
- [4] Giselle Maria Maciel, Luciana Porto Souza Vandenberghe, Ricardo Cancio Fendrich, Bianca Eli Bianca, Charles Windson Isidoro Haminiuk, and Carlos Ricardo Soccol. Study of some parameters which affect xylanase production: Strain selection, enzyme extraction optimization, and influence of drying conditions. *Biotechnology and Bioprocess Engineering*, 14, 2009.
- [5] Myriam L. Izarra, Monica L. Santayana, Gretty K. Villena, and Marcel Gutierrez-Correa. The influence of inoculum concentration on cellulase and xylanase production by aspergillus niger. *Revista Colombiana de Biotecnologia*, 12, 2010.
- [6] M. Jayant, J. Rashmi, M. Shailendra, and Y. Deepesh. Production of cellulase by different co-culture of aspergillus niger and penicillium chrysogenum from waste paper, cotton waste and baggase. *Journal of Yeast and Fungal Research*, 2, 2011.
- [7] Rainer Krull, Christiana Cordes, Harald Horn, Ingo Kampen, Arno Kwade, Thomas R. Neu, and Bernd Nrtemann. Morphology of filamentous fungi: Linking cellular biology to process engineering using aspergillus niger. *Adv Biochem Engin/Biotechnol*, 10, 2009.
- [8] Beln Max, Jos Manuel Salgado, Noelia Rodrguez, Sandra Corts, Attilio Converti, and Jos Manuel Domnguez. Biotechnological production of citric acid. *Brazilian Journal of Microbiology*, 41, 2010.
- [9] Eugen Arts, Christian P. Kubicek, and M. Rhr. Regulation of phosphofructokinase from aspergillus niger: Effect of fructose 2,6-bisphosphate on the action of citrate, ammonium ions and amp. *Journal of General Microbiology*, 133, 1987.
- [10] Sakiko Okumoto, Alexander Jones, and Wolf B. Frommer. Quantitative imaging with fluorescent biosensors. *Annu. Rev. Plant Biol.*, 63, 2012.
- [11] Maria Papagianni. Advances in citric acid fermentation by aspergillus niger: Biochemical aspects, membrane transport and modeling. *Biotechnology Advances*, 25, 2007.

- [12] A. Pfitzner, C. P. Kubicek, and M. Rhr. Presence and regulation of atp:citrate lyase from the citric acid producing fungus aspergillus niger. *Archives of Microbiology*, 147, 1987.
- [13] George J.G Ruijter, Henk Panneman, Ding-Bang Xu, and Jaap Visser. Properties of aspergillus niger citrate synthase and effects of cita overexpression on citric acid production. *FEMS Microbiology Letters*, 184, 2000.
- [14] George J.G Ruijter, Henk Panneman, Ding-Bang Xu, and Jaap Visser. Trehalose-6-phosphate synthase a affects citrate accumulation by aspergillus niger under conditions of high glycolytic flux. *FEMS Microbiology Letters*, 140, 1996.
- [15] C. P. Kubicek and M. Rhr. Influence of manganese on enzyme synthesis and citric acid accumulation in aspergillus niger. *European Journal of Applied Microbiology and Biotechnology*, 4, 1977.
- [16] W.A. de Jongh and J. Nielsen. Enhanced citrate production through gene insertion in aspergillus niger. *Metabolic Engineering*, 10, 2008.
- [17] G. J. G. Ruijter, C. P. Kubicek, and J. Visser. Production of organic acids by fungi. *The Mycota*, 10, 2002.
- [18] C P Kubicek, G Schreferl-Kunar, W Whrer, and M Rhr. Evidence for a cytoplasmic pathway of oxalate biosynthesis in aspergillus niger. *Applied and Environmental Microbiology*, 54, 1988.
- [19] S. Meijer, J. Otero, R. Olivares, M.R. Andersen, L. Olsson, and J. Nielsen. Overexpression of isocitrate lyaseglyoxylate bypass influence on metabolism in aspergillus niger. *Metabolic Engineering*, 11, 2009.
- [20] Sandra Techritz, Susanne Ltzkendorf, Esther Bazant, Silke Becker, Joachim Klose, and Markus Schuelke. Quantitative and qualitative 2d electrophoretic analysis of differentially expressed mitochondrial proteins from five mouse organs. *PROTEOMICS*, 13, 2013.
- [21] F. Lottspeich. Bioanalytik. Book, 2006.
- [22] Jos Miguel P. Ferreira de Oliveira and Leo H. de Graaff. Proteomics of industrial fungi: trends and insights for biotechnology. *Applied Microbiology and Biotechnology*, 89, 2011.
- [23] X. Doua, Y. Yamaguchia, H. Yamamotoa, S. Doia, and Y. Ozaki. Quantitative analysis of metabolites in urine using a highly precise, compact near-infrared raman spectrometer. *Vibrational Spectroscopy*, 13, 1996.
- [24] Patrick Colin Hickey. Luminescent or fluorescent fungal biosensor and assay. Patent, 2004.
- [25] Anja Dietrich, Volker Buschmann, Christian Mller, and Markus Sauer. Fluorescence resonance energy transfer (fret) and competing processes in donoracceptor substituted dna strands: a comparative study of ensemble and single-molecule data. *Reviews in Molecular Biotechnology*, 82, 2002.
- [26] European Molecular Biology Laboratory. http://www.embl.de/eamnet/downloads/modules/fret_teaching_module.pdf visited 4. 9. 2013. Website, 2013.

- [27] Steven S. Vogel, B. Wieb van der Meer, and Paul S. Blank. Estimating the distance separating fluorescent protein fret pairs. *Methods*, June 2013.
- [28] Salk Institute of Biological Studies. <http://flowcyt.salk.edu/fluo.html> visited 4. 9. 2013. Website, 2013.
- [29] Roger Y. Tsien. The green fluorescent protein. *Annual Review of Biochemistry*, 67, 1998.
- [30] Robert E. Campbell, Oded Tour, Amy E. Palmer, Paul A. Steinbach, Geoffrey S. Baird, David A. Zacharias, and Roger Y. Tsien. A monomeric red fluorescent protein. *PNAS*, 99, 2002.
- [31] Xiaokun Shu, Nathan C. Shaner, Corinne A. Yarbrough, Roger Y. Tsien, and S. James Remington. Novel chromophores and buried charges control color in mFruits. *Biochemistry*, 45, 2006.
- [32] David J Kelly and Gavin H Thomas. The tripartite atp-independent periplasmic (trap) transporters of bacteria and archaea. *FEMS Microbiology Reviews*, 25, 2001.
- [33] Naoki Komatsua, Kazuhiro Aoki, Masashi Yamadac, Hiroko Yukinagac, Yoshihisa Fujitac, Yuji Kamiokac, and Michiyuki Matsudaa. Development of an optimized backbone of fret biosensors for kinases and gtpases. *Molecular Biology of the Cell*, 22, 2011.
- [34] Bin Zhang. Design of fret-based gfp probes for detection of protease inhibitors. *Biochemical and Biophysical Research Communications*, 323, 2004.
- [35] European Bioinformatics Institute. http://www.ebi.ac.uk/tools/st/emboss_transeq/ visited 4. 9. 2013. Website, since 1994.
- [36] National Center of Biotechnology Information. <http://blast.ncbi.nlm.nih.gov/> visited 4. 9. 2013. Website, since 1997.
- [37] Nikolaus Pawlowski. <http://www.fr33.net/seqedit.php> visited 4. 9. 2013. Website, 2013.
- [38] Swiss Institute of Bioinformatics. http://web.expasy.org/compute_pi/ visited 4. 9. 2013. Website, 2013.
- [39] K.J. Breslauer, R. Frank, H. Blicher, and LA Marky. Predicting dna duplex stability from the base sequence. *PNAS*, 83, 1986.
- [40] ThermoScientific. <http://www.thermoscientificbio.com/webtools/tmc/> visited 4. 9. 2013. Website, 2013.
- [41] James A. J. Arpino, Pierre J. Rizkallah, and D. Dafydd Jones. Crystal structure of enhanced green fluorescent protein to 1.35 Å resolution reveals alternative conformations for glu222. *PLOS ONE*, 7, 2012.
- [42] Haruko Hosoi, Shoichi Yamaguchi, Hideaki Mizuno, Atsushi Miyawaki, and Tahei Tahara. Hidden electronic excited state of enhanced green fluorescent protein. *The Journal of Physical Chemistry Letters B*, 112, 2008.

- [43] Sigma-Aldrich. <http://www.sigmaaldrich.com/catalog/product/aldrich/w248800?lang=de®ion=de> visited 4. 9. 2013. Website, 2013.
- [44] international Genetically Engineered Machine. <http://parts.igem.org/help:protocols/transformation> visited 4. 9. 2013. Website, 2013.

8 Appendix

8.1 In silico data

8.1.1 Primers

Table 8.1: Primers

Aim	Primer name	Sequence
GFP to GFP F64L	LS.GFP_F64L	5'-CCCTCGTGACCACCTTAACCTACGGCGTG-3'
	LS.GFP_F64L_antisense	5'-CACGCCGTAGGTTAAGGTGGTCACGAGGG-3'
GFP to CFP	LS.GFP_Y66W	5'-CTCGTGACCACCTTCACCTGGGGCGTGCAGT-3'
	LS.GFP_Y66W_antisense	5'-ACTGCACGCCCCAGGTGAAGGTGGTCACGAG-3'
GFP to YFP	LS.GFP_T203Y	5'-GACAACCACTACCTGAGCTATCAGTCCGCCCTGAGCAAA-3'
	LS.GFP_T203Y_antisense	5'-TTTGCTCAGGGCGGACTGATAGCTCAGGTAGTGGTTGTC-3'
GFP to GFP nS	DO_pJetGFP_noStop_del78-80	5'-CATGGACGAGCTGTACAAGATGCATATCTTGCTGAAAA-3'
	DO_pJetGFP_noStop_del78-80_rev	5'-TTTTAGCAAGATATGCATCTTGACAGCTCGTCCATG-3'
GFP to CFP F64L	F64L_Y66W	5'-CCACCCTCGTGACCACCTTAACCTGGGGCGTGCAGT-3'
	F64L_Y66W_antisense	5'-ACTGCACGCCCCAGGTTAAGGTGGTCACGAGGGTGG-3'
Add EcoRI to YFP	LS_EcoRI.YFP_F	5'-GAATTCATGGTGAGCAAGGGCGAGGAGCTGTTC-3'
Add NotI to YFP	LS_NotI.YFP_R	5'-GCGGCCGCTTACTTGTACAGCTCGTCCATGCC-3'
Screen for pyrA in Funbrick	pyrA_FB_F	5'-GACGAAAGGGCCTCGAGCTAACATAC-3'
	pyrA_FB_R	5'-AATAGGCGTATCTCGAGCATCCAAC-3'
Screen for Mito Signal	MS_F	5'-ACTGGCTCAACCATGCAGATGGCTGC-3'
	MS_R	5'-ATGCATAAGCAGGCGGGCGGGCGGGC-3'
Screen for G/CFP	GCFP_F	5'-CTGCAGATGGTGAGCAAGGGCGAGG-3'
	GCFP_R	5'-ATGCATCTTGTACAGCTCGTCCATGC-3'
Screen for mCherry	mCherry_F	5'-GAATTCTGTGAGCAAGGGCGAGGAGG-3'
	mCherry_R	5'-GCGGCCGCCTACTTGTACAGCTCG-3'
Screen for C4core	C4_F	5'-ATGCATACTAGTGAGCCCATCG-3'
	C4_R	5'-ACTAGTTTCTGCGGTTGCAGCC-3'

8.1.2 Sequences

Sequences

Colour mutations

>GFP

```
ATGGTGAGCAAGGGCGAGGAGCTGTTACCGGGGTGGTGCCCATCCTGGTCGAGCTGGACGGC
GACGTAAACGGCCACAAGTTTCAGCGTGTCCGGCGAGGGCGAGGGCGATGCCACCTACGGCAAG
CTGACCCTGAAGTTTCATCTGCACCACCGGCAAGCTGCCCGTGCCCTGGCCCACCCTCGTGACCA
CCTTCACCTACGGCGTGCAAGTGCTTCAGCCGCTACCCCGACCACATGAAGCAGCACGACTTCTT
CAAGTCCGCCATGCCCCGAAGGCTACGTCCAGGAGCGCACCATCTTCTTCAAGGACGACGGCAAC
TACAAGACCCGCGCCGAGGTGAAGTTCGAGGGCGACACCCTGGTGAACCGCATCGAGCTGAAG
GGCATCGACTTCAAGGAGGACGGCAACATCCTGGGGCACAAGCTGGAGTACAACAGCCACAAC
ACAACGTCTATATCATGGCCGACAAGCAGAAGAACGGCATCAAGGTGAAGTTCAGATCCGCCAC
AACATCGAGGACGGCAGCGTGAGCTCGCCGACCACTACCAGCAGAACACCCCCATCGGCGAC
GGCCCCGTGCTGCTGCCCCGACAACCACTACCTGAGCACCCAGTCCGCCCTGAGCAAAGACCCC
AACGAGAAGCGCGATCACATGGTCCTGCTGGAGTTCGTGACCGCCGCCGGGATCACTCACGGC
ATGGACGAGCTGTACAAGTAA
```

>GFP F65L

```
atGGTGAGCAAGGGCGAggagCTGTTACCGGGGTgGTGCCCATCCTGGTCGAGcTGGACGGCGA
CgtAAACGGCCACAAGTTTCAGCGTGTCCGGCGAGGGCGAGGGCGATGCCACCTACGGCAAGCTG
ACCCTGAAGTTTCATCTGCACCACCGGCAAGCTGCCCGTGCCCTGGCCCACCCTCGTGACCACCTT
AACCTACGGCGTGCAAGTGCTTCAGCCGCTACCCCGACCACATGAAGCAGCACGACTTCTTCAAG
TCCGCCATGCCCCGAAGGCTACGTCCAGGAGCGCACCATCTTCTTCAAGGACGACGGCAACTACA
AGACCCGCGCCGAGGTGAAGTTCGAGGGCGACACCctgGTGAACCGCATCGAGCTGAAGGGCAT
CGACTTCAAGGAGGACGGCAACATCCTGGGGCACAAGCTGGAGTACAACAGCCACAAC
GTCTATATCATGGCCGACAAGCAGAAGAACGGCATCAAGGTGAAGTTCAGATCCGCCACAACAT
CGAGGACGGCAGCGTGAGCTCGCCGACCACTACCAGCAGAACACCCCCATCGGCGACGGCCC
CGTGCTGCTGCCCCGACAACCACTACCTGAGCACCCAGTCCGCCCTGAGCAAAGACCCCAACGAG
AAGCGCGATCACATGGTCCTGCTGGAGTTCGTGACCGCCGCCGGGATCACTCACGGCATGGAC
GAGCTGTACAAGTAA
```

>CFP

```
ATGGTGAGCAAGGGCGAGGAGCTGTTACCGGGGTGGTGCCCATCCTGGTCGAGCTGGACGGC
GACGTAAACGGCCACAAGTTTCAGCGTGTCCGGCGAGGGCGAGGGCGATGCCACCTACGGCAAG
CTGACCCTGAAGTTTCATCTGCACCACCGGCAAGCTGCCCGTGCCCTGGCCCACCCTCGTGACCA
CCTTCACCTGGGGCGTGCAAGTGCTTCAGCCGCTACCCCGACCACATGAAGCAGCACGACTTCTT
CAAGTCCGCCATGCCCCGAAGGCTACGTCCAGGAGCGCACCATCTTCTTCAAGGACGACGGCAAC
TACAAGACCCGCGCCGAGGTGAAGTTCGAGGGCGACACCCTGGTGAACCGCATCGAGCTGAAG
GGCATCGACTTCAAGGAGGACGGCAACATCCTGGGGCACAAGCTGGAGTACAACAGCCACAAC
ACAACGTCTATATCATGGCCGACAAGCAGAAGAACGGCATCAAGGTGAAGTTCAGATCCGCCACA
AACATCGAGGACGGCAGCGTGAGCTCGCCGACCACTACCAGCAGAACACCCCCATCGGCGAC
GGCCCCGTGCTGCTGCCCCGACAACCACTACCTGAGCACCCAGTCCGCCCTGAGCAAAGACCCC
AACGAGAAGCGCGATCACATGGTCCTGCTGGAGTTCGTGACCGCCGCCGGGATCACTCACGGC
ATGGACGAGCTGTACAAGTAA
```

>GFP noStop

```
ATGGTGAGCAAGGGCGAGGAGCTGTTACCGGGgtgGTGCCCATCCTGGTCGAGctgGACGGCGA
CGTAAACGGCCACAAGTTTCAGCgtgTCCGGCGAGGGCGAGGGCGATGCCACCTACGGCAAGCTG
ACCCTGAAGTTTCATCTGCACCACCGGCAAGCTGCCCGTGCCCTGGCCCACCCTCgtGACCACCTT
AACCTACGGCGTGCAAGTGCTTCAGCCGCTACCCCGACCACATGAAGCAGCACGACTTCTTCAAG
TCCGCCATGCCCCGAAGGCTACGTCCAGGAGCGCACCATCTTCTTCAAGGACGACGGCAACTACA
AGACCCGCGCCGAGGTGAAGTTCGAGGGCGACACCCTGGTGAACCGCATCGAGCTGAAGGGCA
TCGACTTCAAGGAGGACGGCAACATCCTGGGGCACAAGCTGGAGTACAACAGCCACAAC
CGTCTATATCATGGCCGACAAGCAGAAGAACGGCATCAAGGTGAAGTTCAGATCCGCCACAACA
TCGAGGACGGCAGCGTGAGCTCGCCGACCACTACCAGCAGAACACCCCCATCGGCGACGGCC
CCGTGCTGCTGCCCCGACAACCACTACCTGAGCACCCAGTCCGCCCTGAGCAAAGACCCCAACGA
GAAGCGCGATCACATGGTCCTGCTGGAGTTCGTGACCGCCGCCGGGATCACTCACGGCATGGA
CGAGCTGTACAAGATGCAT
```

>YFP

ATGGTGAGCAAGGGCGAGGAGCTGTTACCGGGGTGGTGCCCATCCTGGTCGAGCTGGACGGC
GACGTAAACGGCCACAAGTTTCAGCGTGTCCGGCGAGGGCGAGGGCGATGCCACCTACGGCAAG
CTGACCCTGAAGTTTCATCTGCACCACCGGCAAGCTGCCCGTGCCCTGGCCCACCCTCGTGACCA
CCTTAACCTACGGCGTGCAGTGCTTCAGCCGCTACCCCGACCACATGAAGCAGCAGCACTTCTT
CAAGTCCGCCATGCCCCGAAGGCTACGTCCAGGAGCGCACCATCTTCTTCAAGGACGACGGCAAC
TACAAGACCCGCGCCGAGGTGAAGTTCGAGGGCGACACCCTGGTGAACCGCATCGAGCTGAAG
GGCATCGACTTCAAGGAGGACGGCAACATCCTGGGGCACAAGCTGGAGTACAACCTACAACAGCC
ACAACGTCTATATCATGGCCGACAAGCAGAAGAACGGCATCAAGGTGAAGTTCAGATCCGCCAC
AACATCGAGGACGGCAGCGTGCAGCTCGCCGACCACTACCAGCAGAACACCCCCATCGGCGAC
GGCCCCGTGCTGCTGCCCGACAACCACTACCTGAGCTATCAGTCCGCCCTGAGCAnAGACCCCA
ACGAGAAGCGCGATCACATGGTCCTGCTGGAGTTCGTGACCGCCGCCGGGATCACTCACGGCA
TGGACGAGCTGTACAAGTAA

>CFP F65L

ATGGTGAGCAAGGGCGAGGAGCTGTTACCGGGGTGGTGCCCATCCTGGTCGAGCTGGACGGC
GACGTAAACGGCCACAAGTTTCAGCGTGTCCGGCGAGGGCGAGGGCGATGCCACCTACGGCAAG
CTGACCCTGAAGTTTCATCTGCACCACCGGCAAGCTGCCCGTGCCCTGGCCCACCCTCGTGACCA
CCTTAACCTGGGGCGTGCAGTGCTTCAGCCGCTACCCCGACCACATGAAGCAGCAGCACTTCTT
CAAGTCCGCCATGCCCCGAAGGCTACGTCCAGGAGCGCACCATCTTCTTCAAGGACGACGGCAAC
TACAAGACCCGCGCCGAGGTGAAGTTCGAGGGCGACACCCTGGTGAACCGCATCGAGCTGAAG
GGCATCGACTTCAAGGAGGACGGCAACATCCTGGGGCACAAGCTGGAGTACAACCTACAACAGCC
ACAACGTCTATATCATGGCCGACAAGCAGAAGAACGGCATCAAGGTGAAGTTCAGATCCGCCAC
AACATCGAGGACGGCAGCGTGCAGCTCGCCGACCACTACCAGCAGAACACCCCCATCGGCGAC
GGCCCCGTGCTGCTGCCCGACAACCACTACCTGAGCACCCAGTCCGCCCTGAGCAAAGACCCC
AACGAGAAGCGCGATCACATGGTCCTGCTGGAGTTCGTGACCGCCGCCGGGATCACTCACGGC
ATGGACGAGCTGTACAAGTAA

>CFP F65L noStop

ATGGTGAGCAAGGGCGAGGAGCTGTTACCGGGGTGGTGCCCATCCTGGTCGAGCTGGACGGC
GACGTAAACGGCCACAAGTTTCAGCGTGTCCGGCGAGGGCGAGGGCGATGCCACCTACGGCAAG
CTGACCCTGAAGTTTCATCTGCACCACCGGCAAGCTGCCCGTGCCCTGGCCCACCCTCGTGACCA
CCTTAACCTGGGGCGTGCAGTGCTTCAGCCGCTACCCCGACCACATGAAGCAGCAGCACTTCTT
CAAGTCCGCCATGCCCCGAAGGCTACGTCCAGGAGCGCACCATCTTCTTCAAGGACGACGGCAAC
TACAAGACCCGCGCCGAGGTGAAGTTCGAGGGCGACACCCTGGTGAACCGCATCGAGCTGAAG
GGCATCGACTTCAAGGAGGACGGCAACATCCTGGGGCACAAGCTGGAGTACAACCTACAACAGCC
ACAACGTCTATATCATGGCCGACAAGCAGAAGAACGGCATCAAGGTGAAGTTCAGATCCGCCAC
AACATCGAGGACGGCAGCGTGCAGCTCGCCGACCACTACCAGCAGAACACCCCCATCGGCGAC
GGCCCCGTGCTGCTGCCCGACAACCACTACCTGAGCACCCAGTCCGCCCTGAGCAAAGACCCC
AACGAGAAGCGCGATCACATGGTCCTGCTGGAGTTCGTGACCGCCGCCGGGATCACTCACGGC
ATGGACGAGCTGTACAAGATG

Sensor

>Sensor

ATGCATACTAGTGAGCCTATAGTCATCAAGTTCAGCCATGTAGTCGCTCCTGACACTCCC
AAAGGGAAGGGTGCAGCTAAATTTCAGAGAGTTGGCCGAGAAATACACCAACGGCGCAGTG
GACGTGGAAGTTTATCCTAACAGCCAGCTTTACAAGGATAAGGAAGAGCTTGAAGCCCTC
CAACTTGGTGCGGTTCAAATGCTGGCACCGTCAATTGGCTAAATTTGGACCGCTTGGTGTG
CAGGATTTTGAAGTTTTTATCTACCTACATCTTCAAGGACTACGAGGCGCTCCACAAG
GTGACCCAAGGCGAAGCTGGTAAGATGCTGCTCTCTAAACTCGAAGCCAAGGGTATCACC
GGGTTGGCCTTCTGGGATAACGGCTTCAAGATTATGTCTGCTAACACGCCGCTAACTATG
CCCGATGATTTCTCGGCTTGAAGATGCGAATCCAGTCTCGAAAGTGTTAGAAGCCGAG
ATGAATGCACTCGGAGCAGTGCCTCAGGTCATGGCCTTCTCGGAAGTCTATCAGGCGTTG
CAAACGGGGGTTGTCGACGGCACTGAAAATCCACCATCAAATATGTTTACGCAAAAAGATG
AATGAGGTGCAGAAACACGCCACCGTCTCCAACCATGGATATCTGGGGTATGCGGTAATC
GTAACAAGCAGTTCTGGGACGGCCTGCCCGCCGATGTCAGAACCGGACTAGAGAAGGCG
ATGGCTGAATCCACAGATTACGCGAATGGAATTGCCAAGGAAGAGAACGAAAAGGCCCTC
CAGGCAATGAAAGACGCTGGCACAACAGAATTTACGAGCTGACCGCGGAAGAGCGCGCT
GCCTGGGAGGAGGTTCTCACACCAGTTCACGACGAAATGGCCGAGCGGATTGGTGCTGAA

ACCATTGCCGCTGTCAAGGCTGCAACCGCAGAACTAGTGAATTCCATGAGGCGGCCGC

Mitochondrial signal

> MitoSignal

CTGCAGATGGCTGCGCCTCGCCTCTTCCGGCCCCGCCGCCCGCCTGCTTATGCAT

pyrA

>pyrA

CTCGAGCTAACATACATTCCGAACCGTGACGCCAAGGCCGAGCAGTTCAACTGCGCTCAGCGC
GCTCATGCCAACTTCCTTGAGAACTCCAGCCAACTATGCTCTTCCTCCTGGTAGCTGGACTGAA
GTACCCCCAGTTGGCGACTGGCCTCGGAAGCATCTGGGTCTCGGTGCTCACTGTTCTTTAC
GGATATGTGTACTCCGGCAAGCCGCGGGGTCGCGGTGTTTTGTACGGCAGCTTCTACTTGCTTG
CACAGGGAGCTCTCTGGGGCTTGACGTCTTTTGGAGTTGCGAGGGAGTTGATTTCTACTTCTAA
GTTTGGACTGAATCCGTGGTGTGATTGAGGTGATTGGCGATGTTTGGCTATACCAGCTATATGTA
ATAATCTCTACTGTATACTACTATTCAACGCATTTTACTATGCGTGCTGCTAGGGTCGGCAATGAC
AATGGCAATCTGACTGACGTGGTCTATTTCTCCATGTGCAGCAGGGAATACGAGCTCCAATGGAC
CTCGGGAGTGCCACAGTCAATGGCAAGGAACTCCGCCTTTGCAGGTGTGGCTGAACCCACG
GGTCGGAGGCGGAGCAATCCACCCCGATGTGGCTGGTGCGTGAGGGGCTCGCGATGATTTT
ACTGAGCTTGCTTTTCTTGTGACATTGAACATTGTCCTTGGTCTTCCTTCAGATTTAAGGGTCAG
TCACTGCTACATTTCTCAGTAGTATCCGCGCACGTCTCTGGATTTACGAATCAGGGTCCACCAGT
CGAAACTTCGAACTACTCTCATTATACAATCCTCTTTCCATTCCCGCATTAACCCCTCCATCAACA
CCATGTCCTCCAAGTCGCAATTGACCTACACTGCCCGTGCCAGCAAGCATCCCAATGCTCTGGC
GAAGAGGCTGTTGAGATTGCCGAGGCCAAGAAGACCAATGTGACTGTCTCGGCTGACGTTACC
ACCACTAAGGAGCTACTAGACCTTGCTGACCGTAGGCCGACCCGCTACTCTGCCTGATTATGCTG
CATGCAAACCTTATTAACGGTGATACCGGACTGCAGGTCTCGGTCCCTACATTGCCGTGATCAAAA
CCCACATCGATATCCTCTCTGATTTAGCAACGAGACCATTGAGGGACTTAAGGCTCTCGCGCAG
AAGCACAACCTTTCTCATCTTCGAGGACCGCAAGTTCATTGACATCGGCAACACGGTCCAGAAGCA
ATACCACGGCGGTACCCTCCGTATCTCGGAATGGGCCACATCATCACTGCAGCATTCTCCCTG
GTGAGGGTATCGTCGAGGCTCTCGCTCAGACGGCGTCTGCACCGGACTTCGCCTACGGCCCCG
AACGCGGTCTGTTGATCTTGGCAGAGATGACCTCTAAGGGCTCCTTGGCTACCGGCCAGTACAC
TACTTCCTCGGTGCGATTATGCCCGGAAATACAAGAACTTCGTTATGGGATTCGTGTCGACGCGCG
CGTTGGGTGAGGTGCAGTCGGAAGTCAGCTCTCCTTCGGATGAGGAGGACTTTGTGGTCTTCAC
GACTGGTGTGAACATTTCTTCCAAGGGAGATAAGCTTGGTCAGCAGTACCAGACGCCCGGATCG
GCTATCGGCCGGGGTGCTGACTTCATTATCGCGGGTCGCGGTATCTACGCCGCGCCGGACCCG
GTGCAGGCTGCGCAACAGTATCAGAAGGAGGGGTGGGAAGCCTACCTGGCCCGTGTGCGCGGA
AACTAATACTATAAAAGGAGGATCGAAGTTCTGATGGTTATGAATGATATAGAAATGCAACTTGCC
GCAACGGATACGGAAGCGGAAACGGACCAATGTGAGCACGGGTAGTCAGACTGCGGCATCGG
ATGTCCAAACGGTATTGATCCTGCAGGCTACTATGGTGTGGCACAAGGATCAATGCGGTACGAC
GATTTGATGCAGATAAGCAGGCTGCGAAGTAGTAACCTTTGCGTAGAGAAAATGGCGACGGGTG
GCTGATAAGGGCGGTGATAAGCTTAATTGTCATCGCAGATAAGCACTGCTGTCTTGATCCAAGT
CAGCGTCAGCAGAAATACGGGACTTCCGAAAGTATATGGCAAATTAAGAAGCTTGACTCTCCAG
CAATGTTTTGCCCTGACCGTCGCTAAACGTTACTACCCCTATACCCGTCTGTTTGTCCAGCCC
GAGGCATTAGGTCTGACTGACAGCACGGCGCCATGCGGGCTTGGGACGCCATGTCCGTGCGGT
GATAAGGGTTGATCCATGCAGCTACTATCCTTCCATCGTTCCATTCCCATCCTTGTCTATCTCCA
TCCTTGAACTTTACTAGTTTAGTTGGATGCTCGAG

8.2 Constructs

Table 8.2: Constructs

Name	Strain	Vector	Insert	Tag
Col. 12	Rosetta	pET52	GFP-Lox	Strep-Tag
Col. 10	Rosetta	pET52	GFP-Lox	Strep-Tag
Col. 5	Rosetta	pET52	GFP-Lox	Strep-Tag
Col. 1	Rosetta	pET52	GFP-Lox	Strep-Tag
Col. 3 "Ruud"	Rosetta	pET52	CFP-Lox	Strep-Tag
Col. 10	Rosetta	pET52	GFP-Lox	Strep-Tag
Col. 3 "Ruud"	Rosetta	pET52	CFP-Lox	Strep-Tag
	DH5- α	pJET	PstI-GFP-NsiI	
Col. I	XL-10 Gold	pJET	GFP F64L	
Col. II	XL-10 Gold	pJET	GFP F64L	
Col. VII	XL-10 Gold	pJET	GFP F64L	
Col. 2A	XL-10 Gold	pJET	YFP F64L	
Col. 2B	XL-10 Gold	pJET	YFP F64L	
Col. 2C	XL-10 Gold	pJET	YFP F64L	
Col. 2D	XL-10 Gold	pJET	YFP F64L	
	DH5- α	pJET	EcoRI-YFP-NotI	
	DH5- α	pFB001	Rcap C4 Sensor	
	DH5- α	pUC57	Mito signal	
Col. I	DH5- α	iGEM BBa_B1003	Amp + Kan resistance gene	
Col. II	DH5- α	iGEM BBa_B1003	Amp + Kan resistance gene	
Col. III	DH5- α	iGEM BBa_B1003	Amp + Kan resistance gene	
Col. 3A	XL-10 Gold	pJET	GFP F64L.nS	
Col. 3B	XL-10 Gold	pJET	GFP F64L.nS	
Col. 3C	XL-10 Gold	pJET	GFP F64L.nS	
Col. 3D	XL-10 Gold	pJET	GFP F64L.nS	
Col. 1A	XL-10 Gold	pJET	CFP	
Col. 1B	XL-10 Gold	pJET	CFP	
Col. 1C	XL-10 Gold	pJET	CFP	
Col. 1D	XL-10 Gold	pJET	CFP	
	DH5- α	pWA 423	pyrA	
Mark GCAM	DH5- α	pET52	GFP-citA-mCherry	
Col. I	XL-10 Gold	pJET	CFP F64L	
Col. II	XL-10 Gold	pJET	CFP F64L	
Col. III	XL-10 Gold	pJET	CFP F64L	
Col. IV	XL-10 Gold	pJET	CFP F64L	
Col. V	XL-10 Gold	pJET	CFP F64L.nS	
Col. VI	XL-10 Gold	pJET	CFP F64L.nS	
Col. VII	XL-10 Gold	pJET	CFP F64L.nS	
Col. VIII	XL-10 Gold	pJET	CFP F64L.nS	
Freddie	DH5- α	pET52	GFP-C4-mCherry	
Brian	DH5- α	pET52	GFP-C4-mCherry	
John	DH5- α	pET52	GFP-C4-mCherry	
Roger	DH5- α	pET52	GFP-C4-mCherry	
Freddie	Rosetta	pET52	GFP-C4-mCherry	
Brian	Rosetta	pET52	GFP-C4-mCherry	
Roger	Rosetta	pET52	GFP-C4-mCherry	
Montserrat	DH5- α	pET52	GFP-C4-YFP	
Martí	DH5- α	pET52	GFP-C4-YFP	
Barnabé	DH5- α	pET52	GFP-C4-YFP	
Mark	DH5- α	pFB200	citA-mCherry	
Michael	XL-10 Gold	pET52	CFP-C4-Frog	
Janet	XL-10 Gold	pET52	CFP-C4-Frog	
Paris	XL-10 Gold	pET52	CFP-C4-Frog	
Jermaine	XL-10 Gold	pET52	CFP-C4-Frog	

8.3 Agarose gels

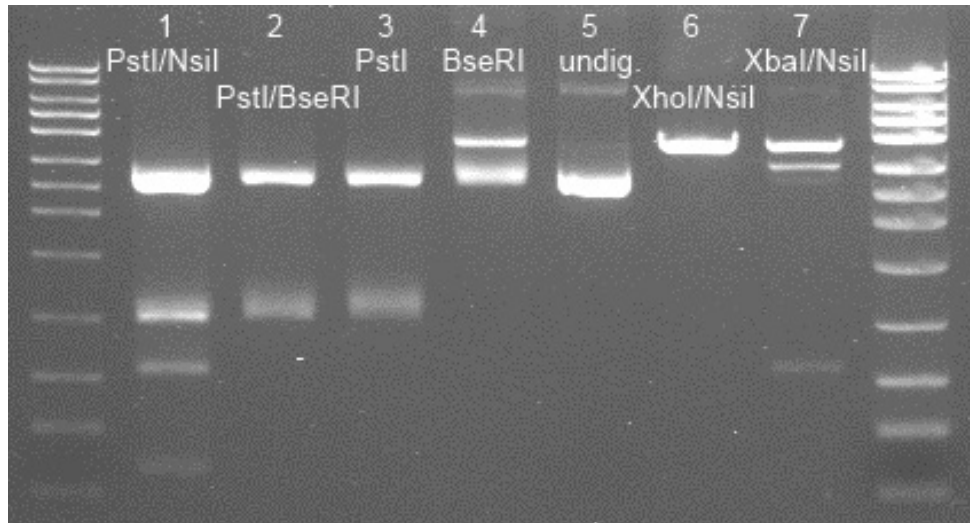


Figure 8.1: GFP restriction digest. The description at the top of each lane corresponds to the restriction enzymes used for that lane. The BseRI used was not a FastDigest enzyme.

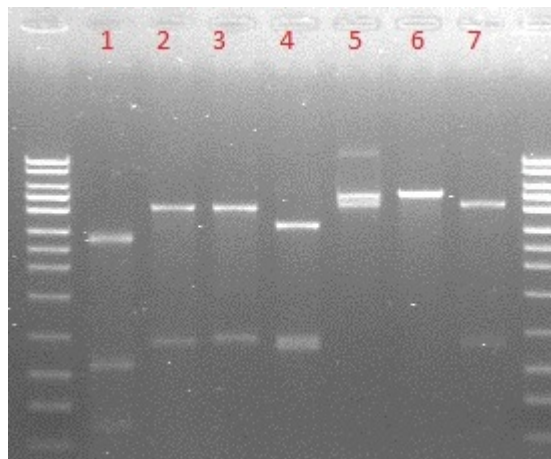


Figure 8.2: Restriction sites check of YFP and Rcap C4.

- 1: YFP in pJET PstI+NsiI
- 2-7: Rcap C4 in FB001
- 2: SpeI
- 3: NsiI+NotI
- 4: NsiI+EcoRI
- 5: uncut
- 6: NsiI
- 7: EcoRI

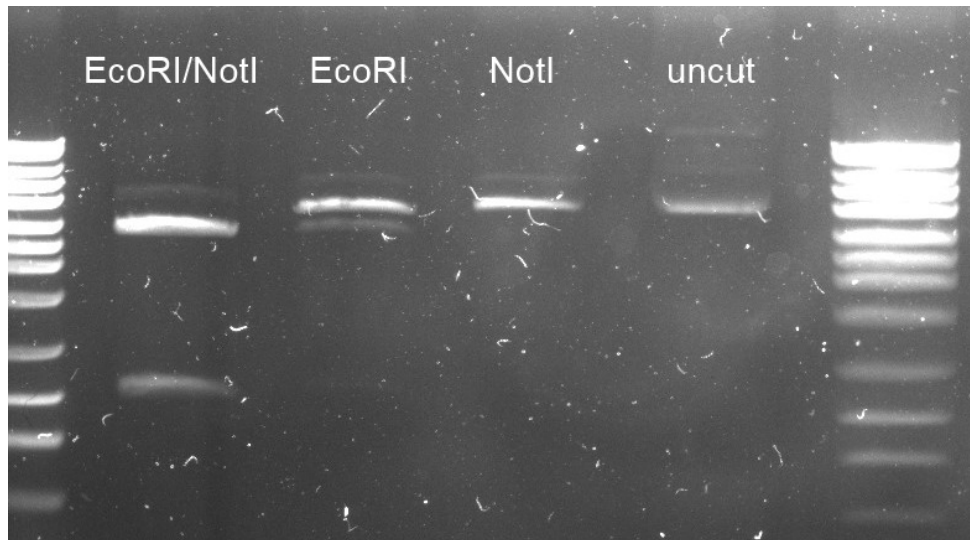


Figure 8.3: EcoRI-YFP-NotI restriction digest

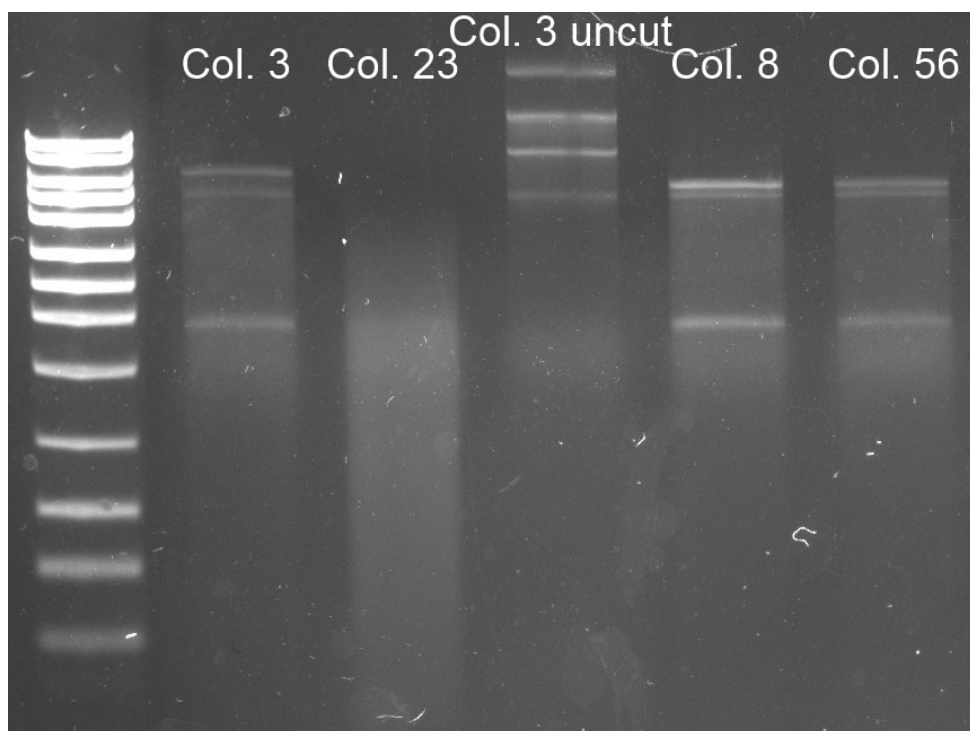


Figure 8.4: CFP-Lox restriction digest

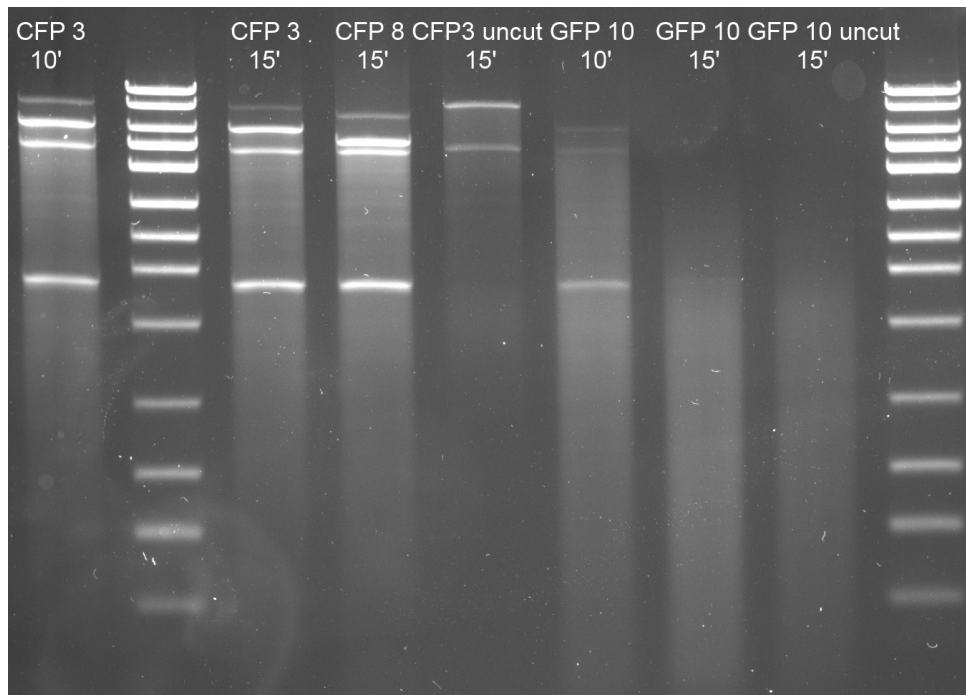


Figure 8.5: CFP-Lox and GFP-Lox restriction digest

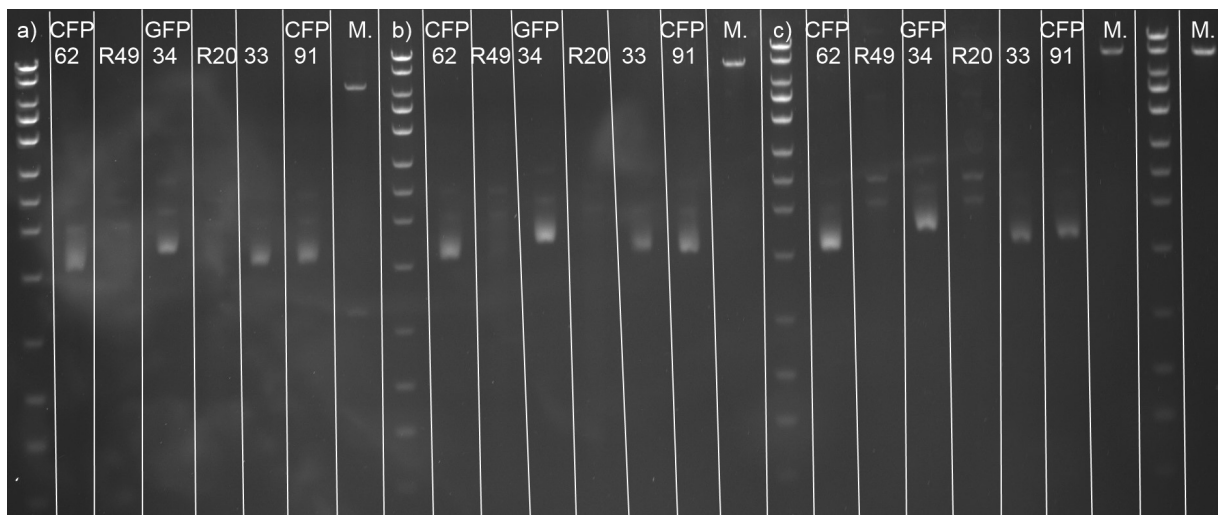


Figure 8.6: Triple point ligation restriction digest

8.4 Protocols

8.4.1 Project outline to build the Khanbrick

The cloning tool should be built. To evaluate whether this selection method is successful, GFP should be used as a test insert. By transforming into Rosetta on 0.02 mM IPTG LB^{KanChl} plates and optical GFP screening of the plates, the cloning tool should be evaluated. If all transformants are fluorescent, the method is successful.

The pET52 backbone was grown, miniprepmed and excised from gel. The Kan resistance gene was transformed into DH5- α according to the iGEM transformation protocol [44]. Primers to add the PstI/antisense stopcodon to the 5' end and the NsiI restriction site to the 3' end of GFP were designed. Primers to add the NsiI and NotI restriction sites to the Kan resistance gene were designed as well (Table 8.3).

Table 8.3: Khanbrick primer designs

Primer	Sequence
GFP forward	5'-CTGCAGTTATTAATGGTGAGCAAGG-3'
GFP reverse	5'-ATGCATCTTGTACAGCTCGTCCATGC-3'
Kan forward	5'-ATGCATATGAGCCATATTCAACGGG-3'
Kan reverse	5'-GCGGCCGCTTAGAAAACTCATCGAGC-3'

The restriction sites could be added to the fragments with the help of PhusionPCR. Next, the PCR products should be loaded on a gel and extracted from the gel. They could be transformed e.g. into pJET and digested with PstI/NsiI and NsiI/NotI, respectively, to verify the functionality of the restriction sites, and be sent to sequencing to make sure the Phusion polymerase did not introduce any mutations. Once this is verified, the Kan gene could be digested, extracted from gel and transformed into DH5- α . The pET52 plasmid should be spread on Kan as a negative control. All transformants should be positive. Some transformants could be picked, grown, miniprepmed and screened for the Kan gene by restriction digest analysis. Positive transformants have the full Khanbrick construct.

To test for selectivity of the cloning tool, positive transformants containing the Khanbrick should be grown, linearised by restriction digest and extracted from gel. The GFP noStop with the antisense stopcodon fragment should be inserted into the Khanbrick. The plasmid should be transformed into Rosetta. 0.02 mM IPTG should be spread on LB^{AmpChl} plates to induce protein production.

If the cloning tool is working properly, only green fluorescent colonies should grow on the plate. If this tool works well with GFP, it can probably be used for many other fragments as well.

With the help of this cloning tool, the need to perform Colony-PCR can be eliminated. Additionally, positive transformants do not have to be screened for the correct orientation of the

insert by restriction digest analysis. However, an additional PCR step to add the antisense stopcodon to the insert has to be performed (and should ideally be verified by sequencing). It is possible that the transcribed insert fused to the Kan resistance protein might prevent the resistance protein from functioning properly. The TAATAA stopcodon might be somewhat leaky which could lead to a success rate of less than 100%. Despite all these potential drawbacks and difficulties, the proposed cloning tool could be a promising method to circumvent Colony-PCR, particularly in cases where performing a PCR to add restriction sites to the insert is unavoidable.

Protocol 9 – Electrotransformation of *E.coli* cells

Materials

SOC: SOB (96 ml) + 10 mM MgCl₂ (1 mL 1M) + 10 mM MgSO₄ (1 mL 1M) + 20 mM glucose (2 mL 1M). Add after autoclaving

1M MgSO₄·7H₂O = 246.5 g/L; dissolve 24.65 g/100 mL

1M MgCl₂·6H₂O = 203.3 g/L; dissolve 20.33 g/100 mL

1M glucose·1H₂O = 198.2 g/L; dissolve 19.82 g/100 mL

SOB: 2% Bacto tryptone (2 g) + 0.5% Bacto yeast extract (0.5 g) + 10 mM NaCl (1mL 1M) + 2.5 mM KCl (250 µL). Complete volume to 96 mL with demi-water.

1M NaCl = 58.44 g/L; dissolve 5.844 g/100 mL

1M KCl = 74.55 g/L; dissolve 7.455 g/ 100mL

LB plates: 5 g NaCl
5 g Bacto tryptone
2.5 g yeast extract
7.5 g agar
(per 500 mL MQ)

Xgal (stock 20 mg/ml) 1:1000

IPTG (stock 200 mM) 1:5000

Ampicillin (stock 100 mg/mL) 1:1000 (Filter sterilize)

Chloramphenicol (stock 10 mg/mL): 1:1000

Kanamycin (stock 50 mg/mL): 1:1000

Protocol

1. Thaw cells @ RT, place on ice
2. In cold eppendorf tube, mix 100 µl of competent cells with 1 or 2 µl of ligation mixture, or 1 ng for whole plasmids, mix well and keep on ice for 30 to 60 sec
3. Set Gene Pulser settings on 25 µF, 2.5 kV, 200 Ω
4. Transfer mixture of cells and DNA to a cold 0.2 cm electroporation cuvette, and tip the suspension to the bottom of the cuvette. Put cuvette in chamber
5. Pulse until a continuous tone sound. Check value (ideally around 5.0)
6. Immediately remove the cuvette from the chamber and add 1 ml of SOC medium and quickly resuspend the cells by pouring the 1 ml SOC two times into the cuvette and eppendorf tube.
7. Transfer the cell suspension to an eppendorf tube and incubate at 37°C for 1 hr .
8. Centrifuge for 20' at max rpm, pour supernatant off, resuspend cells in remaining liquid and plate out 1 µL/ 10 µL/ remaining volume
9. Incubate plates at 37°C overnight
10. The cuvettes are thrown away (single use).

Midiprep of *E.coli*

1. Inoculate 5 mL of LB^{Amp} for 5-6 hours at 37°C.
2. Inoculate Erlenmeyers containing 200 mL LB^{Amp} with E.coli with the 5 mL. Incubate at 37°C o/n.
3. Take the cultures out of the incubator, divide them into 50 mL Falcons and centrifuge them with the ThermoScientific Sorvall Legend XTR Centrifuge.
4. Take out the Falcons and follow the midiprep kit protocol "Plasmid DNA purification" from Macherey-Nagel. (p. 28 7.1 High-copy plasmid purification midi/maxi).

Variations from the Plasmid DNA purification protocol:

Step 10 Don't turn column, just take it out

Step 12 Collect in 15 mL tube with red tip

Step 13 Add iPrOH under chamber. Bring tubes to Sigma 3K12 centrifuge. Centrifuge for 45 min at 10000 g, 4°C

Step 14 Add 2 mL of EtOH and centrifuge with Sigma 3K12 centrifuge for 10-15 min at 10000 g, 4°C

Step 15 Dissolve pellet in 150 µL demi-water and measure concentration on nanodrop

Freeze'n'Squeeze DNA Gel extraction

(works fine for fragments < 2 kb)

1. Cut DNA band from gel.
2. Prepare a microcentrifuge tube (0.5 ml size) with glass wool.
3. Place the gel fragment in the microcentrifuge tube.
4. Freeze the tube in liquid nitrogen for 30 seconds.
5. Punch the tube in the bottom with a needle and let the liquid gel pass to a normal 1.5 ml Eppendorf tube.
6. Centrifuge the resulting solution for 2 minutes at maximum speed.
7. Estimate the volume contained in the tube by pipetting and add a 0.1 volume of 3MNaAc.
8. Add 2 volumes of cold absolute or 96°C ethanol.
9. Keep on ice for 5 minutes.
10. Centrifuge for 5 minutes at 4°C.
11. Discard the ethanol out, dry and dissolve in 20µl of TE.

Protocol 30 - Media for *Aspergilli*

Minimal Medium

Minimal medium salts for 1000 ml:

6.0 g NaNO_3
1.5 g KH_2PO_4
0.5 g KCl
0.5 g $\text{MgSO}_4 \cdot 7 \text{H}_2\text{O}$

0.2% casaminoacids

0,1% yeast extract

pH adjusted to 6.0

For solid medium 15 g agar is added

→ autoclave

Before use:

50 mM carbon source and appropriate supplements, 1 ml Vishniac trace-elements solution (lab fridge)

NB when 10xMM is adjusted to pH=5.45, a 1x MM solution will have pH ~6.0

Complete Medium for 1000 ml:

Minimal medium salts +

2 g meat peptone (pepton 100)
1 g yeast extract
1 g pepton 140 or Casamino acids (vitamins free)
0.3 g yeast ribonucleic acids (cold room shelf)
2 ml vitamins solution (fridge)

pH adjusted to 6.0

For solid medium 15 g agar is added

→ autoclave

Before use:

50 mM carbon source and appropriate supplements (added after sterilization)

1 ml Vishniac trace elements solution

Vishniac solution (Vishniac and Santer, 1957): 1 litre

10 g EDTA
4.4 g $\text{ZnSO}_4 \cdot 7\text{H}_2\text{O}$
1.0 g $\text{MnCl}_2 \cdot 4\text{H}_2\text{O}$
0.32 g $\text{CoCl}_2 \cdot 6\text{H}_2\text{O}$
0.32 g $\text{CuSO}_4 \cdot 5\text{H}_2\text{O}$
0.22 g $(\text{NH}_4)_6\text{Mo}_7\text{O}_{24} \cdot 4\text{H}_2\text{O}$
1.47 g $\text{CaCl}_2 \cdot 2\text{H}_2\text{O}$
1.0 g $\text{FeSO}_4 \cdot 7\text{H}_2\text{O}$

pH adjusted to 4.0 and stored at 4°C.

Vitamins solution: 100 ml, store in protected from light

10 mg thiamine
100 mg riboflavin-5P

Prt. 31 - Preparation spores suspension/inoculation cultures and making spore plates

Materials:

Sterile Pipettes and Pipetting tips
Sterile saline-Tween solution (0.9 % NaCl + 0.005 % (v/v) Tween-80)
Sterile saline solution (0.9 % NaCl)
(for bottles: Sterile glass beads (1 mm))

Protocol:

For bottles:

- 1 Pipette 10 ml saline-Tween on the spore-mat into the culture bottle.
- 2 Add approx. 20 sterile glass beads.
- 3 Shake the bottle for 1 min on a Vortex mixer (max speed).
- 4 Pour the spores suspension to a sterile bottle.

For plates:

1. Inoculate on Thursday six 15 cm CM plates (protocol 30) with a total number of 4×10^5 spores (this is ~ 22 spores per mm^2 on a 15 cm plate; for 9 cm plates, add total 1.4×10^5 spores). Make sure to pour the CM-agar while it is relatively cold, as this will enhance the spore scraping procedure.
Do not add too many spores: with >50 spores per mm^2 the plates will wrinkle and spore concentration will decline since it is more difficult to harvest the spores!
2. Place the plates for 4 days at 30 °C (until Monday).
3. Pipette 10 ml saline-Tween solution on the spore-mat (use 5 mL for small plates).
4. Scrape off the spores using a Drigalski spatula.
5. Transfer the spore suspension to a sterile 50 mL Greiner tube with a sterile 10 ml pipette.
6. Mix 30 seconds on Vortex.
7. Prepare a 50-fold dilution (20 ul spore suspension + 980 ul saline) and determine the concentration of spores by counting the diluted sample in a heamocytometer (see remarks).
8. Calculate the concentration of spores.

Neubauer improved heamocytometer:

depth: 0.1 mm
Minimal area (A): $1/400 \text{ mm}^2$

1. Pipette spore dilution between coverslip and slide enough liquid until the space is flooded (~ 20 ul). *NB: If the coverslip is chipped or in any way damaged, it **must** be replaced: it is no longer functional.*
2. Count the spores (magnification 400 X) in 16 fields. NB: At a magnification of 400x, the square depicted below is seen 9x. The total of spores in one of these counts as one count. Normally, you would count all 9 of them and average it.
3. Calculate the spore concentration in the spores suspension:
 $\text{spores/ml} = \text{count} \times d \times 2.5 \times 10^5$ (d = dilution=50)

(magnification 400 x)

A			

Protocol 32 - Transformation of *Aspergillus*

Reference: L.H. de Graaff (1989), The structure and expression of the pyruvatekinase gene of *Aspergillus nidulans* and *Aspergillus niger*, PhD thesis Agricultural University Wageningen

Materials:

Sterile Büchner funnel with nylon gauze, sterile 10 ml glass tubes), Novozyme 234, sterile funnel with glasswool plug, shake incubator at 30 °C, bench centrifuge, sterile and dry universals (flat bottom 30 ml screw cap tubes), selector and co-transforming gene, sufficient MMS-plates (15 and 9 cm), and molten MMS top-agar at 48 °C.

Saline Tween (ST):

0.8 % NaCl

0.005 % Tween-80 (1:100 dilution from 0.5 % (v/v) Tween-80 stock)

SMC:

1.33 M Sorbitol (242.3 g/L)

50 mM CaCl₂ (7.35 g/L CaCl₂ · 2 H₂O)

20 mM MES buffer pH 5.8

→ filter sterilize store @ 4C

TC:

500 mL

50 mM CaCl₂ 1.86 g

10 mM Tris/HCl pH 7.5 0.61 g

→ Autoclave

STC:

1.33 M sorbitol in TC

→ Autoclave

PEG Buffer (25 % PEG-6000):

Weigh 2.5 g PEG-6000 , add 7.5 ml TC and dissolve by heating to approx. 60°C in a microwave oven (when prepared fresh), or filter sterilize (0.2 um membrane)

→ store filter sterilized at 4°C up to 1 week

TM: Transformation medium for *Aspergillus* per 1000 mL:

10x Minimal Medium salts (protocol 30) 100 mL

Vishniac solution (protocol 30) 1 mL

0.5% Yeast Extract 5 g

0.2 % Casamino acids (vitamins free) 2 g

Adjust pH to 6.0

→ Autoclave

add 2 % glucose after sterilization and appropriate supplements

Stabilized Minimal Medium (St. MM):

per 1000 mL

10x Minimal Medium salts (protocol 30) 100 mL

Vishniac solution (protocol 30) 1 mL

Sucrose (0.95 M) 325.2 g

Adjust pH to 6.0

Add 1.2 % agar 12 g

in case of top agar use 0.6 % agar. 6 g

→ Autoclave

Used as selective/non-selective medium in transformations, depending on the strain used and the supplements added.

Protocol – Optical Screening for GFP and CFP transformants

GFP

Materials

LB^{Amp} plates

Chloramphenicol (stock 10 mg/mL): 1:1000

IPTG stock 10 mM

E. coli Rosetta 2 (DE3) with pRARE plasmid

GeneSys G:Box Chemi-XT4 Gel reader

1. Perform ligation and transformation according to Prt. 09 or with heat-shock competent cells.
2. Prior to plating, spread 20 µL Chloramphenicol stock solution on all agar plates.
3. Prepare a series of IPTG concentrations ranging between 1 and 0.02 mM. For best results, use 0.05 and 0.02 mM (100 µL and/or 40 µL 10mM IPTG stock) IPTG and spread the corresponding volume on agar plates. *NB: Avoid spreading big volumes of IPTG stock solution. If 1 mL is spread, the plate will not dry well.*
4. After incubation for 1 hour, spin down cells, discard supernatant, resuspend cells in remaining volume. Plate 10 µL (or more) of cells per plate.
5. Incubate plates at 37°C overnight.
6. Place plates in the GeneSys G:Box Chemi-XT4 Gel reader. Remove upper lids of the plates.
7. Select AutoCapture > DNA > Type: Blot > Dye: eGFP. Select “continue”.
8. Save and print plate images. Close lids.
9. With the help of the prints, count and mark positive transformants on the plates.
10. Calculate the Colony-PCR mastermix for the number of positive transformants + 5 (positive control, negative control and pipetting errors).
11. Perform Colony-PCR with the DreamTaq polymerase. Make sure to make master plates of all transformants.

CFP and other fluorophores

Materials

LB liquid

Chloramphenicol (stock 10 mg/mL): 1:1000

Ampicillin (stock 100 mg/mL) 1:1000

IPTG stock 10 mM

E. coli Rosetta 2 (DE3) with pRARE plasmid

Molecular Devices SpectraMax M2 96 well-plate reader

Sterile 2 mL Eppendorf tubes

Sterile 1 µL pipette tips

Black 96 well plate

1. Prepare required amount of liquid LB^{AmpChl} medium. Aliquot 1 mL per Eppendorf tube.
2. Pick transformants with sterile 1 µL pipette tips, put tips in Eppis.
3. Incubate transformants at 37°C for one hour. This can be done by placing a rack with the Eppis in a 37°C incubator.
4. Aliquot 250 µL of each culture into one well. Make sure to keep the cultures in the Eppis sterile. Add 0.5 µL of a 10 mM IPTG stock solution to each well. Include a negative control (LB^{AmpChl} medium). *NB: Be sure to measure all samples with the same liquid LB, since different bottles of liquid LB may differ in colour!*
5. Set excitation wavelength to 430 nm and emission wavelength to 475 nm. Measure emission with the 96 well plate reader overnight.
6. Plot emission (ordinate) over time (abscissa). Calculate the slope by comparing the last point with the first point on the ordinate. If the increase is more than 2.8 times bigger than the increase measured in the negative control, then the corresponding well has a positive transformant in it.

NB: By picking the correct wavelengths, this protocol can be adapted for screening of any other fluorophore.

Pr. 23 – Preparation of electrocompetent *E. coli* cells

Equipment

-80°C freezer

37°C incubator

Refrigerated centrifuge that accepts 50 mL Falcons

Chemicals and reagents

~500 mL LB Lennox supplemented with appropriate concentration of antibiotic if appropriate.

~600 mL sterile deionized water chilled to 4°C

50 mL sterile 10% glycerol in deionized water chilled to 4°C

Ice bucket and ice

Dry ice, ethanol bath or liquid nitrogen

Supplies

Many 1.5 mL plastic tubes chilled to -80 °C

14 mL culture tube for starter culture

2 L flask for culture

50 mL Falcons for centrifugation

Pipets

Procedure

1. Prechill all tubes and pipets at 4°C (or -80°C) as appropriate.
Also rinse all flasks with H₂O prior to autoclaving in order to remove residual detergents that may remain on glassware from dishwashing. This step may increase competency.
Autoclaving with water, which is then discarded, is even better.
2. Inoculate 5mL LB medium without salt and grow overnight at 37°C with rotation.
Use LB without sodiumchloride (10 g/l peptone or tryptone and 5 g/l yeast extract)
3. Add the 5mL overnight culture to 450mL LB medium and incubate at 37°C with vigorous shaking until the OD 600nm is between 0.5 and 1.0. It should take about 3 hours.
For recA⁻ strains, the OD 600 nm should be between 0.5 and 0.7 according to one online source.
4. Fast cool the centrifuge with the correct rotor to 4°C
5. Pour the culture into two 225 mL centrifuge tubes.
6. Place the tubes on ice for 15 minutes.
This step can vary in incubation time between 15 minutes and 1 hr. Longer incubation times may lead to higher competency.

Protocol – Heatshock transformation of *E.coli* cells

Materials

SOC: SOB (96 ml) + 10 mM MgCl₂ (1 mL 1M) + 10 mM MgSO₄ (1 mL 1M) + 20 mM glucose (2 mL 1M). Add after autoclaving

1M MgSO₄·7H₂O = 246.5 g/L; dissolve 24.65 g/100 mL

1M MgCl₂·6H₂O = 203.3 g/L; dissolve 20.33 g/100 mL

1M glucose·1H₂O = 198.2 g/L; dissolve 19.82 g/100 mL

SOB: 2% Bacto tryptone (2 g) + 0.5% Bacto yeast extract (0.5 g) + 10 mM NaCl (1mL 1M) + 2.5 mM KCl (250 µL). Complete volume to 96 mL with demi-water.

1M NaCl = 58.44 g/L; dissolve 5.844 g/100 mL

1M KCl = 74.55 g/L; dissolve 7.455 g/ 100mL

LB plates: 5 g NaCl
5 g Bacto tryptone
2.5 g yeast extract
7.5 g agar
(per 500 mL MQ)

Xgal (stock 20 mg/ml) 1:1000

IPTG (stock 200 mM) 1:5000

Ampicillin (stock 100 mg/mL) 1:1000 (Filter sterilize)

Chloramphenicol (stock 10 mg/mL): 1:1000

Kanamycin (stock 50 mg/mL): 1:1000

Protocol

1. Thaw cells on ice.
2. Add 1-2 µL of ligation mix (max. 25 ng) to competent cells.
3. Keep cells on ice for 30 minutes.
4. Heat-pulse cells in a water bath at 42°C for exactly 90 seconds.
5. Keep cells on ice for 2 minutes.
6. Add between 700 µL and 1 mL SOC to each aliquot of cells.
7. Incubate cells at 37°C for 1 hr.
8. Centrifuge for 20' at max rpm, pour supernatant off, resuspend cells in remaining liquid and plate out 1 µL/ 10 µL/ remaining volume.
9. Incubate plates at 37°C overnight.

Gwendolin Isabella Korinek

Date of Birth: 02 August 1988
Nationality: Austrian
Address: Kantweg 10
2201 Gerasdorf/Oberlisse
Telephone: (+43)664/497 87 74
e-mail: gwenkorinek@gmail.com



Education

Since 03/2012

TU Vienna, Study of Biotechnology and Bioanalytics

MSc, Erasmus exchange at **Wageningen UR**,
“Constructing FRET biosensors for intracellular metabolite detection via fluorescence microscopy”
Expected end of study: 6/2014

10/2006 – 04/2012

TU Vienna, Study of Technical Chemistry

BSc, *“Synthesis of amphiphilic block copolymers for potential drug-carrier systems by means of RAFT polymerisation”*

06/2006

School leaving examination (passed with honours)

1999 – 2006

Modern-language grammar school **Sacré Cœur**,
1030 Vienna

Professional experience

since 02/2014 and
06/2010 – 02/2013

Federal Institute of Technology, Department of
Plastics Technology and Environmental
Engineering, Laboratory assistant

Tasks: *performing accredited tests according to
ISO 17025 and non-accredited tests, issuing of test
reports and expertises*

03 – 06/2011 and
03/2012 – 06/2012

TU Vienna, Tutor of Instrumental Bioanalytical
Laboratory

Tasks: *assistance of students with the exercises
GC-FID and F-AAS, handling of gas bottles,
working with software SOLAR and Agilent
ChemStation*

03 – 06/2010

TU Vienna, Tutor of Instrumental Bioanalytical
Laboratory

Tasks: *assistance of students with the exercises
FT-IR spectroscopy and ion chromatography,
preparation of solid samples, handling of liquid
nitrogen, working with software OPUS and
Chromeleon*

10/2008 – 06/2010	Ströck Gastronomiebetriebs GmbH , Gerasdorf branch, Shop assistant <i>Tasks: sale of bakery products such as bread, pastries, spreads, sausage and cheese; taking in charge of dairy products, presentation of bakery products, writing off goods</i>
07– 09/2008	Ströck Gastronomiebetriebs GmbH , Gerasdorf branch, Internship as shop assistant
08/2003 – 12/2007	Radio Orange , project “Funkschatten”, Editorial participation <i>Tasks: development of broadcasting concepts, conduct of interviews, live presenting and technical realisation of live broadcasts, cutting and mixing of contributions on the computer</i>
02/2005	Bundesinstitut für Gehörlosenbildung , Internship as part of the social project “Compassion”

Additional skills

Native language:	German
Foreign languages:	English (fluent) French (fluent) Italian (basic skills) Dutch (basic skills)
Computer skills:	MS Word, MS Excel, MS PowerPoint, Audacity, Cool Edit Pro, Origin (very good knowledge) LaTeX, SOLAR, Agilent ChemStation, OPUS, Chromeleon, OmniSec, SpinWorks, Origin (basic knowledge)

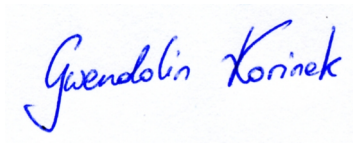
Further education

12/2011	Diplôme d'études en langue française B2
10/2009	“Glass-blowing exercises” course at TU Vienna
10/2009	“Italian for engineers” course at TU Vienna
09/2008	“Technical French” course at TU Vienna
05/2006	1 st place team contest at Chemistry Olympiad Vienna
03-04/2006	3 rd place/1 st place at English Olympiad Austria/Vienna
12/2005	Cambridge Certificate in Advanced English
08/2005 and 2004	Intensive English course at Hertford College, Oxford

06/2005 and 2004 Business English 1 and 2, Sacré Cœur 1030
Vienna
06/2005 Cambridge First Certificate in English

Hobbies and Interests

Sports (triathlon, extreme sports), languages (Klingon), literature (science fiction, fantasy), music (synthpop, indie, deephouse), creative work (drawing, prose, poetry)



Vienna, 15 May 2014